2001

Lithium Isotope Geochemistry of Marine Sediments.

Libo Zhang
Louisiana State University and Agricultural & Mechanical College

INFORMATION TO USERS

This manuscript has been reproduced from the microfilm master. UMI films the text directly from the original or copy submitted. Thus, some thesis and dissertation copies are in typewriter face, while others may be from any type of computer printer.

The quality of this reproduction is dependent upon the quality of the copy submitted. Broken or indistinct print, colored or poor quality illustrations and photographs, print bleedthrough, substandard margins, and improper alignment can adversely affect reproduction.

In the unlikely event that the author did not send UMI a complete manuscript and there are missing pages, these will be noted. Also, if unauthorized copyright material had to be removed, a note will indicate the deletion.

Oversize materials (e.g., maps, drawings, charts) are reproduced by sectioning the original, beginning at the upper left-hand corner and continuing from left to right in equal sections with small overlaps.

Photographs included in the original manuscript have been reproduced xerographically in this copy. Higher quality 6" x 9" black and white photographic prints are available for any photographs or illustrations appearing in this copy for an additional charge. Contact UMI directly to order.

ProQuest Information and Learning
300 North Zeeb Road, Ann Arbor, MI 48106-1346 USA
800-521-0600

LITHIUM ISOTOPE GEOCHEMISTRY OF MARINE SEDIMENTS

A Dissertation

Submitted to the Graduate Faculty of the
Louisiana State University and
Agricultural and Mechanical College
in partial fulfillment of the
requirements for the degree of
Doctor of Philosophy

in

Department of Geology and Geophysics

by
Libo Zhang
B. S., Beijing University, P. R. of China, 1986
M. S., Beijing University, P. R. of China, 1989
M. S., Louisiana State University, U. S. A. 1997
May 2001

ACKNOWLEDGMENTS

Most of all I would like to thank Dr. Lui-Heung Chan, my thesis advisor, for all her inspiration, patience, and scientific advice as well as financial support. Without her support and help, this dissertation would have been very difficult to complete. I am extremely grateful for what she has done for me as a thesis advisor. My deep gratitude also goes to Drs. Ajoy Baksi, Juan Lorenzo, Gary Byerly, Ray Ferrell, and Joris Gieskes for serving as my dissertation committee members and for giving me their advice on my research. Special thanks go to Dr. Joris Gieskes for kindly providing Ocean Drilling Program samples and Dr. Ajoy Baksi for his help in the statistical analysis of my data. Samples used for the reconnaissance study were provided by Oregon State University Core and Rock Repository supported by NSF grant OCE 94-02298.

My gratitude goes to Department of Geology and Geophysics for its financial support through the past few years. I would like to thank the staff of the department, particularly Roselyn Oubre for her excellent help and services. Editorial help from Ed Fitchard and laboratory help from Tommy Blanchard are crucial and are deeply appreciated.

Finally, I would like to thank my wife (Yu Wang), my parents, and parents in law for their patience and confidence in me as well as love. Without their support, this dissertation would have been impossible to complete. Also, thanks to my daughter (Angel, 3 years old) and son (Louis, 10 months old) for effectively letting me know it is time to finish up my schoolwork.

TABLE OF CONTENTS

LIST OF TABLES

LIST OF FIGURES

ABSTRACT

While the isotope geochemistry of lithium in the marine environment is increasingly known, there are still outstanding problems concerning its oceanic budget and mantle-crust recycling that remain to be resolved. To evaluate the role of marine sediments in the oceanic budget, laboratory experiments were conducted to determine the extent of lithium adsorption on marine sediments and the magnitude of isotopic fractionation. Sediments from the Greenland margin were studied to gain further understanding of the sediment-water interaction. The isotopic compositions of the major types of marine sediments were characterized to understand the sedimentary cycle of lithium. The enhanced database permits a re-evaluation of the oceanic lithium budget.

In the adsorption experiments, greater magnitude of adsorption was observed in river water than seawater demonstrating the effect of competition of major ions for sorption sites. The isotopic fractionation factors for adsorption on kaolinite, vermiculite, and Mississippi River suspended sediment are similar within uncertainty, giving a mean value of 1.024 ± 0.003. In the comprehensive study of the sediments from the Greenland margin, the similarity between solid and pore water concentration profiles suggests that the sediments largely control the distribution of lithium in pore water. The isotopic compositions of the sediments are well correlated with source material as defined by lithology and bulk chemistry. Based on the isotopic data of various types of marine sediments, it is concluded that lithium isotopic

compositions of marine sediments are dominated by terrigenous components and reflect local source. Most pelagic and hemipelagic sediments studied have isotopic compositions that are distinct from the mantle, making lithium isotopic ratio a valuable tracer for the subducted component in arc magmas.

Among the sedimentary sinks evaluated in this study, namely incorporation in marine carbonates and biogenic silica, diffusion into sediments, and adsorption on marine sediments, only adsorption appears to be a significant sink for lithium in the oceans. The importance of the oceanic crust alteration at low and moderate temperatures as a lithium sink may be underestimated. Further insight into the lithium balance in the oceans depends on the characterization of water flux on the ocean ridge flank.

CHAPTER 1
INTRODUCTION

Lithium is the first element in the alkali family. It has two isotopes: ^{6}Li and ^{7}Li, with abundances of 7.5 and 92.5% respectively. The large relative mass difference between these two isotopes favors their separation in nature (Heier and Billings, 1970). Thus fractionation of lithium isotopes can be expected during geological processes such as oceanic crust alteration and weathering. This isotope system is therefore a potentially important tool to study provenance and mass transfer processes. However, earlier geochemical applications of lithium isotope system were seriously hampered by the inherent difficulty in the isotopic analysis. The ratio of $^{6}Li/^{7}Li$ is not only sensitive to natural processes but also susceptible to mass fractionation during chemical separation and ionization in the mass spectrometer. Unfortunately, the latter cannot be internally corrected by using another isotope since lithium only has two natural stable isotopes. Due to this analytical problem, the wide range of abundance ratios reported in early literature (Cameron, 1955; Svec and Anderson, 1965; Bowen, 1956; Morozova and Alferovskiy, 1974) is attributable to both instrumental factors and natural variation.

In order to minimize the isotopic effect during mass spectrometric analysis, various techniques have been investigated. Two approaches were adopted: (1) the synthesis of high-mass molecular ions for isotopic measurement (Chan, 1987; Green et al., 1988) and (2) the synthesis of a

loading form that produces Li^+ beam with minimum temperature-induced fractionation (Xiao et al., 1989; Moriguti and Nakamura, 1993, 1998a; You and Chan, 1996). The methods that provide the necessary precision (better than ± 1‰) for geological studies are the use of diborate molecular ion ($LiBO_2^+$) (Chan, 1987) and the analyses of Li^+ from a phosphate ion source (Moriguti and Nakamura, 1993, 1998a; You and Chan, 1996). More recently inductively coupled plasma mass spectrometry has been developed for the measurement of lithium isotopic ratios in geological samples (Tomascak et al., 1999).

With the advancement of the analytical techniques, the initial studies focused on the geochemical cycle of lithium in the marine environment. The isotopic compositions of the major lithium reservoirs, including ocean water, rivers, submarine hydrothermal solutions, fresh and altered basalt, and marine sediments and pore waters, have been gradually characterized. This isotopic system has been applied to study numerous marine processes. It provides a means to determine the direction and magnitude of seawater-basalt exchange during low temperature weathering and high temperature hydrothermal activities in the oceanic crust (Chan et al., 1992, 1993, 1994). Lithium isotope ratios are also a good indicator of fluid expulsion at convergent margins (You et al., 1995; Chan and Kastner, 2000). The isotopic abundance in pore water is extremely sensitive to sediment-water interaction and its variation reveals a multitude of diagenetic processes (Zhang et al., 1998; James et al., 1999; Chan and Kastner, 2000). Lithium isotopic

systematics has also been applied to examine the continental systems such as the rivers (Huh et al., 1998) and the subsurface brines (Bottomley et al., 1999). Finally, lithium isotopes are also used to trace the subduction-related processes and provide insight on the source components in the arc magma (Moriguti and Nakamura, 1998b; Chan et al., 1999). These studies establish an isotopic range of about 60‰ in the geological reservoirs.

While the isotope geochemistry of lithium in the marine environment is increasingly known, there are still outstanding problems concerning the oceanic budget of lithium and its mantle-crust recycling that remain to be resolved. River flux and hydrothermal input are two major lithium sources in the oceans (Stoffyn-Egli and Mackenzie, 1984; Chan et al., 1992; Huh et al., 1998). The only recognized important sink in the oceans is low temperature alteration of oceanic crust, the magnitude of which is much smaller than the total input. Several studies (Seyfried et al.,1984; Stoffyn-Egli and Mackenzie, 1984) have proposed different lithium sinks in the oceans such as adsorption by marine sediments and uptake by authigenic marine sediments. To determine the role of marine sediments in the oceanic budget, there is a clear need to define the distribution of lithium and its isotopes in different types of marine sediments and to understand the interaction between seawater and marine sediments.

The chemical composition and mass of the subducted sediments regulate the growth and chemical composition of the continental crust, as well as the budget of mantle-crust recycling (Plank and Langmuir, 1998). Recent

efforts are directed to characterize the chemical compositions of the subducting sediments at individual convergent margins in order to arrive at a global sedimentary flux (Plank and Langmuir, 1998). Lithium is concentrated in marine sediments relative to the mantle and therefore is an important tracer of the crust-mantle transfer processes. However, lithium and its isotopic flux associated with subducting marine sediment have not been well evaluated due to lack of characterization of its distribution in marine sediments. A systematic study of lithium and its isotopes on marine sediments will provide valuable information for defining the subducting sediment end-member and for assessing the role of sediments in arc magmatism and crust-mantle recycling.

This dissertation is directed to characterize the isotopic compositions of various types of marine sediments including hemipelagic and pelagic clays, and biogenic carbonates and siliceous ooze. A comprehensive study of the sediments from the Greenland margin is included to accompany a previous study of the pore fluids in the same sediments to gain further understanding of the diagenetic reactions in the sediments. With the enhanced isotope database, this dissertation then delineates the controls of lithium isotopic composition in marine sediments and evaluates its potential as a tracer of the contribution of subducted sediments to arc magma genesis. The oceanic budget is also re-evaluated by determining the magnitude of possible sinks such as adsorption by marine sediments, diffusion into bottom sediments, and incorporation into biogenic phases. The overall goal

of this work is to enhance the understanding of lithium isotope geochemistry in the marine environment and the lithium budget in the oceans.

This thesis is divided into six chapters. Chapter 1 presents a general introduction to the lithium isotope geochemistry in the marine environment and the outstanding problems such as imbalance of the oceanic lithium budget and incomplete knowledge of lithium isotope geochemistry on marine sediments.

Chapter 2 examines the adsorption behavior of lithium. To evaluate the extent of lithium absorption by clay minerals, laboratory experiments were carried out in which clay minerals and river suspended sediment were allowed to interact with river water and seawater. The partition of lithium between clay minerals and water, and the isotopic fractionation factor associated with adsorption were then determined. More importantly, by defining the lithium adsorption behavior in river and seawater, this chapter evaluates the role of adsorption by marine sediments in the geochemical cycle of lithium.

Chapter 3 focuses on the geochemistry of lithium and its isotopic composition of marine sediments in the Irminger Basin, offshore of Greenland (Ocean Drilling Program (ODP) Sites 918 and 919). The sediments are from the same depths where pore water lithium was studied (Zhang et al., 1998). In the pore water study, lithium isotope data are accompanied by strontium isotope ratios to decipher diagenetic reactions in the sediments noted for the pervasive presence of volcanic materials and

high accumulation rates. The pore water lithium isotope profiles are complex signifying a variety of exchange reactions with the solid phases including volcanic alteration, cation exchange with NH_4^+, and lithium release during sediment diagenesis. Complementary to the pore water lithium study (Zhang et al., 1998), the detailed lithium concentration and isotopic profiles in marine sediments are reported and the lithium sources and sinks in pore waters are discussed. In addition, the detailed lithium isotope study of marine sediments of known lithology provides a new insight to the control of lithium isotopic composition of marine sediments at Sites 918 and 919.

Chapter 4 presents a reconnaissance study of the lithium isotopic compositions of the major types of marine sediments. The sediments studied include pelagic clay, hemipelagic sediments, biogenic carbonates, biogenic silica, coastal sediments, metaliferous sediments, and river suspended material. With the enhanced database, a conceptual model is formulated to explain the control of lithium isotopic composition of bulk marine sediments. Since the biogenic carbonates and silica incorporates lithium from seawaters and eventually removes it from the oceans, they are sinks for lithium in the oceans. The magnitudes of the lithium flux associated with these sediments are determined by characterizing the lithium content of those components. This work has demonstrated that, because of the distinct isotopic characteristics of marine sediments, lithium and δ^6Li can be a useful tracer for the recycling of marine sediment in the subduction zone.

Chapter 5 summarizes the implications of the findings from the previous three chapters for the oceanic lithium budget. Even though the oceanic lithium budget is not completely resolved, this dissertation provides new constraints on sedimentary sinks such as adsorption by marine sediments, diffusion into bottom sediments, and incorporation into biogenic sediments.

Chapter 6 summarizes the significant findings in this dissertation on the lithium isotope geochemistry of marine sediments: (1) the extent of lithium adsorption on marine sediments and the magnitude of isotopic fractionation associated with the adsorption process, (2) the lithium contents and isotopic compositions of the major types of marine sediments, (3) the isotopic exchange between pore water and sediments, and (4) the controls of the lithium isotopic compositions of marine sediments and the sedimentary cycle of lithium. Overall, this dissertation improves the understanding of the oceanic balance of lithium, as well as contributes to the fundamental knowledge of lithium isotope geochemistry.

1.1 References

BOTTOMLEY D. J., KATZ A., CHAN L. H., STARINSKY A., DOUGLAS M., CLARK I. D., AND RAVEN K. G. (1999) The origin and evolution of Canadian Shield brines: evaporation or freezing of seawater? New lithium isotope and geochemical evidence from the Slave craton. Chem. Geol. 155, 295-320.

BOWEN H. J. M. (1956) The uptake and enrichment of lithium by yeast. J. Nucl. Energy 2, 255.

CAMERON A. E. (1955) Variation in the natural abundance of the lithium isotopes. J. Amer. Chem. Soc. 77, 2731-2733.

CHAN L. H. (1987) Lithium isotope analysis by thermal ionization mass spectrometry of lithium tetraborate. Anal. Chem. 59, 2662-2665.

CHAN L. H., EDMOND J. M., THOMPSON G., AND GILLS K. (1992) Lithium isotopic composition of submarine basalts: Implications for the lithium cycle in the oceans. Earth Planet. Sci. Lett. 108, 151-160.

CHAN L. H., EDMOND J. M., AND THOMPSON G. (1993) A lithium isotope study of hot springs and metabasalts from mid-ocean ridge hydrothermal systems. J. Geophys. Res. 98, 9653-9659.

CHAN L. H., GIESKES J. M., YOU C. F., AND EDMOND J. M. (1994) Lithium isotope geochemistry of sediments and hydrothermal fluids of the Guaymas Basin, Gulf of California, Geochim. Cosmochim. Acta 58, No. 20, 4443-4454.

CHAN L. H., LEEMAN W. P., AND YOU C.F. (1999) Lithium isotopic composition of Central American Volcanic Arc lavas: Implications for modification of subarc mantle by slab-derived fluids. Chem. Geol. 160, 255-280.

CHAN L. H. AND KASTNER M. (2000) Lithium isotope compositions of pore fluids and sediments in the Costa Rica subduction zone: Implications for fluid processes and sediment contribution to the arc volcanoes. Earth Planet. Sci. Lett. 183, 275-290.

GREEN L. W., LEPPINEN J. J., AND ELLIOT N. L. (1988) Isotopic analysis of lithium as thermal dilithium fluoride ions. Anal. Chem. 60, 34.

HEIER K. S. AND BILLINGS G. K. (1970) Lithium. In Handbook of Geochemistry (ed. K. H. Wedepohl), Vol. II – 1, p. 3-H-1. Springer-Verlag.

HUH Y., CHAN L. H., ZHANG L., AND EDMOND J. M. (1998) Lithium and its isotopes in major world rivers: implications for weathering and the oceanic budget. Geochim. Cosmochim. Acta 62, 2039-2051.

JAMES H. J., RUDNICKI M. D., AND PALMER M. P. (1999) The alkali element and boron geochemistry of the Escanaba Trough sediment-hosted hydrothermal system. Earth Planet. Sci. Lett. 171, 157-169.

MORIGUTI T. AND NAKAMURA E. (1993) Precise lithium isotopic analysis by thermal ionization mass spectrometry using lithium phosphate as an ion source material. Proc. Japan Acad. 69, 123 – 128.

MORIGUTI T. AND NAKAMURA E. (1998a) High-yield lithium separation and the precise isotopic analysis for natural rock and aqueous samples. Chem. Geol. 145, 91-104.

MORIGUTI T. AND NAKAMURA E. (1998b) Across-arc variation of Li isotopes in lavas and implications for crust/mantle recycling at subduction zones, Earth Planet. Sci. Lett. 163, 167-174.

MOROZOVA I. M. AND ALFEROVSKIY (1974) Fractionation of lithium and potassium isotopes in geological processes. Geochem. Int. 11, 17-25.

PLANK T. AND LANGMUIR C. H. (1998) The chemical composition of subducting sediment and its consequences for the crust and mantle, Chem. Geol. 145, 325-394.

RYAN J. G. AND LANGMUIR C. H. (1987) The systematics of lithium abundances in young volcanic rocks. Geochim. Cosmochim. Acta 51, 1727-1741.

SEYFRIED W. E. JR., JANECKY D. R., AND MOTTL M. J. (1984) Alteration of the oceanic crust: Implications for geochemical cycles of lithium and boron. Geochim. Cosmochim. Acta 48, 557 – 569.

STOFFYN-EGLI P. AND MACKENZIE F. T. (1984) Mass balance of dissolved lithium in the oceans. Geochim. Cosmochim. Acta 48, 859 – 872.

SVEC H. J. AND ANDERSON A. R. (1965) The absolute abundance of the lithium isotopes in natural sources. Geochim. Cosmochim. Acta 51, 1727-1741.

TOMASCAK P. B., CARLSON R. W., AND SHIRLEY S. B. (1999) Accurate and precise determination of Li isotopic compositions by multi-collector sector ICP-MS, Chem. Geol. 158, 145-154.

XIAO Y. K., QI H. P., WANG Y. H., AND JIN L. (1989) High precision measurement of lithium by thermal ionization mass spectrometry. Int. J. Mass Spectrom. Ion Proc. 94, 101 – 114.

YOU C. F., CHAN L. H., SPIVACK A. J., AND GIESKES J. M. (1995) Lithium, boron, and their isotopes in sediments and pore waters of Ocean Drilling Program Site 808, Nankai Trough: Implications for fluid expulsion in accretionary prisms. Geology 23, No. 1, 37 – 40.

YOU C. F. AND CHAN L. H. (1996) Precise determination of lithium isotopic composition in low concentration natural samples. Geochim. Cosmochim. Acta 60, 909 – 915.

ZHANG L., CHAN L. H., AND GIESKES J. M. (1998) Lithium isotope geochemistry of pore waters from Ocean Drilling Program Sites 918 and 919, Irminger Basin, Geochim. Cosmochim. Acta 62, 2437–2450.

CHAPTER 2
THE ADSORPTION BEHAVIOR OF LITHIUM

2.1 Introduction

Due to its large hydration radius and energy, lithium is generally considered to be the least absorbable element in alkali group (Heier and Billings, 1970). Egli (1979), in her experiments, did not observe adsorption of lithium by clay minerals. In contrast, Lombardi (1963) concluded that nearly all lithium in the saline water of the Vega Spring, California, is removed by clay minerals within sediments. Lithium association with clay minerals is also reflected in its high concentration in sedimentary rocks (Ronov et al., 1970). Anderson et al (1989) and Davey and Wheeler (1980) observed anomalously high uptake of lithium by soils and clay minerals in their experiments. To further test and verify the lithium adsorption behavior of clay minerals, adsorption experiments were designed to mimic natural settings of fresh water and seawater with clay minerals (kaolinite, Na-montmorillonite, vermiculite), and Mississippi River suspended sediment. The lithium adsorption behavior and magnitude determined from the experiments could also provide a basis to evaluate the role of adsorption by marine sediment in the oceanic lithium budget.

Lithium adsorption onto marine sediments was considered an important removal process necessary to balance lithium in the oceans (Seyfried et al., 1984). This hypothesis was proposed largely based on the concentration difference between river sediments and marine sediments.

Since lithium content in sediment is a function of mineral composition (Heier and Billings, 1970), the adsorption onto marine sediment may not be convincingly evident based on the difference of lithium concentration. Controlled adsorption experiments allow the determination of the magnitudes of lithium adsorption by different clay minerals and to better understand the adsorption mechanism. Using the partition coefficients determined from the experiments, we can quantitatively determine the amount of lithium that can be adsorbed from seawater and examine whether this process can serve as an efficient sink in the oceans.

By applying new analytical methods, recent studies have shown a range of ~60‰ in lithium isotopic compositions in geological materials (Chan et al., 1988, 1992, 1993, 1994a, 1994b; You et al., 1995; You and Chan, 1996; Huh et al., 1998; Zhang et al., 1998). With such large isotopic fractionation in natural processes, lithium isotopes have been successfully used to investigate various geological problems, including oceanic crust alteration, submarine hydrothermal activity, and fluid expulsion at convergent margins (Chan et al., 1992, 1993, 1994; You et al., 1995). However, lithium isotopic fractionation during the adsorption process is virtually unknown. This restricts application of lithium isotopes as a diagnostic tracer in adsorption related processes. Besides evaluating the role of marine sediment adsorption in the oceanic lithium budget, this study is also aimed at characterizing lithium isotopic fractionation associated with adsorption based on the experimental

data, thus enhancing our understanding of its isotopic fractionation in the natural processes.

2.2 Method

2.2.1 The experimental systems

The experimental systems consisted of clay minerals suspended in both river water and seawater. The seawater used in the experiments was collected from the Gulf of Mexico (GMW) with a salinity of 34‰ and lithium concentration of 169.5μg/L. The river water was from the Mississippi River (MRW), collected at Baton Rouge in May 1996, and filtered through 0.45μm Nucleopore membrane. Because the Mississippi River has a very low lithium concentration during spring high flow (Chan et al., 1992), a known amount of isotope standard (L-SVEC) solution was added to yield a concentration of 170.8μg/L, comparable to that of the Gulf of Mexico water. The use of lithium-enriched MRW (hereafter referred to as "spiked MRW") is to evaluate the removal of lithium by suspended material in river water.

Solid phases studied consisted of Mississippi River suspended sediment (MRSS), kaolinite, Na-montmorillonite, and vermiculite. MRSS was filtered from river water taken at the high flow stage (May, 1996) and dried at 70°C. In MRSS, three dominant primary minerals were mixed layer illite/smectite, discrete illite, and kaolinite (Kennedy, 1965). The kaolinite sample is a mixture of kaolins from several localities in Georgia. The vermiculite sample is from Libby, Montana and the Na-montmorillonite is from

Crook Country, Wyoming. The clay mineral samples for this study were provided by Dr. Ray Ferrell of Louisiana State University.

2.2.2 Adsorption experiments

Batch experiments were carried out to determine partition coefficients and adsorption kinetics for kaolinite, Na-montmorillonite, and vermiculite. Isotopic fractionation factors between Gulf of Mexico water and these clay minerals were also determined. In each batch experiment, identical amounts of the mineral samples (0.5g for kaolinite and vermiculite, 0.1g for Na-montmorillonite) were placed in 15ml polyethylene centrifuge tubes. Prior to use, the centrifuge tubes were leached with 1N HCl for a week, then rinsed with distilled water and dried. Exactly 10g of solution (either GMW or spiked MRW) were added to each centrifuge tube. The water/rock ratio was maintained at 20:1 for kaolinite and vermiculite, and 100:1 for Na-montmorillonite. The high water/rock ratio for Na-montmorillonite was necessary because of its considerable expansion in solution. It was extremely difficult to filter the solution from Na-montmorillonite with the initial water/rock ratio of 20:1. The centrifuge tubes were closed tightly and agitated on a shaker continuously to keep the fine particles in suspension. At different times after the introduction of the solution, one of the reaction tubes was removed from the shaker and centrifuged, and the supernatant was filtered with 0.45μm membranes. The lithium concentration and isotopic composition of the supernatant were then measured. Following the procedure described above, we carried out the experiments on vermiculite with GMW, vermiculite with the

spiked MRW, kaolinite with GMW, kaolinite with the spiked MRW, and Na-montmorillonite with GMW. In addition, 1.484g of suspended sediment filtered from several liters of Mississippi River water was mixed with 52.465g of GMW to simulate the interaction between river suspended material and seawater. Reactions of the various systems were allowed to proceed for about 4900 hours (approximately 204 days). As a blank used for control, GMW and spiked MRW without clay minerals were also shaken and agitated in the same manner. Lithium concentrations before and after the experiment were identical within the analytical error. Thus, it was concluded that loss of lithium due to wall adsorption and evaporation as well as contamination during reaction was negligible.

2.2.3 Chemical and isotopic analyses

The lithium contents of the initial river water and seawater solutions were determined by isotope dilution mass spectrometry using the procedure of You and Chan (1996). The precision is better than ±0.5% (1σ). Lithium concentrations of the reaction solutions were determined by flame emission with standard addition using a Varian atomic absorption spectrometer. The analytical error is estimated to be ±2% (1σ).

The isotopic composition of lithium was determined by thermal ionization mass spectrometry of lithium phosphate following the procedure of You and Chan (1996). Lithium was separated from the sample by cation exchange chromatography using 0.5N HCl as an eluant. The eluant containing lithium was evaporated to dryness and redissolved in sub-boiling

water. The solution was irradiated with ultraviolet light overnight to destroy any organic materials present, and subsequently evaporated to a small drop. A small amount (0.04ml) of 0.025M H_3PO_4 was added and allowed to react at 130°C on a hot plate for four hours. Lithium was thus converted to phosphate that served as the ion source for isotopic measurement. The sample size used was approximately 100ng, and the procedural and reagent blank was determined to be 0.2ng, which is insignificant. Following this, the lithium phosphate was redissolved in sub-boiling water and loaded on a pre-baked Re filament with a current of 1A. Later the current was raised to 2A to expel the residual phosphoric acid. After the sample was placed in the mass spectrometer (Finnigan MAT 262), the ionization filament current was slowly raised to 2.3A, and the evaporation filament current was increased to 0.6 - 0.7A. The $^6Li/^7Li$ ratios were measured directly on Li^+ using a peak-jumping mode while maintaining the ionization filament temperature at 1300-1350°C. Ten blocks of ten ratios were measured for each sample. Isotopic compositions are expressed as δ^6Li relative to a NBS standard L-SVEC (Flesch et al., 1973):

$$\delta^6Li = [(^6Li/^7Li)_{sample}/(^6Li/^7Li)_{standard} - 1] \times 1000. \quad (1)$$

$(^6Li/^7Li)_{standard}$ was measured to be 0.082738 ± 0.0043 (1σ) by the same method (You and Chan, 1996). The in-run precision ($2\sigma_m$) is about 0.2‰. The reproducibility of this method is ±1.3‰ (1σ), as determined by replicate

analyses of seawater with separate chemical preparation (You and Chan, 1996).

2.2.4 Partition coefficient

The apparent partition coefficient K, in the units of (mole/g)/(mole/g), can be calculated:

$$K = [Li]_{adsorbed}/[Li]_{solution} \quad (2)$$

$[Li]_{adsorbed}$ re$K = [Li]_{adsorbed}/[Li]_{solution}$ration of the adsorbed lithium on clay minerals, and $[Li]_{solution}$ stands for the residual lithium concentration in the solution. $[Li]_{adsorbed}$ was determined using the difference of initial and final lithium concentration in the solutions, the weight of clay mineral and the weight of solution.

2.2.5 Calculation of isotopic fractionation factor

The isotopic fractionation factor, α, associated with adsorption can be expressed as follows:

$$\alpha = [^6Li/^7Li]_{adsorbed}/[^6Li/^7Li]_{solution} \quad (3)$$

Two models are used to calculate the empirical isotopic fractionation factor. The first model is an equilibrium model, which assumes isotopic equilibrium between adsorbed lithium and the bulk solution. Under this model, the isotopic fractionation factor may be written as

$$\alpha = [1/(\delta^6Li_f + 10^3)] \times [(\delta^6Li_i - F \times \delta^6Li_f)/(1-F) + 10^3] \quad (4)$$

where δ^6Li_i is the initial δ^6Li of the solution and δ^6Li_f is the final δ^6Li of the solution. F is the ratio of the final lithium concentration to the initial

concentration. The second model is a Rayleigh fractionation model, which assumes isotopic equilibrium exists between instantaneously adsorbed lithium and lithium in solution. The Rayleigh fractionation model is expressed by the equation.

$$R/R_o = F^{(\alpha-1)} \quad (5)$$

where R_o is the initial $^6Li/^7Li$ ratio and R is the $^6Li/^7Li$ ratio of the remaining lithium in solution. Equation (6) may be used to solve for α:

$$\alpha = 1 + \ln\{[\delta^6Li_f + 10^3]/[\delta^6Li_i + 10^3]\}/\ln F \quad (6)$$

This model also requires that after lithium is adsorbed onto clay minerals, it is no longer accessible in later reactions. Alternatively, α may be determined by plotting lnR against lnF, the slope of the linear regression line being α-1. This method was applied to determine the isotopic fractionation factor using the time series data from the batch experiments. In the experiment where only the initial and final values of the isotope ratios was measured, namely in the experiment involving the river suspended sediment, α was determined by using equation (6) as well as the equilibrium model (equation (4)).

2.3 Results

2.3.1 Initial isotopic compositions of seawater and river water

The lithium isotopic composition (δ^6Li) of Gulf of Mexico water used in the experiment was measured to be -31.5‰ relative to L-SVEC. This value is in agreement with the mean seawater composition (δ^6Li = -31.4 ± 1‰)

determined by You and Chan (1996). The δ^6Li value of the spiked MRW was determined to be -3.6‰ even though the spiked lithium is from L-SVEC (0‰). The negative δ^6Li value is partially caused by the heavier isotopic composition in MRW (Chan et al., 1992) and partially by the analytical uncertainty (1 – 2‰) in the isotopic measurement using the lithium phosphate method (You and Chan, 1996).

2.3.2 Vermiculite with seawater and river water

The change of the concentration and isotopic composition of lithium in the river water with reaction time is given in Table 2.1 and shown in Figure 2.1. Dissolved lithium decreased from the initial value of 170.8μg/L in the river water leveling off to a value of 22.2μg/L. At the end of the experiment, 87% of lithium in the spiked MRW was adsorbed by vermiculite. With the decrease of the lithium concentration, the isotopic composition of the water also shifted from initial value of -3.6‰ to a final δ^6Li value of -36.9‰. The negative shift in δ^6Li indicates that the lighter isotope (^{6}Li) was preferably adsorbed by vermiculite. The adsorption experiment of vermiculite with GMW showed a similar trend and displayed adsorption of up to 60.7μg/L, 35.8% of lithium in GMW (Table 2.2 and Figure 2.2). The smaller magnitude of lithium adsorption in seawater is probably caused by the higher abundance of major ions in seawater, which competed for exchangeable sites. The δ^6Li value decreased from -31.5‰ to -43.6‰ again indicating preferential uptake of the lighter

Table 2.1 Lithium concentrations and isotopic compositions of the solutions and lithium partition coefficients from the experiment of vermiculite with the spiked Mississippi River water

Time (Hours)	Li Concentration (μg/L)	δ^6Li (‰)	Partition coefficient
0	170.8	-3.6	0
73	123.1	-15.2	7.75
191	99.5	-25.2	14.33
332	84.7	-25.5	20.33
647	63.9	-30.9	33.46
1775	37.8	-38.8	70.37
3215	25.1	-37.7	116.10
3935	22.6		131.15
4295	22.2	-36.9	133.87

Table 2.2 Lithium concentrations and isotopic compositions of the solutions and lithium partition coefficients from the experiment of vermiculite with Gulf of Mexico water

Time (Hours)	Li Concentration (μg/L)	δ^6Li (‰)	Partition coefficient
0	169.5	-31.5	0
2	160.8		1.08
6	161.7		0.96
18	161.8	-32.9	0.95
48	147.7	-36.2	2.95
95	151.4	-34.9	2.39
221	137.7	-39.2	4.61
409	139.4	-42.2	4.32
673	137.0		4.74
1151	127.0	-42.9	6.69
2447	108.3	-43.9	11.30
4967	108.8	-43.6	11.16

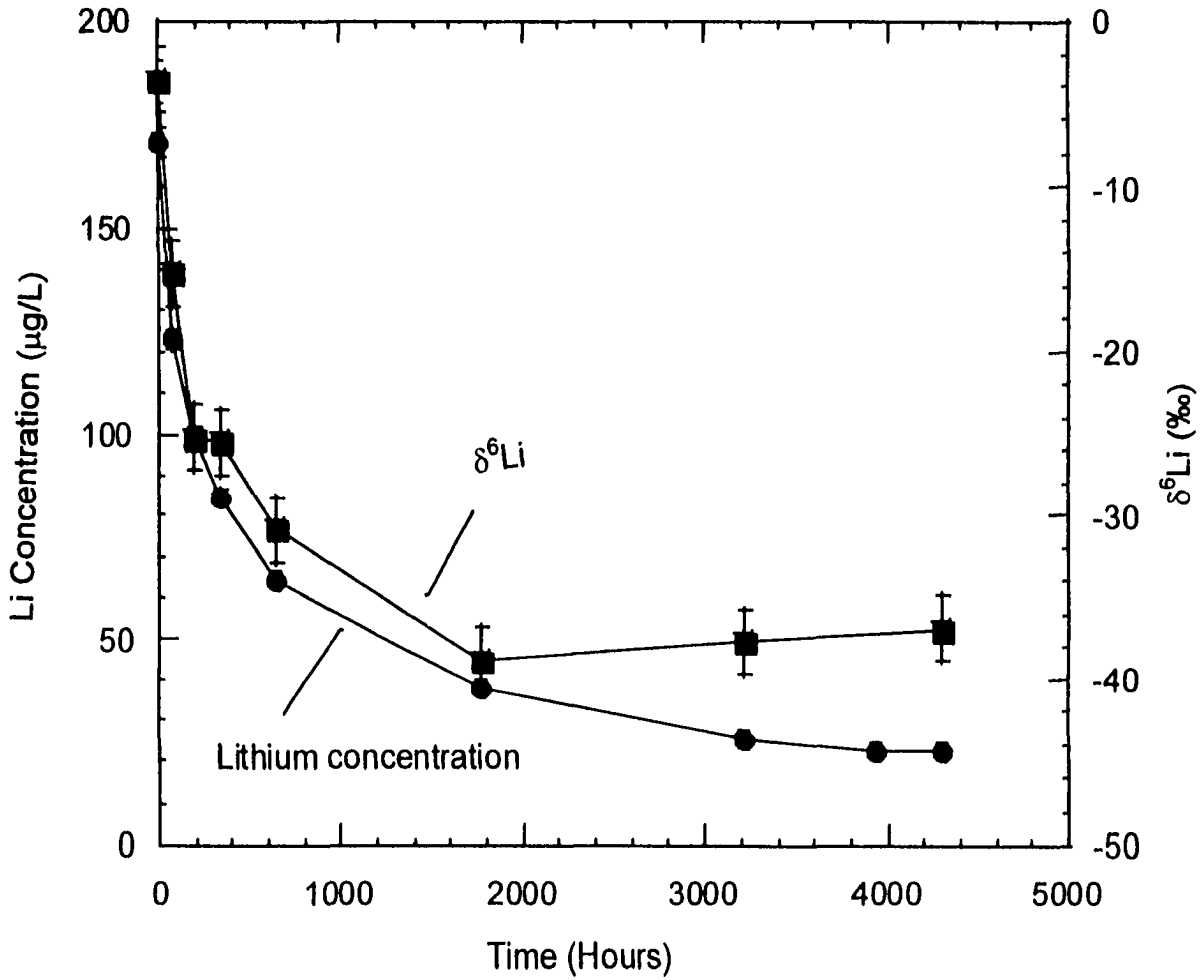

Figure 2.1 Lithium concentration and isotopic composition of the solutions from the experiment of vermiculite with the spiked MRW over time. Error range is indicated by error bar.

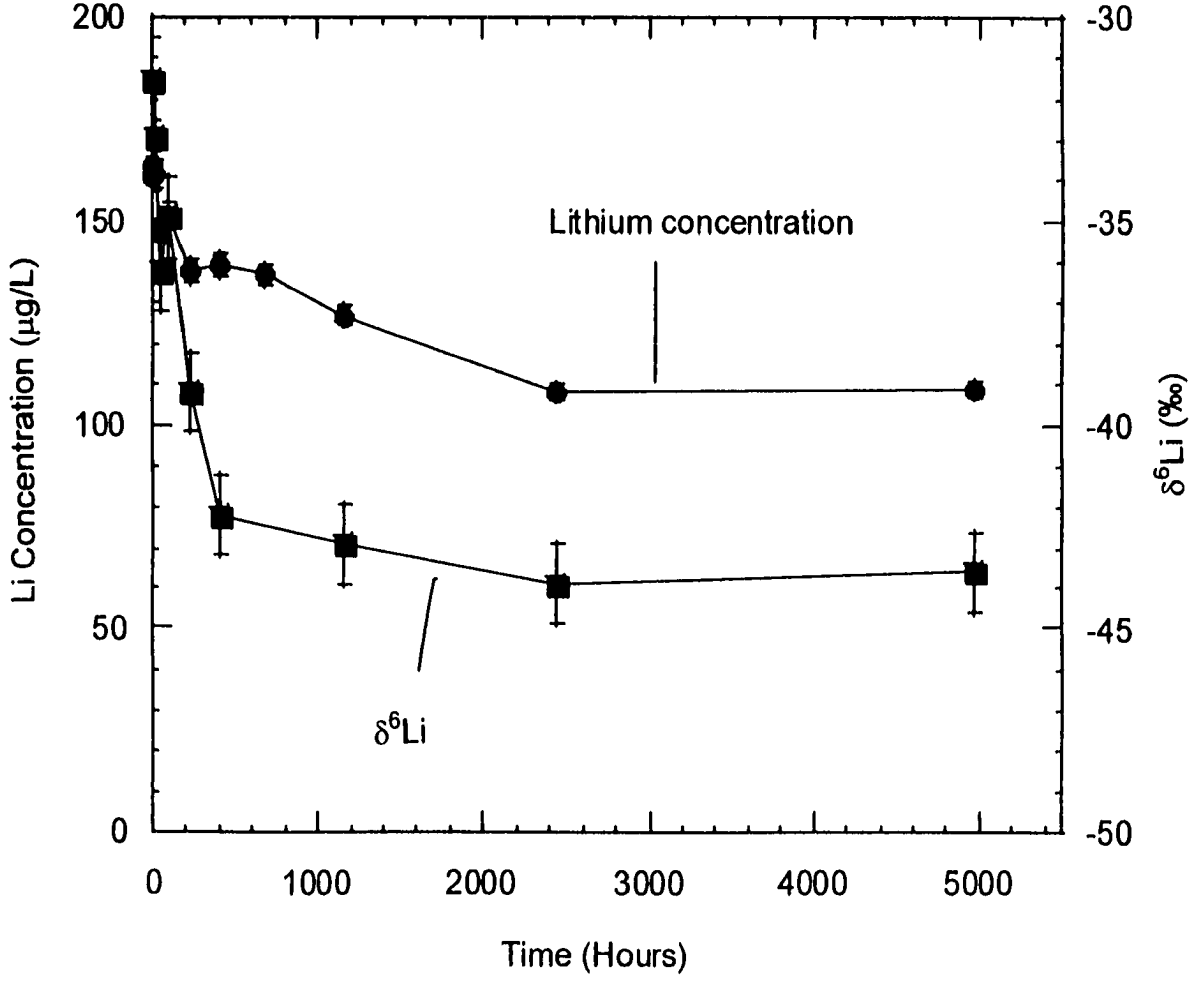

Figure 2.2 Lithium concentration and isotopic composition of the solutions from the experiment of vermiculite with GMW experiment over time. Error range is indicated by error bar.

isotope by the clay mineral. The apparent partition coefficients calculated for the final seawater and river water solutions (presumed to be at equilibrium with the solid phase) are 133.9 and 11.2 respectively.

2.3.3 Kaolinite with seawater and river water

A similar trend was also observed in the experiment of kaolinite with GMW. The concentration dropped rapidly in the first few weeks and thereafter, decreased slowly reaching a minimum concentration of 86.4μg/L (Table 2.3 and Figure 2.3), 49% of lithium in GMW partitioned into kaolinite. The isotopic composition shifted from an initial value of -31.5‰ to a final value of -40.9‰. In the river water experiment, more than 95% of lithium partitioned into kaolinite and the isotopic composition shifted from -3.6‰ to -38.7‰ (Table 2.4 and Figure 2.4). The larger amount of lithium taken up from river water again suggests the effect of ionic strength on lithium adsorption. The time curves of the apparent partition coefficients resemble those on vermiculite but with larger partition coefficients on both the spiked MRW and GMW experiments, 441.6 and 16.3, respectively.

2.3.4 Na-montmorillonite with seawater

In the experiment of Na-montmorillonite with GMW, the lithium concentration remained essentially constant with time (Table 2.5). The δ^6Li value in the final solution was -30‰, approximately 1.5‰ lighter than the initial solution. Given the analytical uncertainty in isotopic measurements (1-2‰), the isotopic composition was essentially unchanged. The data therefore suggests no significant adsorption of lithium by Na-montmorillonite.

Table 2.3 Lithium concentrations and isotopic compositions of the solutions and lithium partition coefficients from the experiment of kaolinite with Gulf of Mexico water

Time (Hours)	Li Concentration (μg/L)	δ^6Li (‰)	Partition coefficient
0	169.5	-31.5	0
72	140.2	-33.8	4.18
168	129.7	-34.2	6.14
360	129.1	-35.7	6.25
672	121.4	-38.5	7.92
1344	118.1	-41.4	8.70
2680	86.4	-45.5	19.24
4900	93.5	-40.9	16.26

Table 2.4 Lithium concentrations and isotopic compositions of the solutions and lithium partition coefficients from the experiment of kaolinite with the spiked Mississippi River water

Time (Hours)	Li Concentration (μg/L)	δ^6Li (‰)	Partition coefficient
0	170.8	-3.6	0
72	112.3	-14.5	10.41
168	105.8	-14.4	12.28
360	95.7	-28.5	15.70
672	78.3		23.62
1344	61.6	-36.4	35.45
2680	12.7	-36.3	248.98
4900	7.4	-38.7	441.62

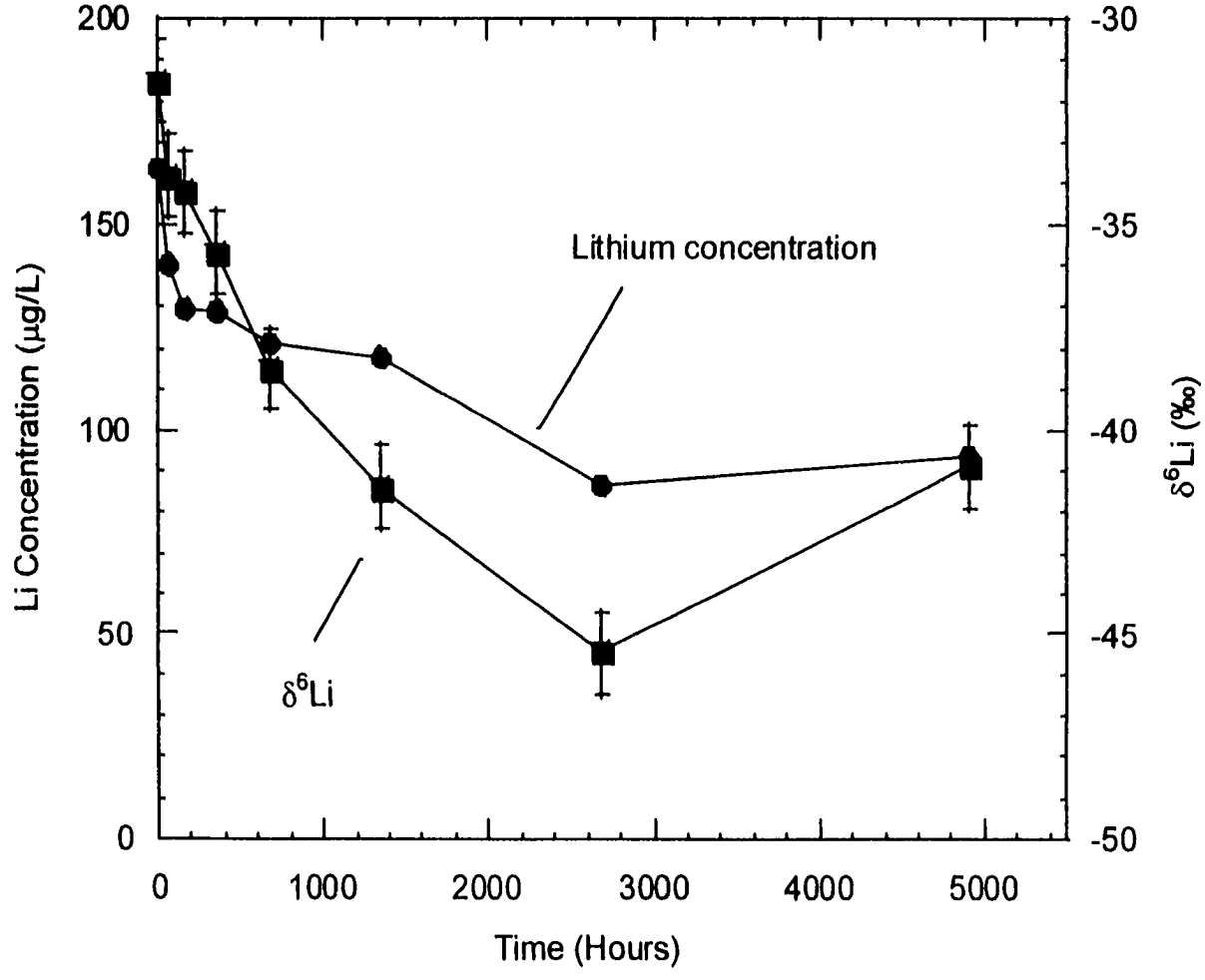

Figure 2.3 Lithium concentration and isotopic composition of the solutions from the experiment of kaolinite with GMW over time. Error range is indicated by error bar.

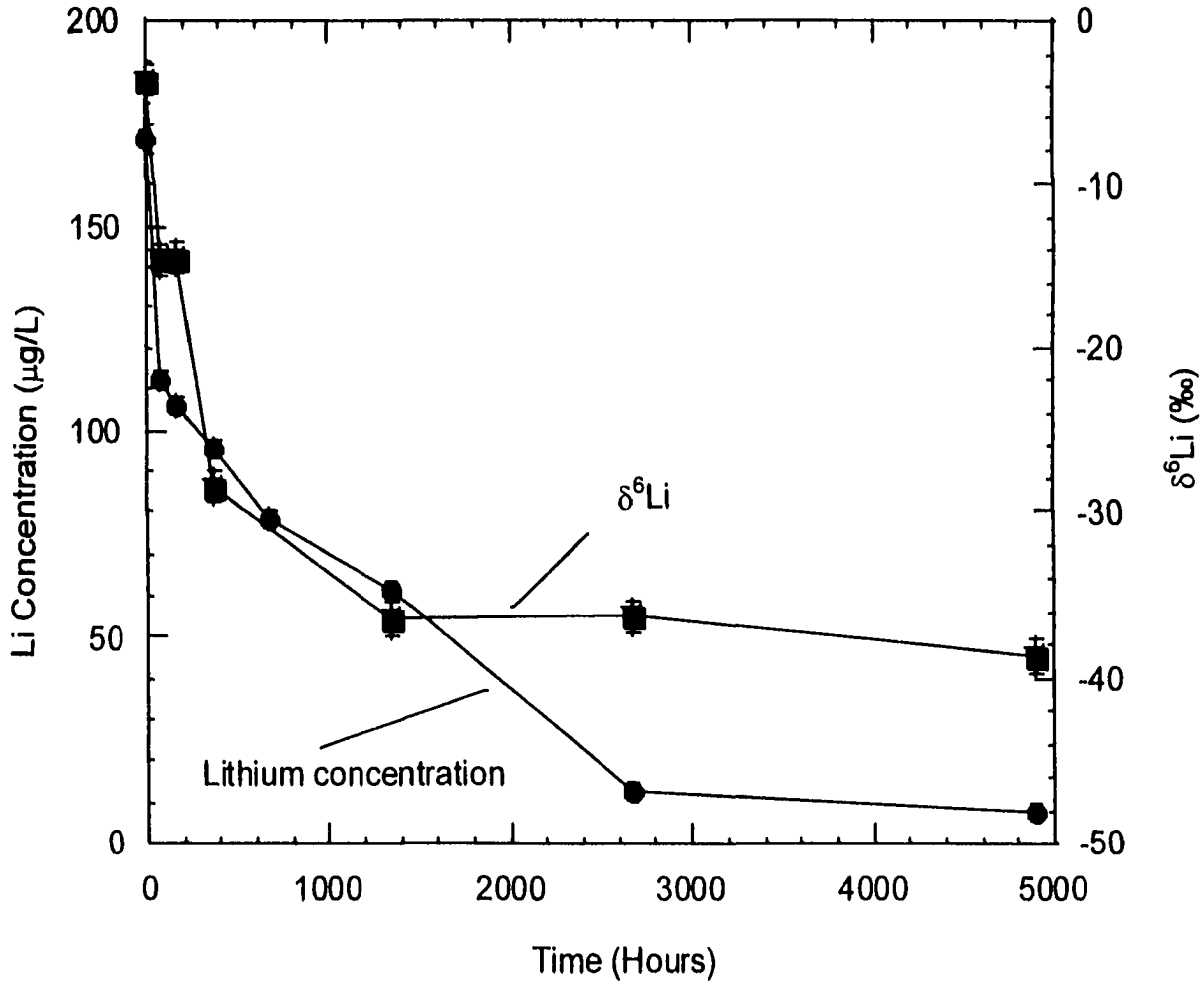

Figure 2.4 Lithium concentration and isotopic composition of the solutions from the experiment of kaolinite with the spiked MRW. Error range is indicated by error bar.

2.3.5 Mississippi River suspended sediment with seawater

After 4800 hours (200 days), the sediment took up 23% of the dissolved lithium. δ^6Li decreased from -31.5‰ to -36.7‰, consistent with the direction of isotopic shift observed for individual clay minerals. The calculated partition coefficient between river suspended material and seawater is 10.6 (Table 2.5), close to the value for lithium adsorption on vermiculite (11.2) but lower than kaolinite in a seawater medium (16.3). This may in part be due to the fact that river suspended sediment contains material with lower ion exchange capacity such as quartz.

2.3.6 Isotopic fractionation (α)

The values of the isotopic fractionation factor for the clay minerals and river suspended material are presented in Table 2.6. For the Mississippi River suspended sediment, the concentration and isotopic composition of lithium in the solution were determined initially and at the end of the reaction after 4800 hours. The isotopic fractionation between the sediment and seawater was calculated using both the equilibrium model (eq. 4) and the Rayleigh fractionation model (eq. 6). The errors in α were estimated based on the analytical uncertainty in concentration (±0.5% or ±2%) and δ^6Li (±1.3‰) as discussed in the methods section. The calculated values of α are 1.024 ± 0.008 and 1.0021 ± 0.007 for the equilibrium model and Rayleigh fractionation model respectively. The two values agree within error.

Table 2.5 Lithium concentrations and isotopic compositions of the solutions and lithium partition coefficients from the experiments of Na-montmorillonite and Mississippi River suspended sediment with Gulf of Mexico water

Time (Hours)	Li Concentration (μg/L)	δ^6Li (‰)	Partition coefficient
Na-montmorillonite			
0	169.5	-31.5	—
95	169.5		—
191	164.6		—
863	169.0		—
2900	165.0		—
4800	169.5	-30.0	—
Mississippi River suspended sediment			
0	169.5	-31.5	0
4800	130.5	-36.7	10.6

For experiments involving individual minerals, concentration (C) and isotopic ratio R were acquired at successive reaction times. It was therefore possible to employ the Rayleigh fractionation model and determine α from the slope of the "best" straight line that fit the data points. The data fitting was carried out by least squares fitting following the procedure developed by York (1966, 1969). Analytical errors result in an uncertainty in the estimate of the slope, hence in the magnitude of the isotopic fractionation. In this study, the calculation of the slope takes into account the errors both in the x-coordinates (natural log of isotopic ratios) and y-coordinates (natural log of concentration ratios). The derivations of errors in the coordinates are as follows:

$$\Delta \ln(C/C_o) = \Delta(C/C_o)/(C/C_o)$$

$$= (C/C_o)\,[(\Delta C/C_o)^2 + (\Delta C_o/C_o)^2]^{1/2}/(C/C_o)$$

$$= [(\Delta C/C_o)^2 + \Delta C_o/C_o)^2]^{1/2} \quad (7)$$

$\ln(R/R_o)$ may be written as $\ln[1 + (R/R_o - 1)]$ which in turn can be approximated as $R/R_o - 1$ since $R/R_o - 1$ is small. Then,

$$\Delta\ln(R/R_o) = \Delta(R/R_o - 1)$$

$$= (R/R_o)\,[(\Delta R/R_o)^2 + (\Delta R_o/R_o)^2]^{1/2}/(R/R_o)$$

$$= [(\Delta R/R_o)^2 + \Delta R_o/R_o)^2]^{1/2} \quad (8)$$

The relative 1σ error in C (i.e., $\Delta C/C_o$) is 2%, that in C_o (i.e., $\Delta C_o/C_o$) is 0.5 %. $\Delta R/R_o$ and $\Delta R_o/R_o$ are both 1.3‰ (1σ), as discussed in the methods section. The isotopic fractionation factor α and errors therein determined in this way are given in Table 2.6. Also presented is the GFE (goodness of fit estimator) as defined by York (1969). The goodness of fit is evaluated using chi-square (χ^2) distribution with n-2 degrees of freedom (Devor et al., 1992). The GFE parameter that represents a "good" fit is a function of the number of measurement (n). For the results to be within the 95% probability limit, the GFE values must be smaller than or equal to 2.0, 2.1 and 2.6 for n = 9, 8, and 5 respectively for the four sets of linear regression performed. By this criterion, the data fitting for the kaolinite and vermiculite in the seawater experiments are acceptable. The fitting for vermiculite in river water is marginal, and that for kaolinite is unacceptable (Table 2.6).

Table 2.6. Empirical fractionation factors for kaolinite, vermiculite, and Mississippi River suspended sediment using equilibrium and Rayleigh fractionation models. The fractionation factor with ^ is calculated using Rayleigh fractionation model and time-series data (n). The fractionation factor with # is determined using the fractionation model with initial and final solutions only and with * is using equilibrium model with initial and final solutions only. F stands for the ratio of lithium content in the final solution to that in the initial solution. GFE stands for goodness of fitting estimator that is used to determine the validity of the fractionation factor.

	δ^6Li(i) (‰)	δ^6Li(f) (‰)	Fractionation factor
Kaolinite			
GMW experiment (n = 8, GFE = 1.18)	-31.5	-40.9	1.021±0.004^
MRW experiment (n = 5, GFE = 6.17)	-3.6	-36.4	1.035±0.004^ (not valid due to large GFE)
Vermiculite			
GMW experiment (n = 9, GFE = 1.25)	-31.5	-43.9	1.030±0.005^
MRW experiment (n = 5, GFE = 2.75)	-3.6	-30.9	1.029±0.004^
Suspended Mississippi River sediment			
F = 0.770	-31.5	-36.7	1.024±0.008* 1.021±0.007#
F = 0.770	-31.5	-36.6	1.024±0.008* 1.021±0.007#

The regression lines for vermiculite in seawater and kaolinite in seawater yield, respectively, isotopic fractionation factors of 1.030 ± 0.005, and 1.021 ± 0.004 (Figures 2.5 and 2.6). These values agree at the 95% confidence level. Thus any mineralogical difference cannot be discerned with present analytical precision. The α values of kaolinite and vermiculite are also analytically indistinguishable from the mean value (1.022 ± 0.004) determined for Mississippi River suspended sediment in seawater (Table 2.6). The data for these minerals in river water however show complications (Figures 2.7 and 2.8). There is a reduction of slope when $\ln C/C_o < -1$, indicating little change in isotopic ratio when C becomes extremely small. For river waters, α was determined from data where $\ln C/C_o > -1$. The fitness parameter for kaolinite in river water is extremely large (6.17) and the fractionation factor, 1.035 ± 0.007, cannot be considered reliable. For vermiculite in river water, the slope of the regression line coincides with that for seawater, yielding an α of 1.029 ± 0.004 (Figure 2.9). However, the GFE value of 2.75 (Table 2.6) is just outside of the limit of acceptance, as discussed above.

2.4 Discussion

2.4.1 Lithium adsorption behavior on clay minerals

Adsorption is normally accomplished by ion exchange reactions. Although the exchange reaction is stoichiometric and thereby differs from simple sorption, it is difficult to distinguish one from the other in reality (Grim, 1968). Ion exchange is associated with six predominantly active sites on clay

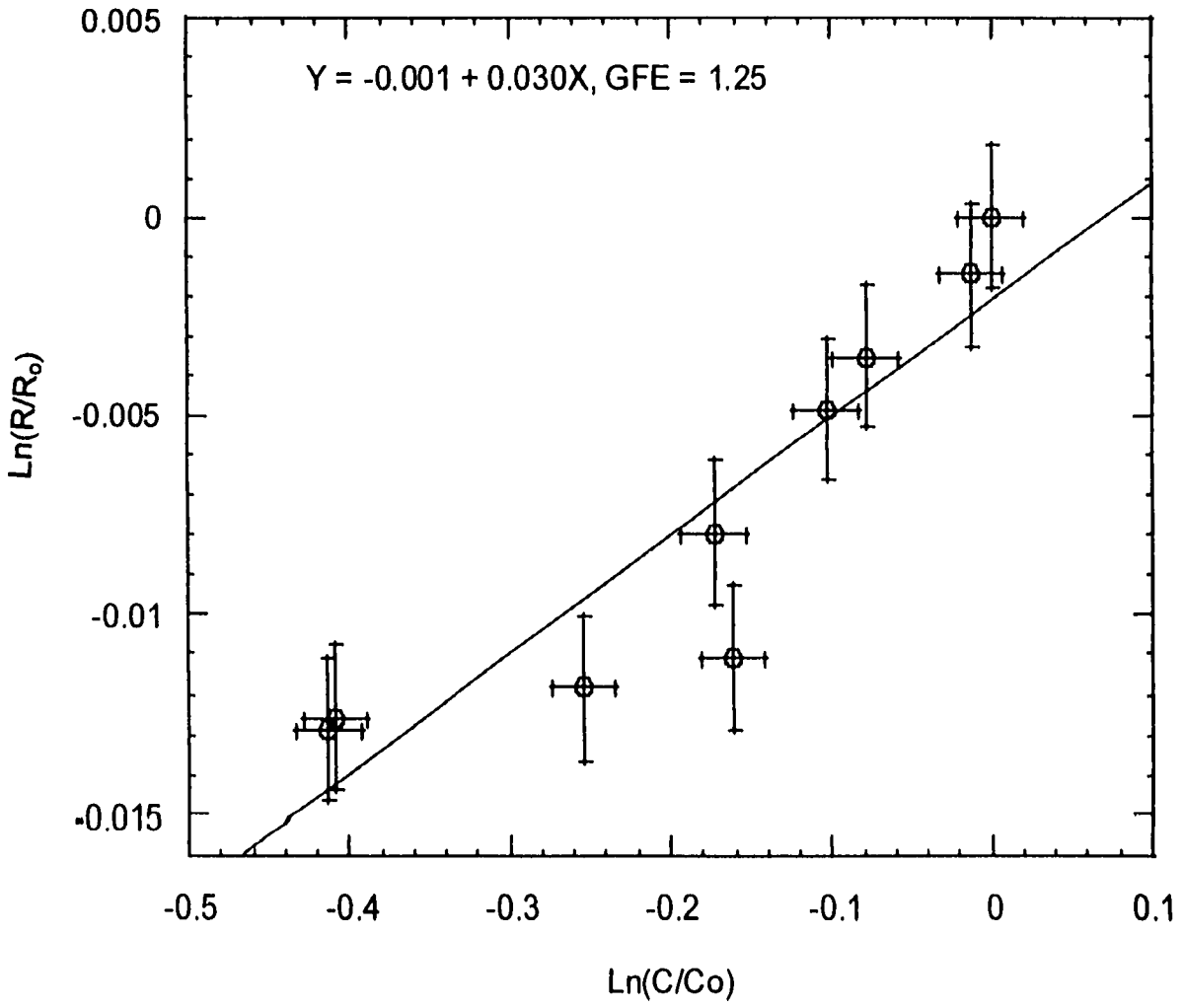

Figure 2.5 Empirical fractionation factor estimated using Raleigh fractionation model with all data from the experiment of vermiculite with GMW.

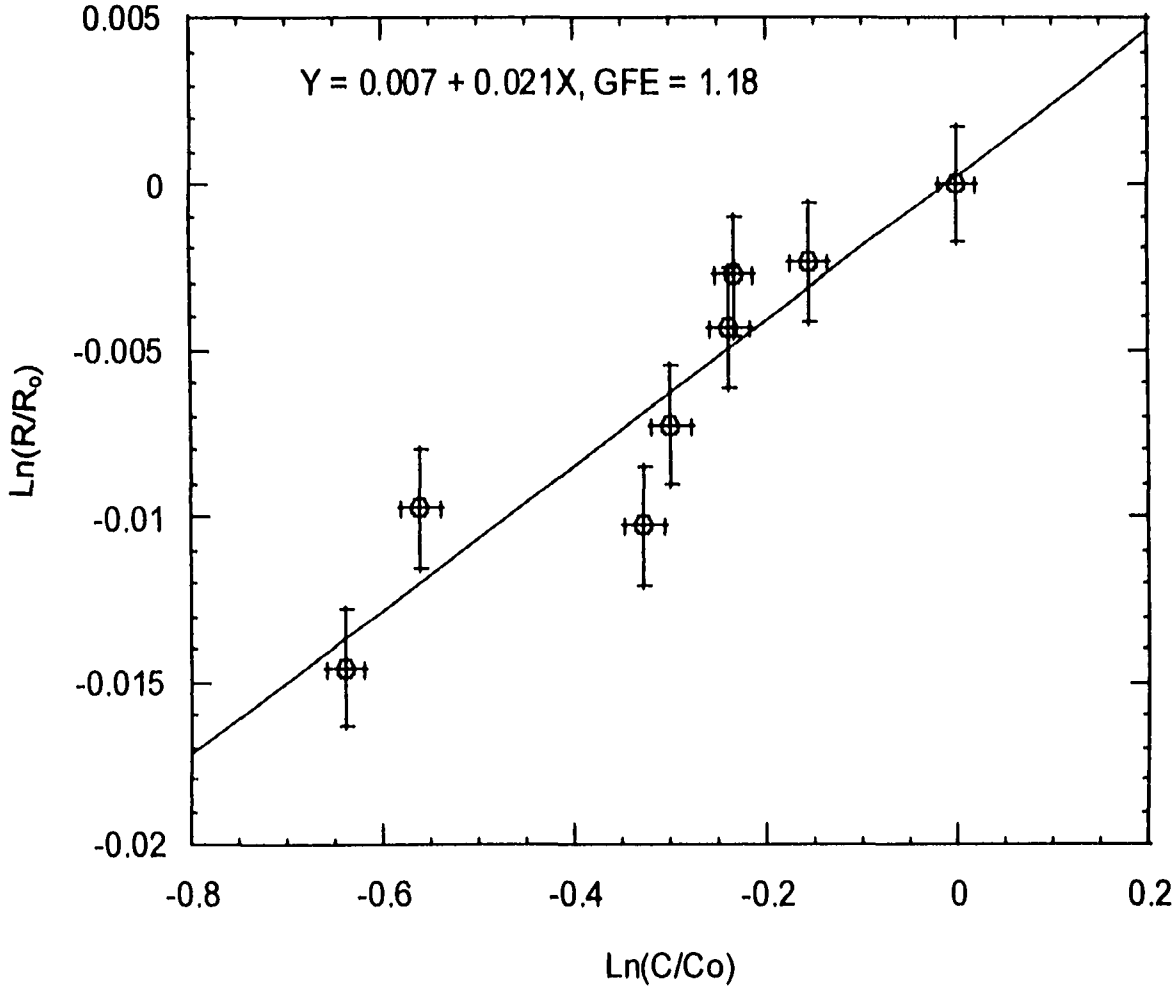

Figure 2.6 Empirical fractionation factor estimated using Raleigh fractionation model with all data from the experiment of kaolinite with GMW

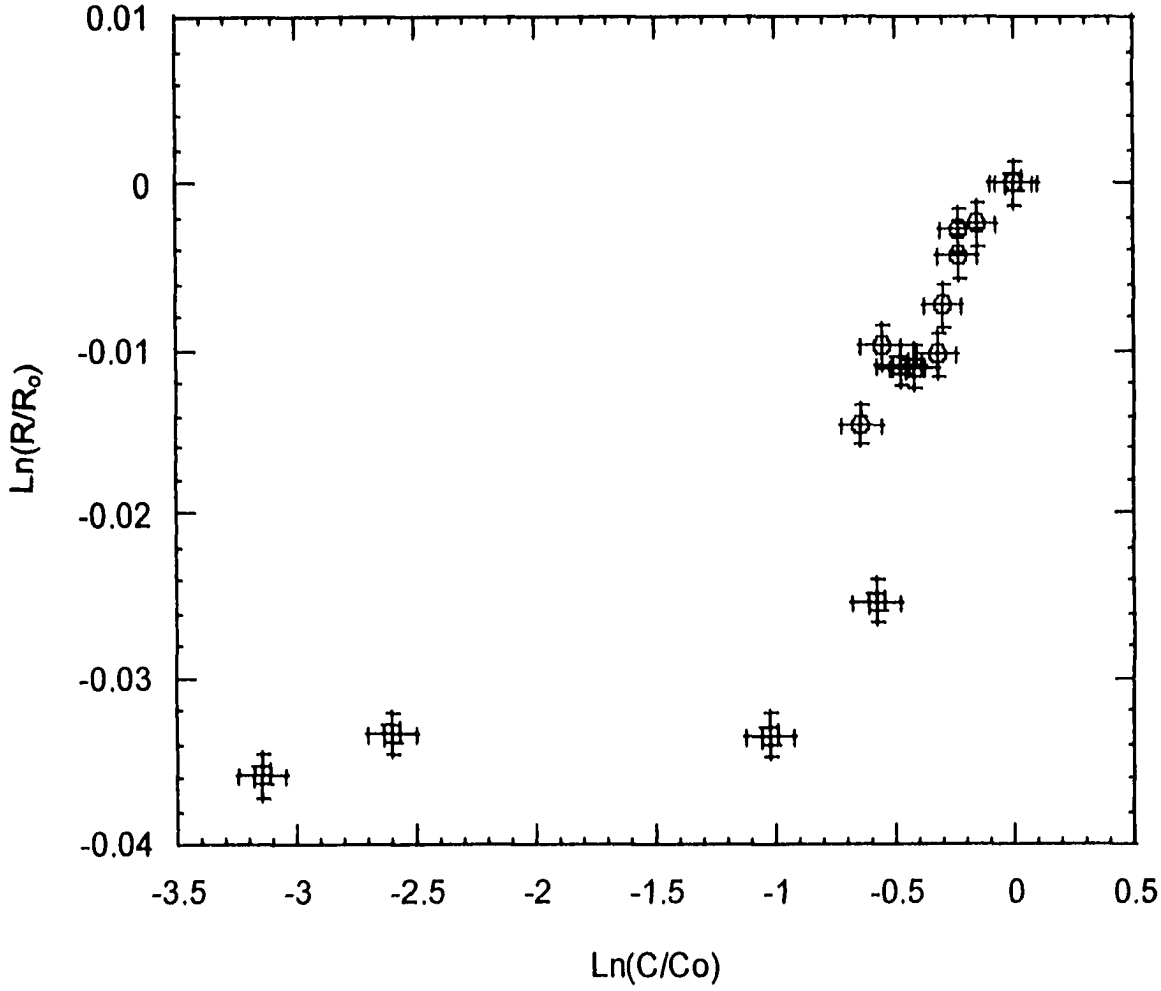

Figure 2.7 Different slopes indicated by all data from the experiments of kaolinite.
Open circle represents GMW experiment and open square for spiked MRW experiments

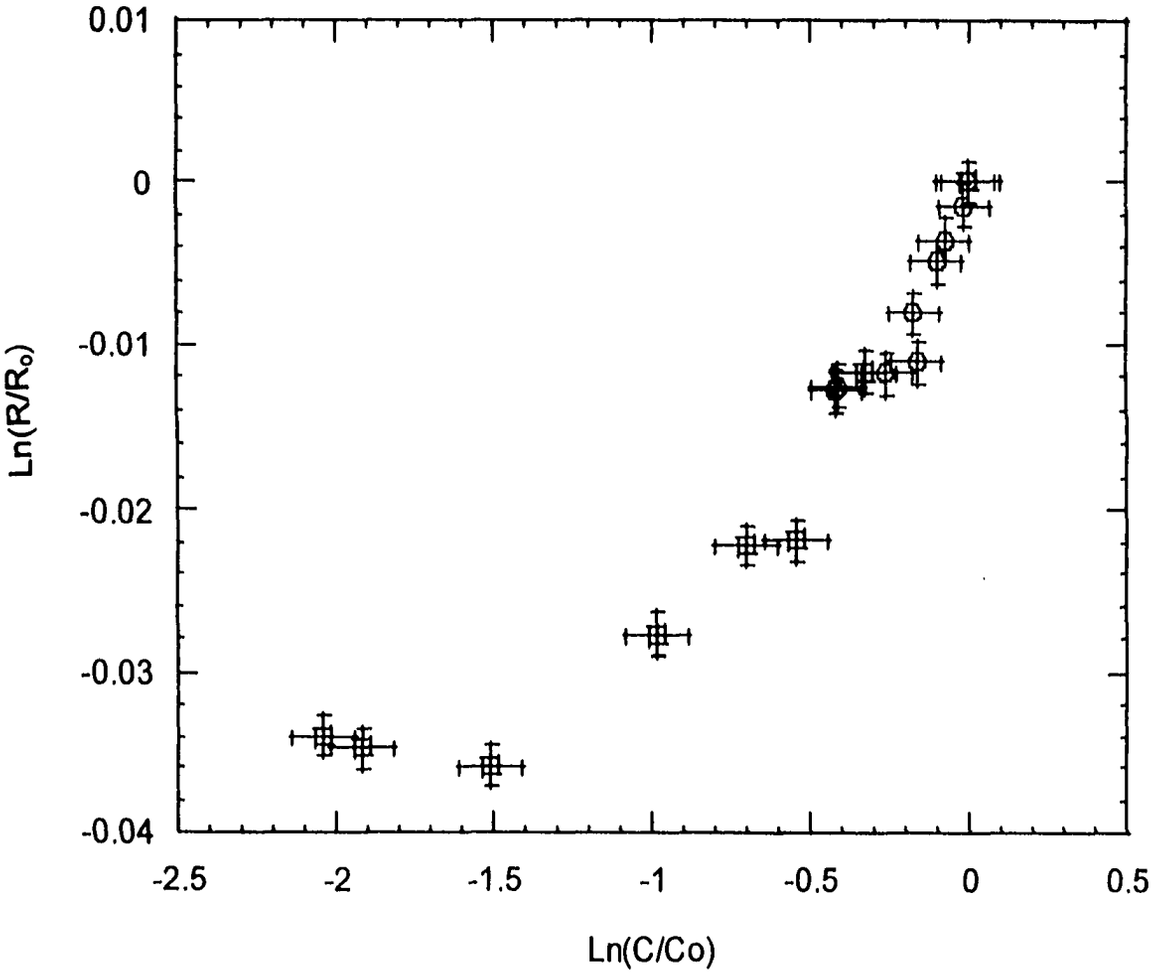

Figure 2.8 Different trends are indicated by the data from the experiments of vermiculite. Open circle stands for GMW experiment and open square for spiked MRW experiments.

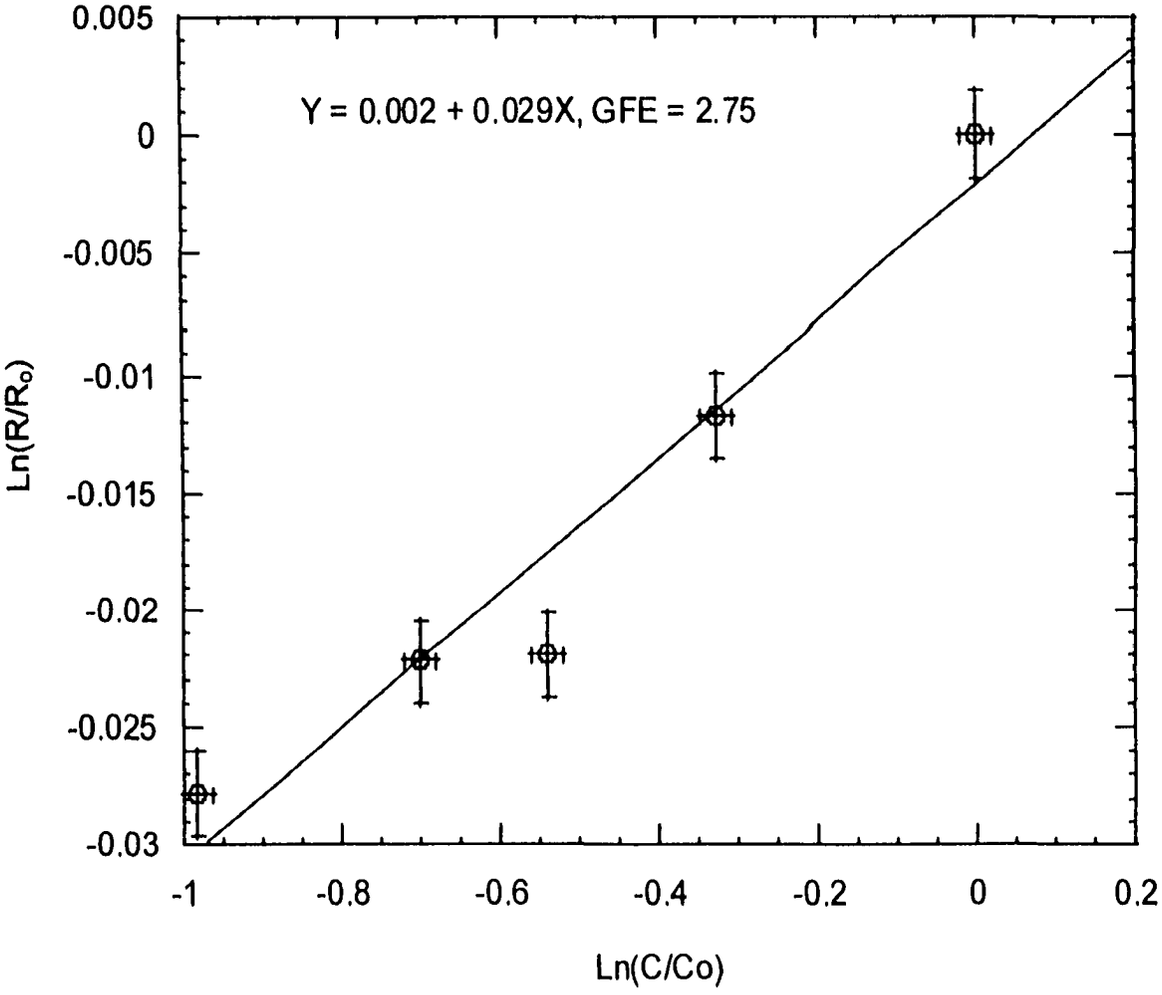

Figure 2.9 Empirical fractionation factor estimated using Raleigh fractionation model with the data from early stage of vermiculite experiment with MRW

minerals, namely neutral siloxane surface, isomorphic substitution sites, metal cations occupying cation exchange sites, water molecules surrounding exchangeable cations, hydrophobic sites, and broken edge sites with exposed surface silanol and aluminol groups (Johnston, 1996). It is also influenced by a variety of factors such as other cations and anions in the solution and clay, particle size, structural distortion, and clogging of exchange positions.

The adsorption of lithium due to cation exchange reactions and the selectivity for lithium can be expressed in the following reaction.

$$Li^+ + Clay\text{-}X \rightarrow X^+ + Clay\text{-}Li \qquad (9)$$

The selectivity coefficient of ideal ion exchange reaction is

$$K_s = \frac{(Clay\text{-}Li)[X^+]}{(Clay\text{-}X)[Li^+]} \qquad (10)$$

where parentheses denote concentrations or mole fractions of ions on the clay surface and brackets denote activities of ions in solutions and on the clay surfaces (Macbride, 1994). Generally cations with the largest ionic radii and the lowest hydration energy are adsorbed most strongly on permanent charge sites of clay minerals. The hydration energy of the alkali ions decreases with increasing atomic weight and size. Therefore the order of selectivity (K_s) is $Li^+ < Na^+ < K^+ < Rb^+ < Cs^+$ (McBride, 1994).

Vermiculite is generally considered to have the highest cation exchange capacity (CEC: 100 –150meq/100g) among the clay minerals (McBride, 1994). Smectite has slightly lower CEC, 70 –120meq/100g. Kaolinite possesses little or no permanent charge and have much lower CEC

values, 1 – 15meq/100g. For vermiculite and montmorillonite, the cation exchange capacity is the result of isomorphic substitution in the 2:1 layer silicate structure (Johnston, 1996). Isomorphic substitution leads to permanent negative charge sites on tetrahedral and octahedral sheets. Kaolinite does not have isomorphic substitution and consequently there are no charges on the structure. The broken edge sites with exposed surface silanol group on kaolinite is the most likely edge sites to adsorb cations. The adsorption at the broken edge sites is a function of pH. At appropriate pH (<7 or even lower), these sites develop a negative charge to retain cations (McBride, 1994).

Lithium adsorption by kaolinite and vermiculite in the experiments are small compared to their CEC values. Only 0.043 and 0.017meq/100g were adsorbed by vermiculite in the spiked MRW and GMW experiments respectively. Slightly higher values (0.047 and 0.022meq/100g) were obtained for kaolinite. Those results show that (1) lithium accounts for a small part of the CEC in the clay samples used; (2) there is no correlation between the amount of lithium adsorbed and the hypothetical CEC of the minerals; and (3) the magnitude of adsorption is greater in river water than in seawater. Accordingly, partition coefficients determined from MRW experiments are 10 times larger than those from GMW experiments. These observations may be understood in the following ways: a) Lithium is a trace element (26μM) in seawater and its percentage of CEC has to be very low compared to other

major ions in GMW. b) Lithium is at the bottom of the selectivity sequence: $Cs^+ > Rb^+ > K^+ > Na^+ > Li^+ > H^+$ (Heier and Billings, 1970; McBride, 1994).

Lithium contents in the spiked MRW and GMW are comparable, but the ionic strength of seawater is 0.7 and that of river water is less than 0.01 (Berner, 1971). There is therefore relative lack of cation competition in the river water medium. In addition, lithium to major cation ratios in the spiked MRW are one to two orders of magnitude larger in river water than in seawater, based on the chemical composition of Mississippi River water at St. Francisville in May, 1996 (Garrison et al., 1996). According to the ion exchange equation (9), a greater magnitude of lithium uptake in the spiked MRW experiment is expected.

The present results may be compared to previous experimental studies (Egli, 1979; Anderson et al., 1989). In Egli's experiment, 1g/L of disordered kaolinite (from Boom, Belgium) was mixed with artificial seawater containing approximately 300μg Li/L. No significant change of lithium concentration in the solution was observed after a period of 178 days, comparable to the reaction time of this study. The difference in our observations for the seawater-kaolinite system may be attributed to water/rock ratios in the two experiments (1000:1 in Egli's experiment and 20:1 in ours). The apparent partition coefficient from our kaolinite-seawater experiment is determined to be 16.3. Given the concentration of 300μg Li/L and water/rock ratio of 1000:1 in Egli's experiment, the apparent partition coefficient of 16 would only allow 1.6% of lithium to be removed from the solution, which is

close to the analytical uncertainty. In contrast, Anderson et al (1989) carried out a similar experiment mixing clay minerals (Wyoming bentonite, Georgia kaolinite, and Texas vermiculite) from 0.1g to 0.5g with 10ml of 0.25mmol lithium solution in the presence of magnesium for 5 days. Rapid removal of lithium from the solutions was observed. Experiments with soils (Anderson et al., 1989) showed that the extent of lithium adsorption is larger in the absence of other electrolytes, consistent with our observations.

We now consider the mechanisms of lithium retention in the minerals. Because vermiculite has the highest structural charge, lithium is probably adsorbed on permanent octahedral and tetrahedral charge sites. The contribution of edge sites to the overall ion exchange depends on size of clay mineral (Johnston, 1996). Because vermiculite is coarse-grained, its edge sites would be relatively insignificant as exchange sites.

Although the structural charge of montmorillonite is smaller than vermiculite (McBride, 1994), lithium is still expected to be adsorbed on isomorphic substitution sites. The absence of lithium uptake by Wyoming Na-montmorillonite may be explained as follows. The selectivity coefficient K_s of the reaction

$$Li^+ + \text{montmorillonite-Na} \rightarrow Na^+ + \text{montmorillonite-Li} \qquad (11)$$

is 0.71 and is constant with the ion composition on the clay (McBride, 1994). Because lithium has the lowest hydration energy and thus the largest hydrated ionic radii, it is not possible for Li^+ to replace Na^+ on montmorillonite as discussed previously.

In kaolinite, the silanol group is the most likely edge site to adsorb cations (McBride, 1994). The adsorption of lithium on dissociated silanol ion may be expressed as

$$Si-OH \rightarrow Si-O^- + H^+ \quad (12)$$

$$Si-O^- + Li\,(H_2O)_y^{n+} \rightarrow Si-O^- - Li\,(H_2O)_y^{n+} \quad (13)$$

In summary, cation exchange in vermiculite and montmorillonite is dominated by a high degree of isomorphic substitution. On the other hand, kaolinite does not have structural charge, and exchange on kaolinite is mainly due to broken bonds on the edges. The CEC reflect these mineralogical effects. It is therefore expected that vermiculite and montmorillonite would retain more lithium by adsorption than kaolinite. Contrary to this predicted trend, comparable amounts of lithium was removed by kaolinite to vermiculite from identical solutions (river and Gulf water) and with the same water/sediment ratio (Table 2.1 to 2.4). This implies other processes than adsorption may also be involved in the uptake of lithium.

Our experiments on kaolinite and vermiculite indicate that much longer periods of time (~200 days) are required to attain a steady state than for ion exchange reaction that are essentially completed within hours. This supports the notion that a more complex process is responsible for lithium uptake in kaolinite and vermiculite experiments. Anderson et al (1989) observed that 60% of the lithium adsorbed by kaolinite and vermiculite could not be displaced by NH_4Cl. They suggest that vacant octahedral positions at the mineral edge may be responsible for the fixation. Jaynes and Bogham (1987)

observed a reduction of layer charge when Li-saturated montomorillonite was heated at 250°C. This result supports that lithium migrated into octahedral sites during mild heat treatment as originally suggested by Hofmann and Klemen (1950). Migration of this type with dehydration of adsorbed lithium could occur over a longer time frame at temperature used in our experiment.

This study supports the speculation that after initial adsorption at edge sites and interlayer sites, lithium is further dehydrated, migrates into vacant octahedral sites and becomes fixed. Such fixation of lithium, if confirmed, has important geochemical implications because ion exchange is an important mode of lithium exchange in the sediment-water system (Zhang et al., 1998; Chan and Kastner, 2000).

2.4.2 Implication on oceanic lithium budget

As discussed in the introduction section, processes for lithium mass balance in the oceans have not been completely identified. Using the partition coefficients determined in our experiments, it is possible to estimate the amount of lithium adsorbed by suspended sediments in the oceans. The estimation will establish the role of adsorption by clay minerals in removing lithium from the oceans. Based on the GMW experiments, lithium partition coefficients for clay minerals vary, kaolinite and vermiculite having values of 16.3 and 11.2 respectively. The Mississippi River suspended sediment contains mostly illite and mixed layered illite/smectite (Kennedy, 1965), and has a partition coefficient of 10.6 in seawater. In our estimation we assume that the Mississippi River suspended sediment is representative of river-

transported material to the ocean. Given a suspended load of 150 x 10^{14}g/yr for the world's rivers (Milliman and Meade, 1983) and uptake of 1.9ppm based on MRSS partition coefficient and 26μM for lithium concentration in seawater, the total lithium removed from the oceans by suspended sediments would be about 4.1 x 10^{9}moles/yr. This constitutes about 20% of the total input from continental runoff and submarine hydrothermal source (Huh et al., 1998). Thus, adsorption onto clays is a significant process for the removal of lithium from the oceans.

2.4.3 Empirical fractionation factors

Using time series data from the experiments with GMW and Rayleigh fractionation model, we determine the fractionation factors of 1.021 ± 0.004 and 1.030 ± 0.005 for kaolinite and vermiculite with extremely low GFE (goodness of fit estimator) values (1.18 and 1.25) respectively (Figures 2.5 and 2.6).

In the experiment of MRSS with GMW, there are only initial and final solutions available. The empirical fractionation factors are estimated as 1.021 ± 0.007 and 1.024 ± 0.008 respectively using Rayleigh fractionation and equilibrium models. In order to reduce the uncertainty in isotopic measurement, a duplicate run was carried out and almost identical empirical fractionation factors were acquired (Table 2.6). These values agree with the empirical fractionation factors of vermiculite and kaolinite within the limits of uncertainty. The constancy of the data suggests that the fractionation factors associated with adsorption from seawater for kaolinite, vermiculite, and the

Mississippi River suspended sediment are similar despite the complexity in the partition process of lithium into clay minerals. The weighted average of the four values is 1.024 ± 0.003. This value is comparable to the value of 1.022 determined by Taylor and Urey (1938) for ion exchange with zeolite. It is greater than the fractionation (1.019) during incorporation of lithium in alteration clay (smectite) during low temperature alteration of submarine basalt (Chan et al., 1992)

Considering the fact that the fractionation factors from GMW experiments are consistent for different models and different data sets, the fractionation factors from the spiked MRW experiments are difficult to explain. The plots of lnR vs. lnF for kaolinite and vermiculite show a change of slope at about lnF = -1 (Figures 2.7 and 2.8). Evidently, the fractionation factors of kaolinite and vermiculite at later stages of the spiked MRW experiments are not in agreement with those from GMW experiments. The data from the early stage of the adsorption experiments seem to be consistent with GMW experiment. Although the linear regression for vermiculite is marginally acceptable, the fractionation factor (1.029) is almost identical to the one (1.030) determined from the GMW experiment. The similar values from two different experiments suggest that the fractionation factors are similar for adsorption from seawater and river water.

After two thirds of the lithium was removed from the river water, however, lithium concentration decreases without much change in δ^6Li in the solution, suggesting very small isotopic fractionation associated with the late

stage adsorption process (Figures 2.7 and 2.8). This is analogous to lithium scavenged on to hydrogenous Mn crust, the isotopic composition of which is similar to seawater (Chan et al., 1994b).

The isotopic fractionation of the lithium isotopes depends on the difference in the binding of the two isotopic ions with water and with the clays. The isotopic fractionation during lithium exchange with zeolite has been determined to be an equilibrium process rather than one due to differences in the rate of diffusion or reaction (Taylor and Urey, 1938). The change of isotopic fractionation in the course of the river experiment may be caused by the change of the dominant sorption sites. As the usual interlayer and edge sites, and perhaps structural sites are becoming filled in the case of extreme uptake from the river water medium, the residual lithium may be held loosely at the mineral surface, surrounded by water, and hence with negligible isotopic fractionation. This explanation is highly speculative, but it is generally accepted that a given cation can be held by a clay mineral with different bonding energies, and the bonding energy depends on the position of the adsorbed ion on the mineral surface and electronic charge (McBride, 1994). We propose that the change of isotopic fractionation factor at the end of experiment is a manifestation of the occupation of a sorption position in an extremely weak field when the charge is greatly reduced or neutralized.

2.5 Summary and conclusion

Several conclusions can be drawn from the results of the adsorption experiments:

(1) In the experimental systems, lithium is taken up by kaolinite and vermiculite but not Na-montmorillonite in seawater and river media. The extent of uptake is not correlated to the cation exchange capacity of the minerals. Lithium is also adsorbed on river suspended material from seawater.

(2) Greater magnitude of adsorption is observed from river water than seawater demonstrating the effect of competition of major ions for sorption sites. The uptake of lithium by kaolinite and vermiculite is a more complex process than simple cation exchange reaction, possibly involving both cation exchangeable sites such as interlayer region, edge sites and non-exchangeable sites such as collapsed interlayer and structural sites.

(3) The lighter isotope, ^{6}Li, is favored in the adsorption process. The isotopic fractionation factors for adsorption on kaolinite, vermiculite and Mississippi River suspended sediment are similar within the limits of uncertainty, and the mean value was determined to be 1.024 ± 0.003.

(4) After extensive uptake, the isotopic fractionation becomes negligible. It is speculated that the residual lithium is held loosely on the mineral surface with similar bonding energies for the two isotopes as those in hydrated ions in the external reservoir.

(5) Based on the empirical partition coefficient, the flux of dissolved lithium in the oceans to river-transported sediments is about 4.1×10^{9} moles/yr, approximately 20% of the total input to the ocean.

2.6 References

ANDERSON A. M., BERTSCH M. P., AND MILLER P. W. (1989) Exchange and apparent fixation of lithium in selected soils and clay minerals. Soil Sci. 148, No. 1, 46-52.

BERNER R. A. (1971) Principles of Chemical Sedimentology. McGraw-Hill, New York.

CHAN L. H. AND EDMOND J. M. (1988) Variation of lithium isotope composition in the marine environment: A preliminary report. Geochim. Cosmochim. Acta 52, 1711-1717.

CHAN L. H., EDMOND J. M., THOMPSON G., AND GILLS K. (1992) Lithium isotopic composition of submarine basalts: Implications for the lithium cycle in the oceans. Earth Planet. Sci. Lett. 108, 151-160.

CHAN L. H., EDMOND J. M., AND THOMPSON G. (1993) A lithium isotope study of hot springs and metabasalts from mid-ocean ridge hydrothermal systems, J. Geophys. Res. 98, 9653-9659.

CHAN L. H., GIESKES J. M., YOU C. F., AND EDMOND J. M. (1994a) Lithium isotope geochemistry of sediments and hydrothermal fluids of the Guaymas Basin, Gulf of California, Geochim. Cosmochim. Acta 58, No. 20, 4443-4454.

CHAN L. H. AND KASTNER M. (2000) Lithium isotope compositions of pore fluids and sediments in the Costa Rica subduction zone: implications for fluid processes and sediment contribution to the arc volcanoes. Earth Planet. Sci. Lett. 183, 275-290.

CHAN L. H., ZHANG L., AND HEIN J. R. (1994b) Lithium isotope characteristics of marine sediments. EOS 75, No. 44, 314.

DAVEY B. G. AND WHEELER R. C. (1980) Some aspects of the chemistry of lithium in soils. Plant Soil 57, 49-60.

DEVOR R. E., CHANG T. H., AND SUTHERLAND J. W. (1992) Statistical quality design and control, contemporary concepts and methods. Prentice Hall, NJ.

EGLI P. (1979) Cycling behavior of dissolved lithium in the Oceans. Ph. D. Thesis, Northwestern University, Illinois, 175p.

FLESCH G. D., ANDERSON A. R. JR., AND SVEC H. J. (1973) A secondary isotopic standard for Li determinations. Intl. J. Mass Spectrom. Ion Phys. 12, 265-272.

GARRISON C. R., LOVELACE W. M. AND MONTGOMERY P. A. (1996) Water Resource Data Louisiana, Water Year 1996. U. S. Geological Survey, Water Data Report LA 96-1.

GRIM E. RALPH (1968) Clay Mineralogy, McGraw-Hill Book Company.

HEIER K. S. AND BILLINGS G. K. (1970) Lithium. In Handbook of Geochemistry (ed. K. H. Wedepohl), Vol. II – 1, p. 3-H-1. Springer – Verlag.

HOFMANN (U.) AND KLEMEN (R.) (1950) Verlust der Austauschfahigkeit vun Lithiumionen an Bentonit durch Erhitzung. Zeits. Anorg. Chem., Vol. 262, pp. 95 – 99.

HUH Y., CHAN L. H., ZHANG L., AND EDMOND J. M. (1998) Lithium and its isotopes in major world rivers: implications for weathering and the oceanic budget. Geochim. Cosmochim. Acta 62, 2039-2051.

JAYNES W. F. AND BIGHAM J. M. (1987) Charge reduction, octahedral charge, and lithium retention in heated, Li-saturated smectites. Clays and Clay Minerals 35, No. 6, 440-448.

JOHNSTON C. T. (1996) Sorption of organic compounds on clay minerals: A surface functional group approach. The CMS Workshop Lectures Vol. 8, Organic Pollutants in the Environment, Sahwney B., ed. The Clay Minerals Society, Boulder, CO.

Kennedy U. C. (1965) Mineralogy and cation-exchange capacity of sediments from selected streams, U. S. Geol. Surv. Prof. Paper 433-D, pp 28.

LOMBARDI O. W. (1963) Observations on the distribution of chemical elements in the terrestrial saline deposits of Saline Valley, California, U. S. Naval Ordinance Test Station NOTS TP 2916.

MCBRIDE M. B. (1994) Environmental chemistry of soils, Oxford Press.

MILLIMAN J. D. AND MEADE R. H. (1983) World-side delivery of river sediments to the oceans. J. of Geol. 91, 1-21.

RONOV A. B., MIGIDSOV A. A., VOSKERSENSKAYA N. T., AND KORZINA G. A. (1970) Geochemistry of lithium in the sedimentary cycle. Geochm. Int. 7: 75 –102.

SEYFRIED W. E. JR., JANECKY D. R., AND MOTTL M. J. (1984) Alteration of the oceanic crust: Implications for geochemical cycles of lithium and boron. Geochim. Cosmochim. Acta 48, 557 – 569.

TAYLOR S. R. AND UREY H. C. (1938) Fractionation of the Li and K isotopes by chemical exchange with zeolites. J. Chem. Phys. 6, 429 – 438.

YORK D. (1966) Least-square fitting of a straight line. Can. J. Phys., 44, 1079 – 1086.

YORK D. (1969) Least-square fitting of a straight line with correlated errors. Earth Planet. Sci. Lett. 5, 320 –324.

YOU C. F., CHAN L. H., SPIVACK A. J., AND GIESKES J. M. (1995) Lithium, boron, and their isotopes in sediments and pore waters of Ocean Drilling Program Site 808, Namkai Trough: Implications for fluid expulsion in accretionary prisms. Geology, 23, No. 1, 37 – 40.

YOU C. F. AND CHAN L. H. (1996) Precise determination of lithium isotopic composition in low concentration natural samples. Geochim. Cosmochim. Acta 60, 909 – 915.

ZHANG L., CHAN L. H., AND GIESKES J. M. (1998) Lithium isotope geochemistry of pore waters from Ocean Drilling Program Sites 918 and 919, Irminger Basin, Geochim. Cosmochim. Acta 62, 2437 – 2450.

CHAPTER 3
LITHIUM ISOTOPIC COMPOSITIONS OF MARINE SEDIMENTS AT ODP SITES 918 AND 919, IRMINGER BASIN

3.1 Introduction

Lithium takes an active part in sediment diagenesis and is, therefore, highly mobile in the sediment-interstitial water system. Lithium isotopic compositions of pore fluids provide insight on sediment-water exchange and fluid processes. You et al. (1995) first investigated the sediments and fluids at the Nankai Trough where a lithium isotopic anomaly in the décollement zone indicates expulsion of fluids generated deep in the accretionary prism. At ODP Sites 918 and 919 (Zhang et al., 1998), the vertical isotopic profiles of pore waters reflect intense sediment-water reactions, including alteration of volcanic matter, ion exchange, and release of lithium under elevated temperatures. The isotopic systematics at Escanaba Trough largely reflects interactions between hydrothermal fluids and sediments (James et al., 1999). The study of the Costa Rica subduction zone (Chan and Kastner, 2000) follows the paths of the subducted sediments, providing a view of the diagenetic reactions, fluid processes, and an estimate of the sedimentary flux at this convergent margin. Because of sample size constraints, the first lithium isotope study of pore fluids (You et al., 1995) required pooling pore water samples from adjacent depths which strongly hampered depth resolution. Following development of a technique of high analytical sensitivity (You and Chan, 1996), it has become possible to measure small samples such as pore fluids. To date, lithium isotope studies of pore fluids and

associated sediments are still relatively few. This chapter, as a companion of the pore water study (Zhang et al., 1998), focuses on the isotopic systematics of lithium on the sediments from Leg 152 of the Ocean Drilling Program (ODP), offshore of Greenland.

ODP Leg 152 extends from the continental shelf to the rise of the southeast Greenland coast (Figure 3.1). The objectives of the expedition were to investigate the structure and evolution of the volcanically rifted margin, and the oceanographic and climatic history of the North Atlantic (Larsen et al., 1994). Sites 918 and 919 are located on the continental rise and are characterized by exceptionally high sediment accumulation rates. At Site 918, a 1200m thick sediment section ranging from the Eocene to the Quaternary was recovered. The sediments are derived from both volcanic and continental sources. They therefore provide an excellent setting for determining the lithium isotopic compositions of volcaniclastic and siliciclastic sediments, as well as a high-resolution record of sediment-water exchanges. In a previous study, detailed measurements of $^{87}Sr/^{86}Sr$ and $\delta^{6}Li$ in pore water samples were carried out at these two sites (Zhang et al., 1998). This companion study analyzes lithium concentration and isotopic composition of marine sediments at the depths corresponding to the pore water lithium study.

The objectives of the sediment study at Sites 918 and 919 are twofold. They complement the pore fluid study to gain further understanding of the sources and sinks of lithium in the pore fluid, thereby providing better constraints on the sediment-water exchange. The investigation is also

intended to relate lithium isotope characteristics of the sediments to lithology and source materials, including terrigenous, volcaniclastic and glacial components. The results will add to the global lithium isotope database of marine sediments and aid the understanding of the controls of lithium isotope composition in marine sediments.

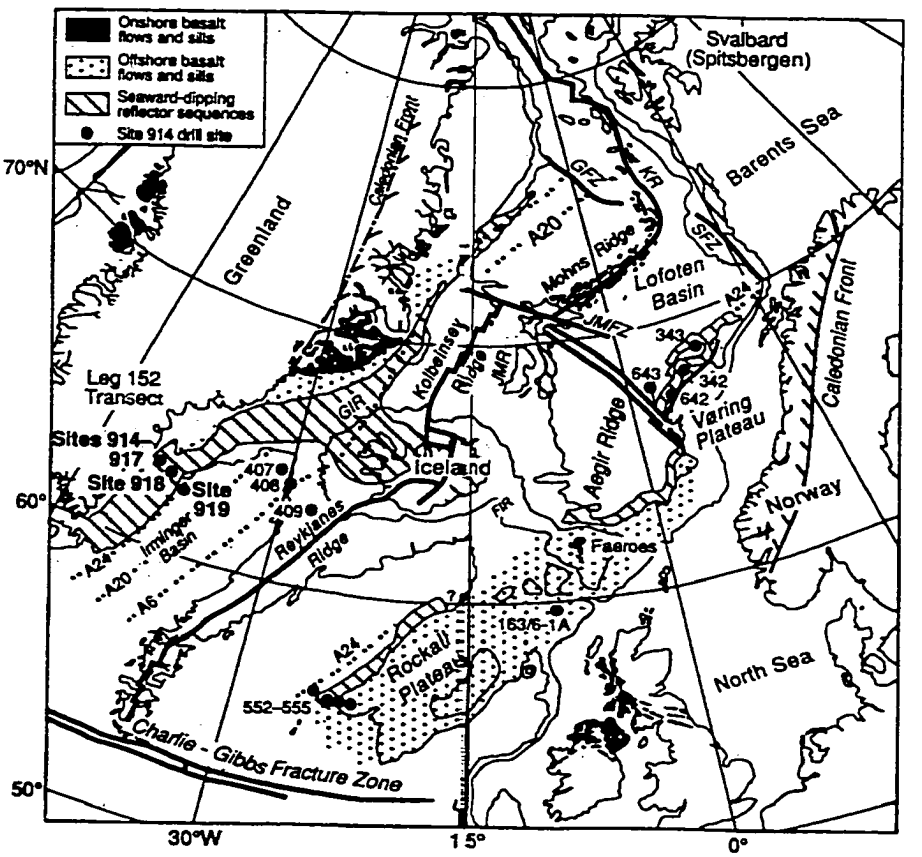

Figure 3.1 Location map of ODP Sites 918 and 919 (from Larsen et al., 1994).

3.2 Lithology and sample description

Samples were retrieved from ODP Sites 918 and 919, Leg 152, located on the upper continental rise of southeast Greenland within the western part of Irminger Basin (Figure 3.1). The volcanic basement at Site 918 is covered with approximate 1200m of sediments (Larsen et al., 1994). The sedimentary section at Site 918 can be divided into five lithologic units (Figure 3.2). Unit I (Holocene – late Miocene) is comprised of volcanogenic and nonvolcanic components and forms the top 600m of the section. It is divided into five sub-units (IA, IB, IC, ID, IE). Sub-unit IA (0 – 71.1mbsf) comprises graded turbidite beds of fine sand to silt. The dominant minerals of the sand are quartz and feldspars with amphibole and garnet as minor components. Dropstones and smaller IRD (Ice Rafted Debris) are scattered throughout the sub-unit. Dropstones are coarse detritus brought in to the basin by ice sheets. They are predominantly basalt, gneiss, granite, and sediments, with minor components of gabbro, dolerite, and limestone. Samples A-2H-4 and A-7H-4 are from this sub-unit. Sub-unit IB (71.1 – 236mbsf) is similar to sub-unit IA but contains microfossils. IRD is also present throughout the sub-unit. Samples A-16H-4 and A-26X-4 from this sub-unit are similar to A-2H-4 and A-7H-4 in mineral composition. Sub-unit IC (236 – 317.8mbsf) is characterized by a high concentration of IRD and dropstones. The sediment matrix contains 50-65% quartz and 5-15% feldspar with amphibole, sphene, chlorite, garnet, and pyroxene as accessories. Sample A-31X-1 is from this sub-unit. Sub-unit ID (317.8 – 543.6mbsf) consists of silt with IRD. There is a decrease in

concentration of dropstones within this sub-unit. Sample D-25R-2 contains volcanic, terrigenous, and siliciclastic components. Sub-unit IE (543.6 – 600mbsf) is lithologically identical to ID except for the absence of IRD and dropstones. Sample D-31R-CC is from the sub-unit 1E. A list of analyzed samples is presented in Table 3.1 with their lithologic units and dominant mineral compositions. Based on the lithology of Unit I, it is evident that the cold condition lasted from the late Miocene to the Holocene. Mechanical erosion by ice probably dominated the weathering process.

Unit II (early – late Miocene) is 206.5m (600 – 806.5mbsf) thick and comprises moderate to heavily burrowed nannofossil chalk and silt. Climate was in the transition from the warm condition in early – middle Miocene to the cold condition in middle – late Miocene (Heiden and Holmes, 1998). The silt beds in this section contain a mixed suite of minerals derived from both volcanic and nonvolcanic sources. Two samples (D-40R-1 and D-51R-2) from Unit II were analyzed at depths corresponding to lithium concentration maximum in the pore fluid. Unit III (late Oligocene – early Miocene) consists of nannofossil chalk and turbiditic sands and is interbedded with silt (806.5 – 1108.2mbsf). Sample D-68R-1 was analyzed to understand low pore water lithium concentration in sandy layers. It contains quartz, quartz feldspar, nannofossils, pyrite and volcanic grains. Unit IV (middle Eocene) comprises nannofossil chalk and volcanic silt (1108.2 – 1157.9mbsf) and is in a phase of contact metamorphism. Sample D-91R-1 mainly contains nannofossils and volcaniclastic altered glass, basaltic clasts, and volcanic derived smectite

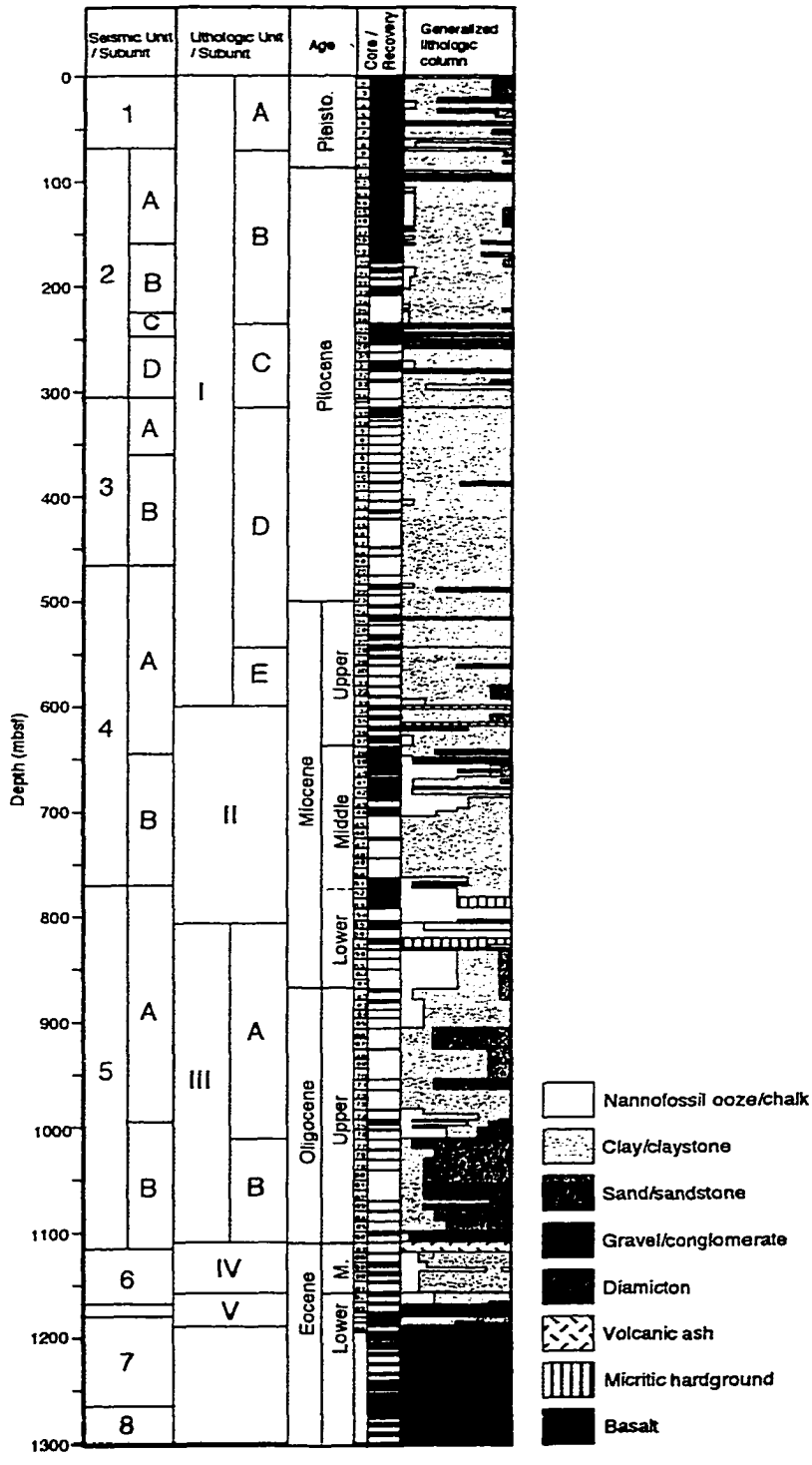

Figure 3.2 Lithological section of Site 918 (from Saito, 1998).

Table 3.1 Lithological Units and dominant mineral compositions of the analyzed sediment samples at Sites 918 and 919.

Site	Core-Section	Interval(cm)	Lithological Unit	Dominant Mineral Composition
918				
	A-2H-4	150-155	IA	Quartz and feldspars with amphbole and garnet with dropstones and IRD (ice rafted debris). Dropstones are Basalt, gneiss, granite with minor components of gabbro, Dolerite, and limestone.
	A-7H-4	145-150	IA	
	A-16H-4	140-150	IB	Similar to A-2H-4 and A-7H-4 but contain microfossils
	A-26H-4	140-150	IB	
	A-31X-1	0-20	IC	High concentration of IRD and dropstones. 50-65% quartz and 5-15% feldspar with amphibole, sphene, chlorite, garnet, and pyroxene as accessories.
	D-25R-2	140-150	ID	Decrease in dropstones. Volcanic, terrigenous, and siliciclastic components.
	D-31R-CC	----------	IE	Similar to ID without IRD and dropstones
	D-40R-1	140-150	II	Nannofossil chalk and tunbiditic sands with silt.
	D-51R-2	140-150	II	
	D-68R-1	91-100	IIIA	Quartz, quartz feldspar, nannofossils, pyrite and volcanic Grain.
	D-91R-1	119-129	IV	Nannofossil and volcaniclastic altered glass, basaltic clasts, And volcanic derived smectite with enrichement in iron oxide

(table 3.1 continued)

(table 3.1 continued)

Site	Core-Section	Interval(cm)	Lithological Unit	Dominant Mineral Composition
919				
	A-1H-4	140-150	I	Predominantly clay and silt. IRD and dropstones are
	A-4H-2	145-150	I	presented. Volcaniclastic and continentally derived silt
	A-7H-3	145-150	I	clays are generally fine-grained than the equivalent
	B-3H-3	145-150	I	sediments at Site 918.
	B-7H-3	145-150	I	

with enrichment in iron oxide. Unit V (early Eocene) consists of glauconitic sandy silt with interbeded calcareous sands (1157.9 – 1189.4mbsf). The sediment sequence is underlain by highly weathered basaltic lava flows (Larsen et al., 1994).

Site 919 is located in 2088.2m of water on the continental rise of Southeast Greenland, within the western part of the Irminger Basin (Figure 3.1). Sediments recovered at Site 919 extend to 134mbsf and belong to the upper Pliocene and Pleistocene sequence. The sediments are composed predominantly of distinct beds of clay and silt, many of which can be identified as deposits from turbidity currents. Other beds have poorly sorted sediments indicating deposition from melting icebergs. Overall, IRD and dropstones are present throughout the whole section of Site 919. The volcaniclastic and continentally derived silt clays are generally finer-grained than the equivalent sediments at Site 918 (Larsen et al., 1994). Quartz is ubiquitous. The volcanic detritus are mostly from Iceland. Erosion of volcanic sequences outcropping in the East Greenland is a source for the lithic volcanogenic material (Larsen et al., 1994). Five samples were analyzed at Site 919 and the whole section of Site 919 is assigned to lithologic unit I (Table 3.1). It is evident that climate condition is extremely cold and mechanical erosion dominates the weathering process.

3.3 Analytic method

Sediment samples consisted of dried squeezed cakes. They were washed with distilled water to remove residual salts from the pore water and

oven-dried. The dissolution procedure was adapted from Crock and Severson (1980). Dissolution was achieved by digestion with HF-$HClO_4$. The salts were converted to perchlorates by treatment with $HClO_4$. Finally H_2O_2 were added to insure complete dissolution of manganese oxide. By this procedure, all solids were dissolved completely. The lithium concentrations were determined by flame emission using the standard addition method. The precision is determined to be 2% (1σ). Isotopic analysis was carried out using Finnigan MAT 262 thermal ionization mass spectrometer. To reduce isotopic fractionation during analysis, lithium borate complexes as $Li_2BO_2^+$ or $LiNaBO_2^+$ were measured. The precision is between 0.5 to 1‰ (1σ). Detailed procedures for chemical preparation and isotope analysis have been given by Chan (1987). Isotopic compositions are expressed as δ^6Li relative to a NBS standard L-SVEC (Flesch et al., 1973):

$$\delta^6Li = [(^6Li/^7Li)_{sample}/(^6Li/^7Li)_{standard} - 1] \times 1000, \quad (1)$$

where $(^6Li/^7Li)_{standard} = 0.083062 \pm 0.000054$.

Pore waters were extracted from 5 to 10 cm long, whole-round sediment samples by using the standard procedure of Mannheim and Sayles (1974). The pore water samples were then filtered through an in-line filtration apparatus. Lithium concentrations were measured by atomic absorption spectrophotometry (Larsen et al., 1994). Lithium isotope data of the pore waters have been reported by Zhang et al. (1998). Lithium isotope measurements of pore waters were carried out following the procedure of You

and Chan (1996). In this technique, isotopic ratios were measured on Li^+ ions, hence providing superior sensitivity suitable for pore water study. Replicate analyses of the seawater (n=6) produced a mean value for δ^6Li of -31.4 ± 1‰ (You and Chan 1996). The precision of the method is estimated to be 1.3‰ (1σ).

Lithium concentrations of the sediments were determined by flame emission with standard additions. The concentrations of major ions were measured on a dual view inductively coupled plasma optical emission spectrometer (Perkin Elmer DV3000).

3.4 Results

Lithium concentration and isotopic composition of pore waters have been presented in a previous paper (Zhang et al. 1998). For a better comparison with the lithium profiles in marine sediments, the pore water profiles are also shown here (Figures 3.3 and 3.4). At Site 918, pore water lithium decreases rapidly to half of the seawater value within the top 20m (Figure 3.3). At greater depths (> 100mbsf) the pore water lithium concentration increases gradually downcore. The lithium concentration profile resembles a diffusion-controlled curve and the concentration reaches a maximum (~163μM) at 765mbsf. In contrast to pore water lithium concentration, lithium concentration of marine sediments increases gradually with depth from 13.6ppm at the surface to a maximum 52.7ppm at 575mbsf (Figure 3.5 and Table 3.2). Then, it decreases slightly to 40.4ppm at 660mbsf and increases to 47.1ppm at 765mbsf. Below, from the turbidite sand layers

to the basal section, lithium concentration decreases to the range of 32ppm, corresponding to the lowering of lithium concentration in the pore water. Overall, the concentration profile of the pore waters roughly resembles that of the sediments.

Lithium isotopic composition of the sediments at Site 918 appears to vary with lithology. In the uppermost turbidite section with abundance of IRD (sub-units IA and IB, 0 – 250mbsf), the δ^6Li values of sediments increase slightly with depth from -9.5‰ to -8.4‰ (Figure 3.6). Below, in sub-units IC and ID the δ^6Li values are slightly heavier: -10.5 and -9.7‰. At 575mbsf in sub-unit IE where IRD are absent and where the strongest volcanic alteration zone is inferred from the early study (Zhang et al., 1998), the marine sediment has the highest lithium concentration of 52.7ppm and the heaviest isotope composition of -11.5‰. In Unit II where volcaniclastic components are abundant, δ^6Li value reaches the extremely light value of -4.9‰ at 660mbsf, corresponding to a dip in lithium concentration. At the depth of maximum lithium concentration in pore water profiles (~765mbsf), the sediment sample has a δ^6Li value of -8.7‰. A similar isotopic value (-8.4‰) is observed in the sandy layer below (Unit IIIA). At the interface of the sediment and basement, the sediment sample has an isotopic composition of -3.2‰ similar to MORB (Mid-Ocean Ridge Basalt) value (Chan et al., 1988).

At Site 919, lithium concentrations generally correlate with grain size. The sediments above 80mbsf contain a larger proportion of clays than the

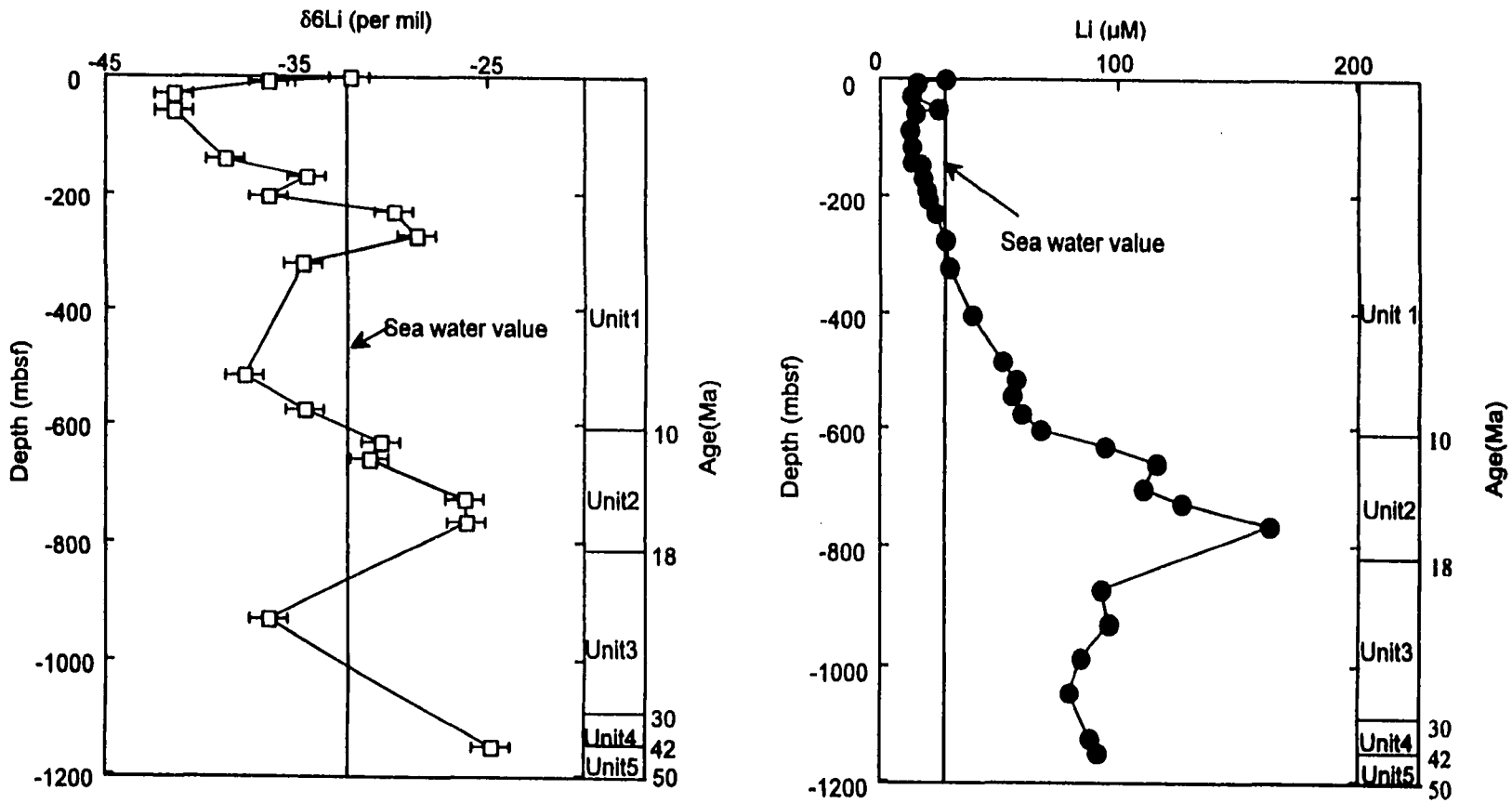

Figure 3.3 Lithium concentration and isotopic composition of pore waters at Site 918.

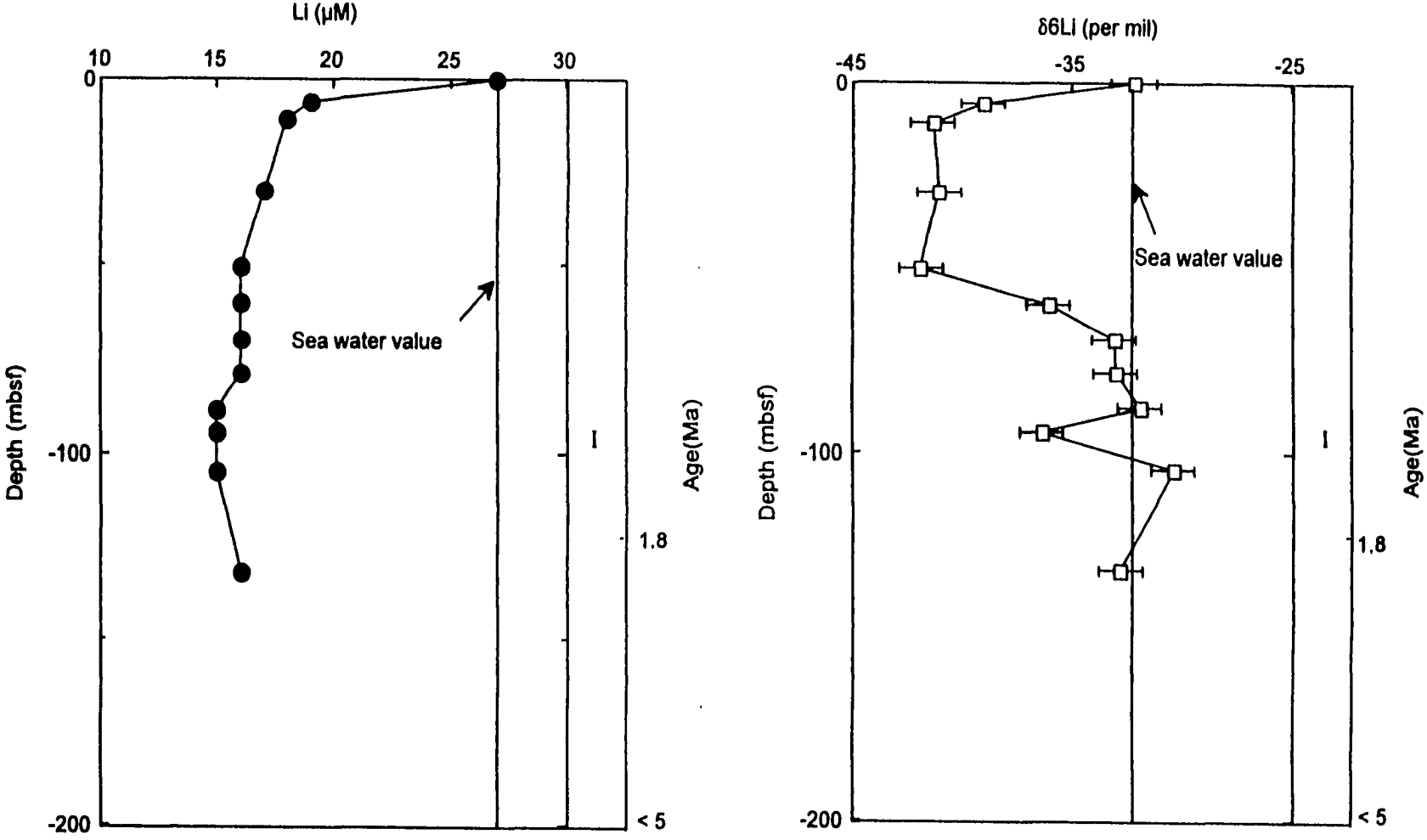

Figure 3.4 Lithium concentration and isotopic composition of pore waters at Site 919.

Table 3.2 Lithium concentrations and isotope compositions of the analyzed sediment samples at Sites 918 and 919

Site	Core-Section	Interval(cm)	Depth(mbsf)	Li(ppm)	δ^6Li ± 2σ_m (‰)	Lithological Unit
918						
	A-2H-4	150-155	7.8	13.6	-9.5 ± 0.6	IA
	A-7H-4	145-150	55.3	16.5	-9.3 ± 0.8	IA
	A-16H-4	140-150	139	17.5	-8.9 ± 0.8	IB
	A-26H-4	140-150	232	19.1	-8.4 ± 0.7	IB
	A-31X-1	0-20	276	24.3	-10.5 ± 0.6	IC
	D-25R-2	140-150	515	32.8	-9.7 ± 0.8	ID
	D-31R-CC	----------	575	52.7	-11.7 ± 0.7	IE
	D-40R-1	140-150	660	40.4	-4.9 ± 0.5	II
	D-51R-2	140-150	765	47.1	-8.7 ± 0.7	II
	D-68R-1	91-100	930	32.9	-8.4 ± 0.6	IIIA
	D-91R-1	119-129	1157	32.1	-3.2 ± 0.8	IV
919						
	A-1H-4	140-150	6	29	-8.2 ± 0.7	I
	A-4H-2	145-150	30	33	-7.3 ± 0.8	I
	A-7H-3	145-150	60	53.2	-8.8 ± 0.8	I
	B-3H-3	145-150	94.5	27.9	-10.6 ± 0.6	I
	B-7H-3	145-150	133	31.4	-12.4 ± 0.8	I

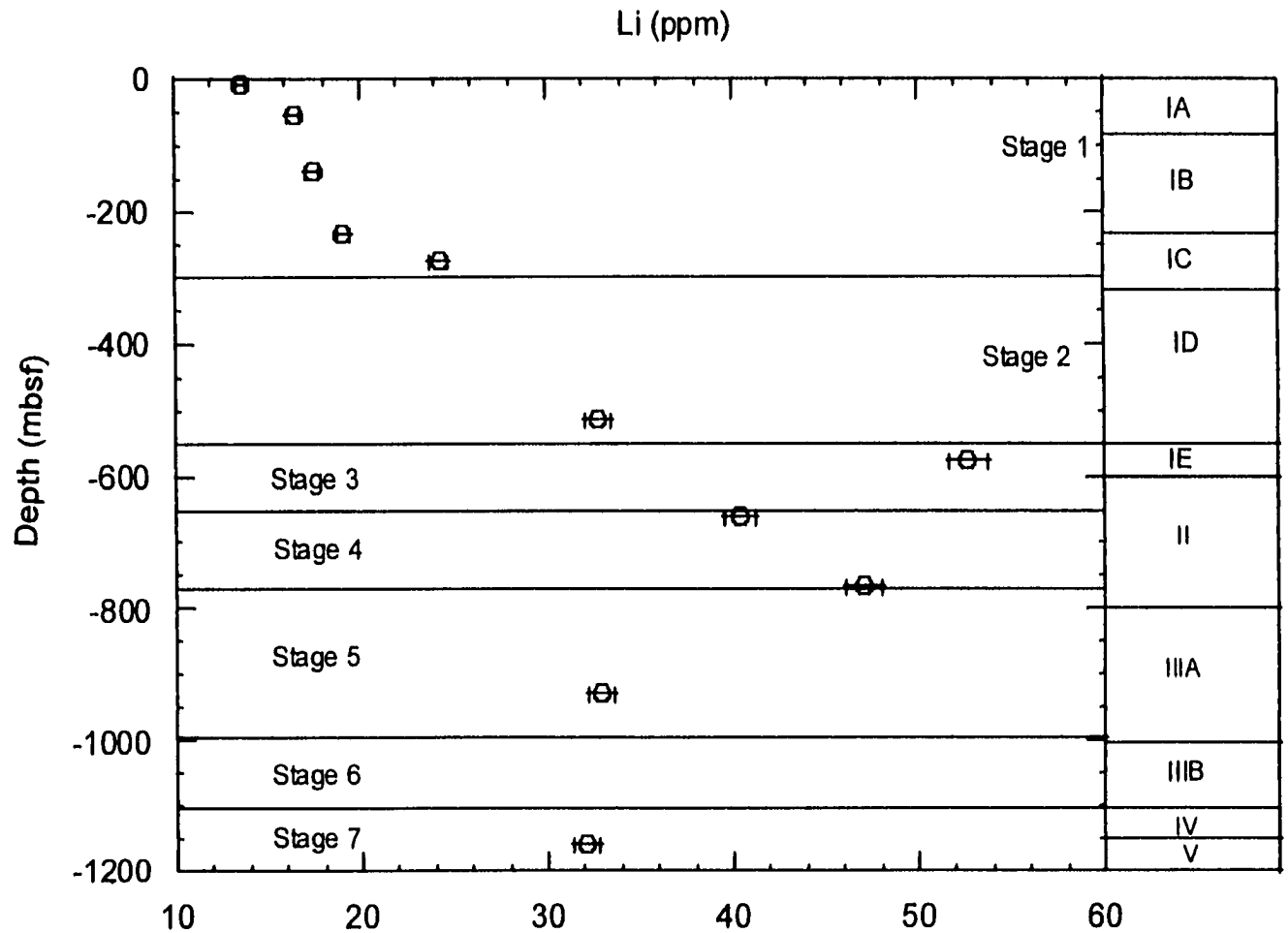

Figure 3.5 Lithium concentration of bulk marine sediments at Site 918 shown with lithologic units (Larsen et al., 1994) and geochemical stages (Saito, 1998).

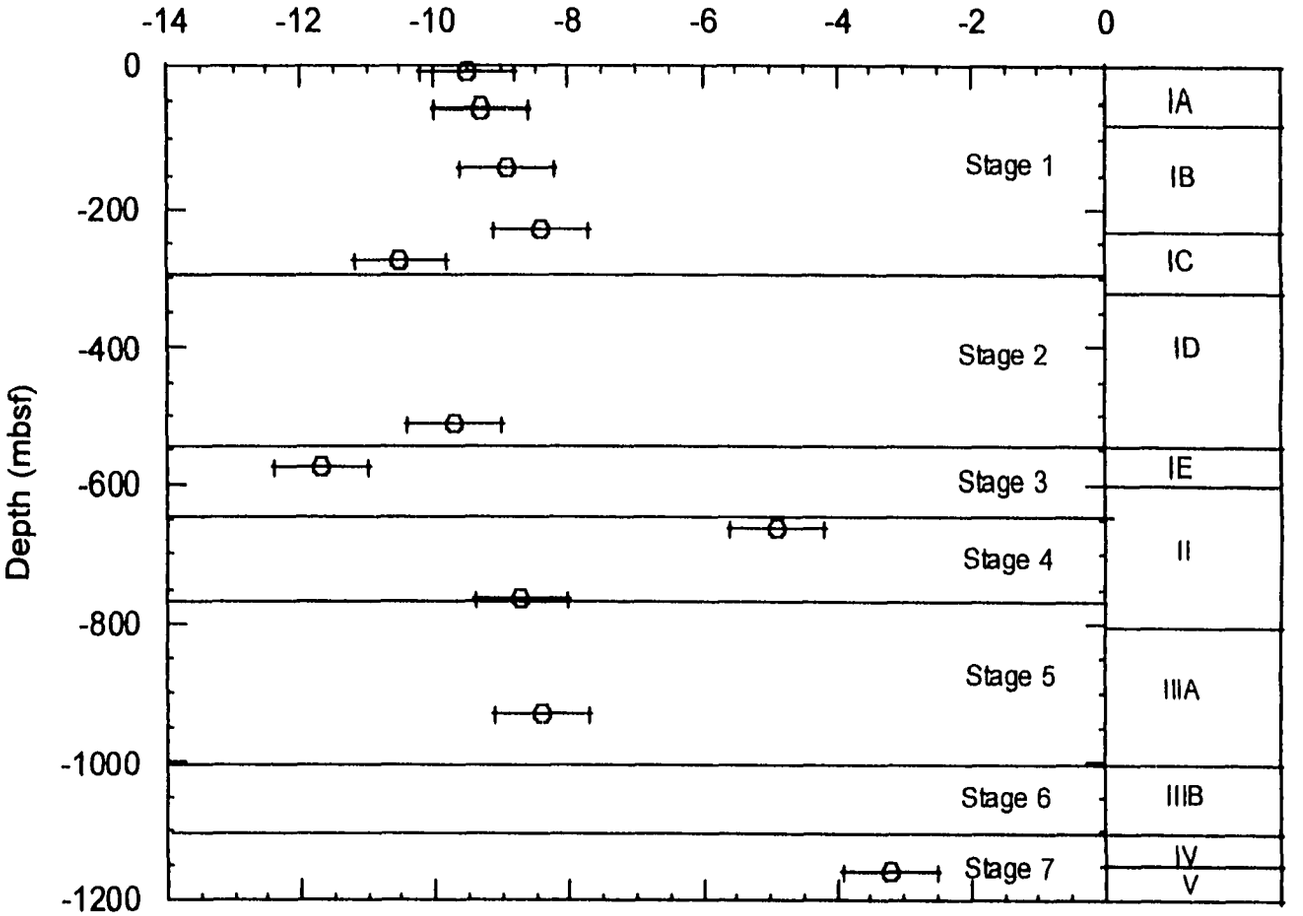

Figure 3.6 Lithium isotopic composition of bulk marine sediments at Site 918 shown with lithologic units (Larsen et al., 1994) and geochemical stages (Saito, 1998).

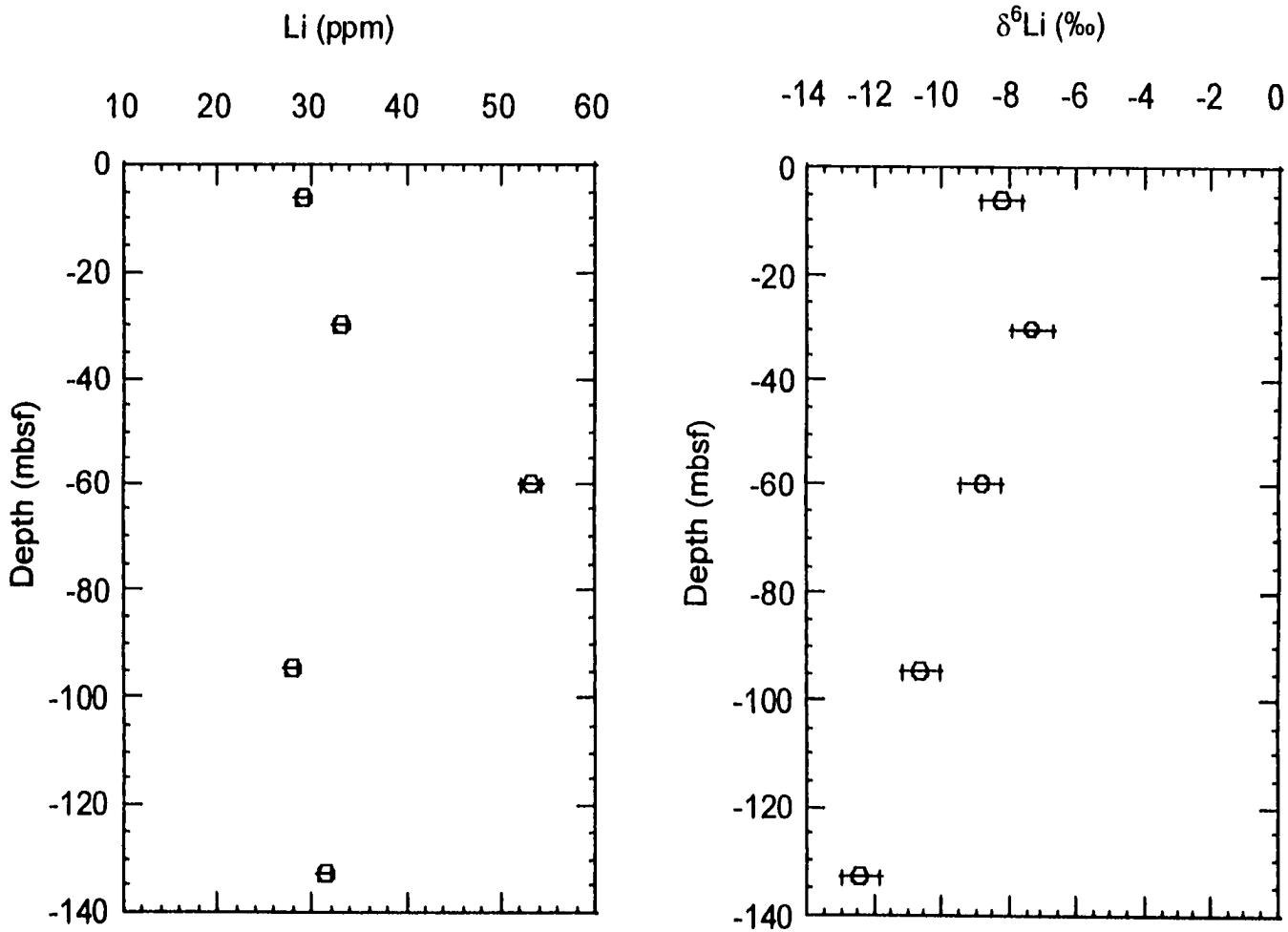

Figure 3.7 Lithium concentration and isotopic composition of the marine sediments at Site 919

deeper section and are therefore finer grained (Larsen et al., 1994). The concentrations of the upper sediments vary from 29 to 33ppm reaching 53.2ppm at 60mbsf (Table 3.2 and Figure 3.7). Lithium isotopic compositions exhibit a narrow range -7.3 to -8.8‰. The coarser sediments in the deeper section have lower concentrations (27.9 and 31.4ppm) and lower δ^6Li values (-10.6 and -12.4‰).

The concentrations of Al, Na, Fe, Ca, K, Mg, Ti, and Mn of the bulk sediments from Site 918 are listed in Table 3.3 as weight percentage of oxide. In most cases, the results of Al, Fe, Ca, Ti, and Mn agree within 10% with those reported for the same samples by Murray et al. (1998). Na_2O/Fe_2O_3 and TiO/Al_2O_3 ratios are plotted against lithium contents and δ^6Li values of sediments to illustrate the relationship of lithium isotopic composition with major ion chemistry.

Table 3.3 Major and trace element data from the analyzed samples at Site 918. All values are in Wt.% as oxide.

Sample	Al_2O_3	Fe_2O_3	CaO	Na_2O	K_2O	TiO_2	MnO	MgO
A-2H-4	14.17	6.45	5.06	3.30	1.90	0.96	0.01	2.89
A-7H-4	14.55	7.51	4.59	3.09	1.96	0.98	0.01	3.43
A-16H-4	14.03	12.78	7.18	2.55	1.15	2.03	0.16	5.30
A-26X-4	13.85	12.62	6.66	2.49	1.26	2.07	0.16	5.00
A-31X-1	15.17	7.36	3.97	3.13	2.07	0.93	0.09	3.13
D-25R-2	11.90	6.29	6.83	1.78	2.45	0.91	0.11	2.57
D-31R-CC	13.55	9.68	2.72	1.92	2.13	1.54	0.08	3.76
D-40R-1	11.10	6.98	13.05	1.10	1.56	1.15	0.06	0.21
D-51R-2	11.67	8. 47	12.36	1.16	1.53	1.39	0.06	2.84
D-68R-1	11.34	14.17	1.47	1.65	2.25	1.67	0.04	8.43
D-91R-1	13.39	9.91	7.37	0.74	1.47	1.45	0.04	3.32

3.5 Review of pore water study

The pore water study (Zhang et al., 1998) demonstrates that lithium isotopic compositions of pore water are a useful indicator of sediment-water interactions. Three processes are identified at different depths of Site 918: alteration of volcanic material within marine sediments, exchange of lithium with NH_4^+, and release of lithium under elevated temperatures.

3.5.1 Pore water lithium depletion at shallow depths

At shallow depths (< 50mbsf) of Sites 918 and 919, $^{87}Sr/^{86}Sr$ data indicate alteration of volcanic material that constitutes a sink for lithium. While the lithium concentration of pore waters decreases to half of the sea water value (Gieskes et al., 1998), δ^6Li value becomes heavier than the sea water value indicating preferential incorporation of the lighter isotope into the alteration clay. The decrease in lithium concentration at the shallow depths, therefore, is caused by uptake during alteration of volcanic materials based on δ^6Li and $^{87}Sr/^{86}Sr$ data.

3.5.2 Source of lighter lithium isotope of pore water at 250 – 350mbsf

Although pore water $^{87}Sr/^{86}Sr$ and $\delta^{18}O$ data indicate that alteration of volcanic material occurs in the interval of 250 to 350mbsf at Site 918 (Gieskes et al., 1998), δ^6Li shows an increase to a maximum of -28‰, suggesting that other processes besides alteration of volcanic material occur in this depth interval. The reversal of δ^6Li to lighter isotopic values corresponds to the NH_4^+ maximum in the zero SO_4^{2-} zone. NH_4^+ produced during sulfate reduction of

organic matter undergoes ion exchange with cations in clay minerals (Gieskes et al., 1983). It has been experimentally verified that NH_4^+ expels lithium from exchangeable positions in clay minerals (Zhang et al., 1998). Desorbed lithium has a relatively light isotopic composition (-8‰) (Zhang el al., 1998). The net result of two competing processes, volcanic alteration and exchange of NH_4^+ with lithium, could cause the observed shift in δ^6Li. Thus cation exchange of NH_4^+ with lithium in clay minerals exerts an important control on the lithium isotopic composition at 250-350mbsf.

3.5.3 Lithium enrichments in deeper interstitial water

From 500 to 800mbsf, lithium concentration and δ^6Li steadily increase with depth at Site 918, reaching a maximum concentration of 163μM and the lightest isotopic composition (-25‰) at 765mbsf. The maximum concentration and the lightest isotopic composition suggest a lithium source within the sediment column. Experimental studies (You, 1994; Chan et al., 1994) have shown that lithium can be released from marine sediments at the elevated temperatures. Therefore, the enrichment most likely originates from the marine sediments.

3.6 Discussion

3.6.1 Effect of sediment-water interaction on lithium isotopic distribution of the marine sediments

Lithium concentrations of marine sediments at shallow depths (0 – 230mbsf) of Site 918 show a gradual increase from surface to downcore. In the same interval, lithium concentrations of the pore waters are below

seawater value indicating removal. The sediments at this site contain considerable amounts of volcanic matter as evidenced by high Ti/Al ratios, and decreases in $^{87}Sr/^{86}Sr$ and δ^6Li in the pore fluids (Gieskes et al., 1998; Zhang et al., 1998). Lithium can be incorporated in the product of alteration, mainly smectite. At the concentration minimum of the pore water (~140mbsf), Site 918, the concentration is 13μM and the porosity is 50% (Larsen et al., 1994). In a unit volume ($1cm^3$) of sediment with 50% porosity and an initial pore water lithium concentration of 26μM (seawater value), the total amount of lithium incorporated into the marine sediment would be at most 45ng. The average concentration of marine sediments at the pore water concentration minimum is approximately 15ppm, equivalent to 20μg lithium/$0.5cm^3$ sediment assuming a sediment density of $2.7g/cm^3$. Thus lithium removed from the fluid amounts to only 0.2% of lithium inventory in the solid phase. The lowest δ^6Li value in the residual fluid is -41‰ (Figure 3.3). Therefore, the alteration mineral in equilibrium with this fluid should have a δ^6Li of -22‰, based on an isotopic fractionation factor of 1.019 observed for low temperature alteration of submarine basalt (Chan et al., 1992). Thus the addition of pore water lithium to the sediment would at most cause a -0.03‰ shift in the sediment.

The above calculation assumes a closed system. Even if diffusive input is considered, the result would be similar. Using the maximum concentration gradient (10μM/10m) at Site 919 and a diffusion coefficient of 1.48 x

$10^2 cm^2$/year for lithium at 0°C (Li and Gregory, 1974) and a porosity of 50%, the diffusive flux of lithium into the sediments is estimated to be 3.7×10^{-4} $\mu M/cm^2$.year (flux = (porosity)^2 x diffusion coefficient x concentration gradient, Stoffyn-Egli and Mackenzie, 1984). Since the concentration gradient and porosity decrease with depth at Site 918, the calculation here is considered as the maximum of lithium flux into the pore waters of marine sediments. With the sedimentation rate of 8cm/1000 years at shallow depth of Site 918 (Larsen et al., 1994), the maximum diffusion flux to $0.5cm^3$ volume sediment is 0.023μM (0.16μg) lithium. This maximum lithium input from diffusion is still two orders in magnitude smaller than the lithium concentration of the sediments. The maximum change on the isotopic composition of marine sediments from the addition of pore water lithium would be only -0.24‰. Therefore, even considering an open system with a lithium diffusive flux into the marine sediments, the addition of pore water lithium is still not adequate to affect the isotopic distribution in the solid phases.

The simple mass balance calculations above demonstrate that the incorporation of lithium into altered products could not lead to any significant variation in concentration and isotopic composition of marine sediments. In any case, the isotopic composition of the marine sediments should become heavier if the increase of lithium content is due to the addition of pore water lithium. However, the isotopic compositions of the sediments in the upper 230m display slightly lighter isotopic composition with higher lithium content. Therefore, the variation of lithium content and isotopic composition at the

shallow depths would be better explained by the difference in the compositions of source materials.

At the depths of 250-350mbsf, the exchange of NH_4^+ with lithium in clay minerals accounted for the source of the lighter lithium isotope based on pore water lithium study (Zhang et al., 1998). Lithium desorption by NH_4^+ was also observed on three coastal sediments from Gulf of Mexico treated with 1N ammonium. An average of 0.5 - 0.6μg lithium is desorbed from 1g sediment (Zhang et al., 1998), indicating ion exchange between NH_4^+ and lithium at exchangeable sites. Given the lithium concentration (24.3ppm) of sample 918A-31X-1, 0.5 to 0.6ppm only accounts for slightly over 2% of the lithium in marine sediment. Lithium adsorbed on clays from seawater has a δ^6Li of -8‰ (Zhang et al., 1998). It can be shown by mass balance, release of the adsorbed lithium would not significantly affect the lithium content and isotopic composition in the sediments.

Between 575 and 800mbsf, the concentration profile of the sediments displays a shape similar to the dissolved lithium profile, with the peak concentration occurring at 765mbsf. The lithium enrichment in the pore water most likely originates from the sediments. Experimental studies have shown that mobilization of lithium into the fluid phase can occur at temperatures as low as 50 – 60°C (You, 1994; Chan et al., 1994). At Site 918, the geothermal gradient is 5 – 6 °C/100m (Larsen et al., 1994). Thus the temperature at 765mbsf would be approximately 45°C, making it possible for lithium to be mobilized from the sediments. However, dissolved lithium in the most

concentrated pore water (163μM) represents still only 1% of the lithium inventory in the solid.

In summary, lithium inventory in the sediments of Site 918 is two to three orders of magnitude higher than that in the pore waters. Hence water-sediment interaction during ash alteration, ion exchange, and diagenesis at elevated temperatures exerts important control on the concentration and isotopic composition of dissolved lithium while having little effect on the lithium isotope composition of the solid phase. Thus, the observed concentration and isotopic variation of marine sediments at Sites 918 and 919 must be attributed to other factors, such as the provenance and lithology of the sediments.

3.6.2 Effect of source materials on isotopic distribution of marine sediments

Based on major and the trace element variations in bulk sediments at Site 918, Saito (1998) proposed seven different geochemical stages. The boundaries of the geochemical stages coincide with significant lithological boundaries (Figures 3.5 and 3.6). Lithium isotopic characteristics of the sediments are discussed in the framework of geochemistry and lithology.

Geochemical Stage 1 covers from 0 – 300mbsf and corresponds to lithologic sub-units IA and IB. The dominant sediment type is marine silt with IRD and dropstones. The large sediment influx at this horizon was caused by glacial erosion of the Greenland continent. This stage is characterized by relatively high sodium and calcium contents and low iron content. The high sodium content is attributed to fresh plutonic rocks that contain an abundance

of sodium-rich feldspars (Vallier et al., 1998). Another important component in this stage is IRD and dropstones that consist of a large component of basalt, as well as granitic and metamorphic rocks (Larsen et al., 1994). The basalt is derived from the North Atlantic Volcanic Province. According to bulk chemistry, the dominant sources of the sediments are unweathered plutonic and volcanic rocks eroded by ice sheets (Saito, 1998). Lithium concentrations of the analyzed marine sediments at Stage 1 range from 13.6 to 24.3ppm with relative narrow lithium isotopic composition from -8.4‰ to -9.5‰ (Figures 3.5 and 3.6). Low lithium content is probably due to the great abundance of quartz and feldspar and low clay mineral contents. The knowledge on lithium isotopic composition of granitic and metamorphic data is limited and can be summarized as follows (Chan, unpublished data): the granite and tonalite samples from the Greenstone Belt of South Africa have δ^6Li of -8‰ to -10‰ and schist and gneiss samples from the Canadian Shield have -10 to -14‰. From an earlier study (Chan et al., 1992), lithium isotopic compositions of mid-ocean ridge basalt have been determined to be -3 to -5‰. Thus basalt-rich IRD should be isotopically light. The lithium isotopic compositions for Stage 1 are consistent with mixing of volcanic material and plutonic component.

Geochemical Stage 2 (300 –550mbsf) corresponds to lithologic sub-units IC and ID. Silt is composed of terrigenous debris and volcaniclastics. IRD and dropstones are present. The dominant source is transitional between Stage 1 and Stage 3 based on bulk geochemical data (Saito, 1998).

δ^6Li of samples from the base of Stage 1 and within Stage 2 also show intermediate values of -9.7 to -10.5‰, heavier than Stage 1 and lighter than Stage 3.

Geochemical Stage 3 (550-650mbsf) includes lithologic sub-unit IE, which has the same lithology as sub-unit ID but no dropstones. The main sediment type is characterized as turbidites derived mainly from weathered plutonic materials with a minor volcanic component (Saito, 1998). The sediment sample at the depth of 575mbsf (D31R-CC) reaches a maximum in lithium concentration and minimum (-11.7‰) in δ^6Li at Site 918. The heaviest isotopic composition can be in part attributed to the absence of IRD and dropstones at this depth, which are abundant in Stage 1 and Stage 2. The isotopic value -11.7‰ falls within the range for granitic and metamorphic rocks of South Africa and the Canadian Shield (-8 to -14‰) (Chan, unpublished). This supports the assumption that isotopic compositions of plutonic materials on Greenland are similar to the Archean rocks of South Africa and the Canadian Shield. The maximum lithium concentration at the depth is also accompanied by high rubidium, thorium, lead, and potassium and low sodium and calcium (Saito, 1998). Based on the study of Heiden and Holmes (1998), the warm climate occurred from early Miocene to middle Miocene and was followed by a cooling trend in late Miocene that cover the sediment sequence from the depths of 515 to 615mbsf. The high lithium, rubidium, thorium, and potassium concentrations can be explained by weathering of plutonic materials during the warm period and these elements

are preferentially retained in weathered residues. Again, concentration and isotopic data can be explained rather well in the light of source materials.

At the depth of 660mbsf, lithium content of the sediment sample (D40R-1) decreases from the maximum to 40.4ppm and isotopic composition shifts to -4.9‰, which is at the top of Stage 4. This layer (lithologic unit II) is rich in volcaniclastics (Larsen et al., 1994). The chemical composition displays high Na_2O/Fe_2O_3 and K_2O/CaO ratios indicating predominance of fresh volcanics in its source material (Saito, 1998). The lithium isotopic composition of -4.9‰ falls in the range of fresh basaltic values (-3 to -5‰) (Chan et al., 1992), which supports the conclusion that Stage 4 mainly consists of sediments of volcanic origin.

At 765mbsf, where the maximum dissolved lithium is found, the lithium content of the sediment sample (D-51R-2) is 47.1ppm with an isotopic value of -8.7‰. This sample is at the boundary between geochemical Stage 4 and Stage 5. Stage 4 is mainly basaltic, whereas Stage 5 is mainly turbidite. Its lithium isotopic composition is similar to that of a deeper sample (D-68R-1) in Stage 5, which has a δ^6Li value of -8.4‰. From the isotopic composition, the sediment sample at 765mbsf probably is derived from a source material similar to Stage 5. Chemical data indicate that the dominant source is transitional between volcanic and weathered plutonic and metamorphic material (Saito, 1998). Lithium isotopic values are also intermediate between the signatures of these two sources.

At 1157mbsf, the silt is dominantly composed of volcaniclastic sediments (altered glass and basalt clasts) as well as volcanic derived smectite (Larsen et al., 1994). The alteration might have occurred by meteoric groundwater or by cool seawater (Heiden and Holmes, 1998). If the smectite were formed during low temperature seawater alteration, the isotopic composition of the alteration product would be close to -14‰, as determined from low-temperature alteration of submarine basalt by seawater (Chan et al., 1992). The MORB-like lithium isotopic composition (-3.2‰) of the sample at 1157mbsf (D-68R-1) suggests that the basaltic lava was altered in fresh water because fresh water is dilute in lithium and the system is rock-dominated. The presence of abundant kaolinite and some gibbsite in the weathered basaltic lava flows directly below this unit also suggests that subaerial exposure to warm, wet climate occurred in the late Paleocene and/or early Eocene (Heiden and Holmes, 1998).

In a plot of δ^6Li against TiO_2/Al_2O_3 (Figure 3.8), three end-member components may be distinguished in Site 918 sediments. IRD and turbidites that are rich in basalt and ash are characterized by the highest TiO_2/Al_2O_3 ratios and have δ^6Li of about -8‰, whereas plutonic rocks have the lowest TiO_2/Al_2O_3 ratios and lower δ^6Li (~ -10‰). Volcaniclastic sediments have intermediate TiO_2/Al_2O_3 and the lightest isotopic compositions. Only a highly weathered sample (D31R-CC) falls off the triangular field and may represent a distinct source rock composition.

In Saito's study (1998) Na_2O/Fe_2O_3 ratio was used to characterize the sediment source. Lithium concentration and δ^6Li are plotted against this ratio to illustrate the effect of weathering, and relationship between source materials and the lithium isotopic compositions of the sediments (Figures 3.9 and 3.10). Lithium is concentrated in clays and is therefore enriched in chemically weathered turbidites (Figure 3.9). IRD have low lithium contents indicating domination of physical weathering (Figure 3.9). The volcaniclastic sediments have low Na_2O/Fe_2O_3 and are isotopically light, while sediments derived from plutonic rocks have higher Na_2O/Fe_2O_3 and relatively heavy isotopic composition. Figure 3.10 shows a decrease of δ^6Li with increasing Na_2O/Fe_2O_3, corresponding to increasing plutonic input. Such correlation suggests that mixing of plutonic and volcanic materials that were transported into the Irminger Basin largely controls the lithium isotopic compositions of the sediments at Site 918. As defined by the geochemical characteristics, four components are used to model lithium concentrations and isotopic compositions of bulk sediments at Site 918. These four components are volcaniclastic, basalt-rich IRD, fresh plutonic, and weathered plutonic. The end-member compositions (Li, δ^6Li, Na_2O, Fe_2O_3) of these components are listed in Table 3.4. Volcaniclastic component has high lithium content (50ppm) and basalt-like isotopic composition (-3.2‰). The high lithium content with basalt-like isotopic is mainly caused by sub-aerial weathering as discussed earlier. The IRD end-member is rich in basaltic dropstones and ash. It is actual a mixture of plutonic and volcanic component and therefore

has intermediate isotopic composition (-8‰). The fresh plutonic component is assumed to have lithium content (15ppm) and isotopic composition (-10.5‰), consistent with the data from South Africa and Canadian Shield (Chan, unpublished data). The weathered plutonic component has higher lithium content (50ppm) and lighter isotopic composition (-8‰) than plutonic component due to weathering because clay minerals preferentially concentrate δ^6Li. It also has low Na_2O/Fe_2O_3 ratio because Na is lost during the course of weathering. Two mixing curves are generated to model mixing of plutonic component with the weathered plutonic component and with the IRD (Figures 3.9 and 3.10). Although the modeling is crude, it generally explains the lithium content and isotopic composition of the bulk sediments at Site 918. The scattering of the actual data points around the mixing curve may be caused by the uncertainty of the weathering effect on the Na_2O/Fe_2O_3 ratio, lithium content, and δ^6Li value of the sediment samples in our end-member estimation. One sample from Stage 3 (D31R-CC) falls off the trend, having very low Na_2O/Fe_2O_3 ratio but heavy isotopic composition (-11.7 ‰). This sample is a turbidite derived from dominantly weathered plutonic rock. Sodium was mobilized by weathering and consequently is depleted in this sample. As mentioned above, the more negative isotopic value may be due to a distinct source rock composition.

At Site 919, lithium concentration ranges from 27.9 to 53.2ppm with isotopic composition of -7.3 to -12.4‰. The sediments at this site grade from quartz silt downward to silty clay (Larsen et al., 1994). The high concentration

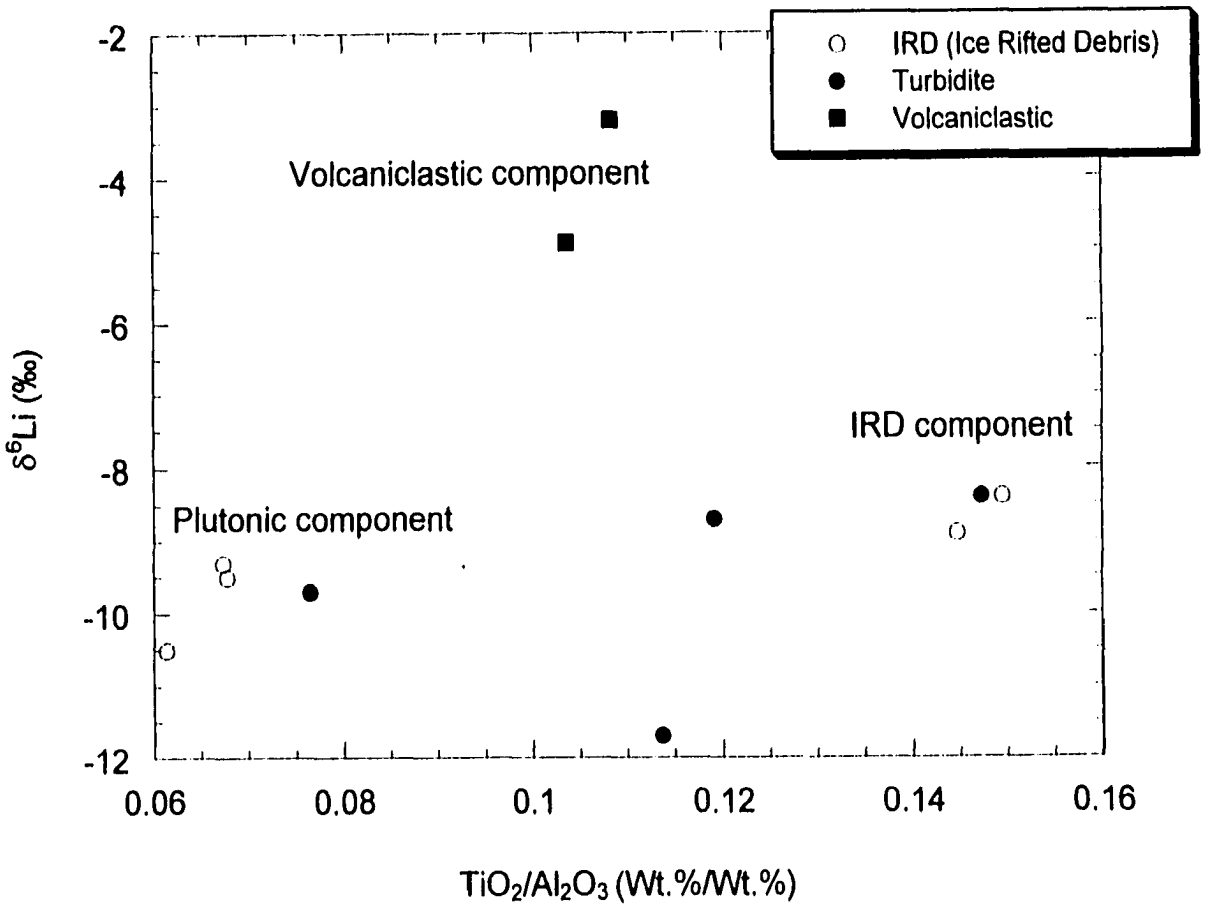

Figure 3.8 Variation of lithium isotopic compositions of the marine sediments from Site 918 with TiO_2/Al_2O_3 ratios. Three components: volcaniclastic, plutonic, basalt-rich IRD, are identified.

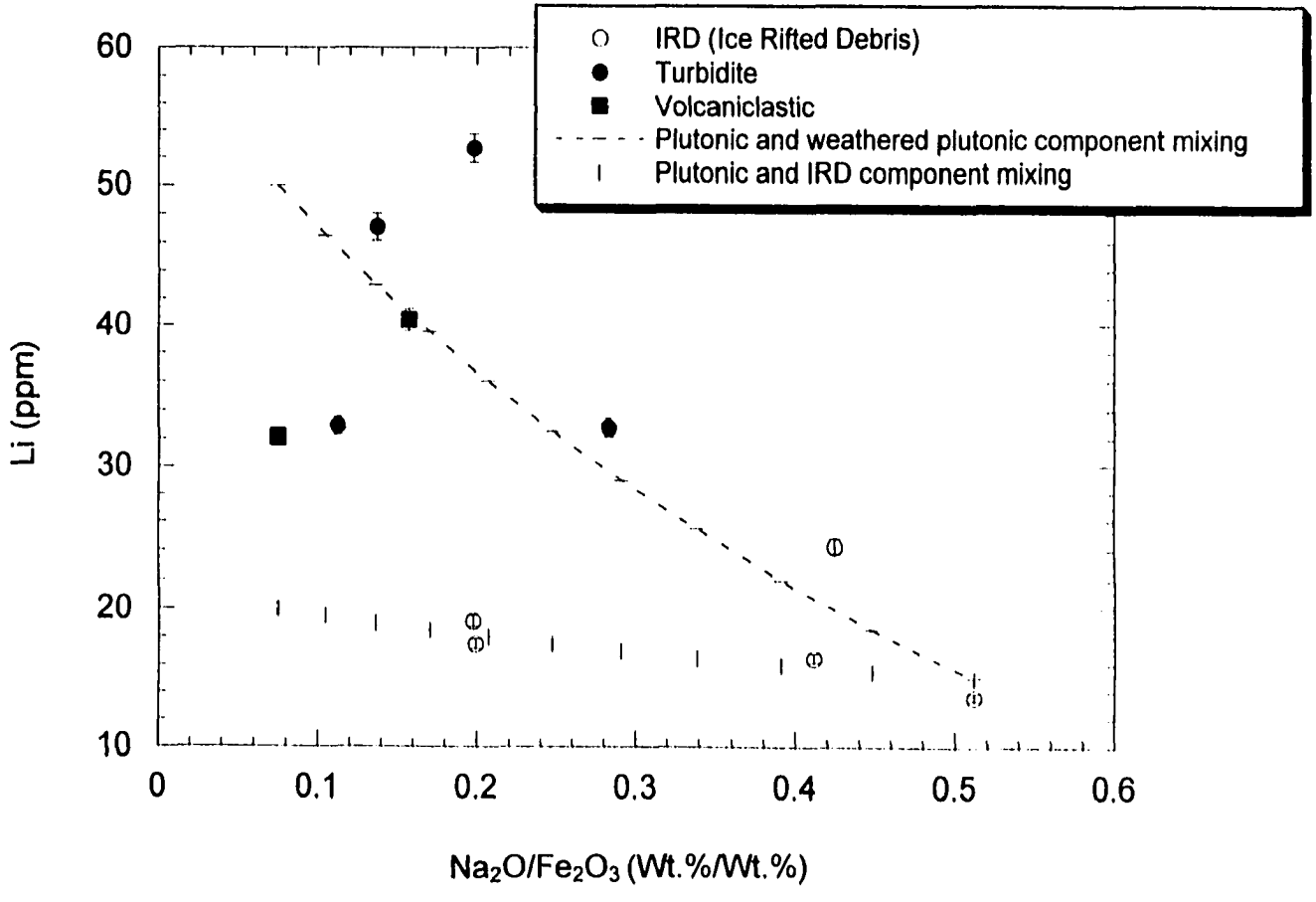

Figure 3.9 Variation of lithium concentrations of the marine sediments from Site 918 with Na_2O/Fe_2O_3 ratios. Two mixing curves are generated to model the mixing of the fresh plutonic component with the IRD, and with weathered plutonic component respectively.

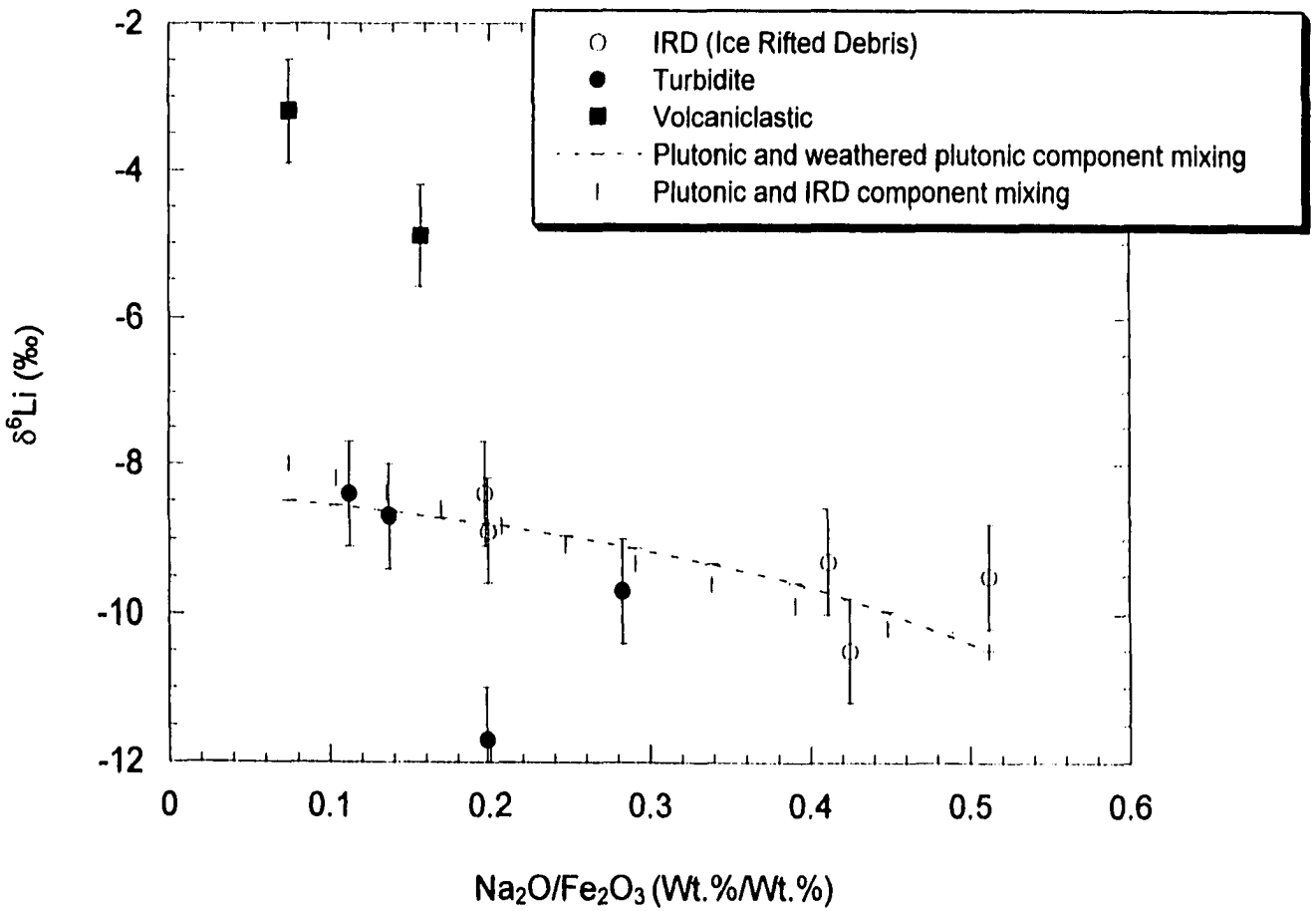

Figure 3.10 Variation of lithium concentrations of the marine sediments from Site 918 with Na_2O/Fe_2O_3 ratios. Two mixing curves are generated to model the mixing of the fresh plutonic component with the IRD, and with weathered plutonic component respectively.

Table 3.4 The estimated Na_2O, Fe_2O_3, lithium concentrations and isotopic compositions, for four sediment end-members at Site 918.

Sediment component	Li concentration (ppm)	δ^6Li (‰)	Na_2O (Wt.%)	Fe_2O_3 (Wt.%)
Plutonic	15	-10.5	3.302	6.448
Volcaniclastic	50	-3.2	0.741	9.906
IRD	20	-8	0.741	9.906
Weathered plutonic	50	-8.5	3.302	6.448

at 60mbsf probably reflects an abundance of clay minerals. Site 919 is located further from the East Coast of Greenland compared to Site 918. The increased amount of smectite at Site 919 relative to Site 918 indicates eastward transport of fine clays (Heiden and Holmes, 1998). The clay mineral assemblage at Site 919 is similar to the upper Pliocene-Pleistocene section (Unit I) of Site 918 (Larsen et al., 1994). The higher lithium concentration at Site 919 than at Site 918 is probably due to the particle size difference of the marine sediments at these two sites since lithium is enriched in clay minerals. Sediments in the section above 60mbsf of hole 919A have relatively light isotopic compositions (-7.3 to -8.8‰), compared to the deeper sediments of 919B (-10.6 and -12.4‰). Figure 3.9 shows that 919A sediments are isotopic lighter than the IRD of the same lithologic unit at 918, relative to Na_2O/Fe_2O_3 ratios. Thus the lighter isotopic composition cannot be due to higher contents of volcanic material, but probably the result of greater abundance of clay minerals which preferably concentrate the lighter isotope. The more negative

isotopic values of the deeper sediments in Hole 919B may be characteristic of turbidites derived from weathered continental rocks, as observed at Site 918.

3.7 Summary and conclusion

The concentration profile of the marine sediments displays a shape similar to the dissolved lithium profile. The similarity between solid and pore water profiles suggests that the sediments largely control the distribution of lithium in pore water. However, due to at least two orders of magnitude difference in lithium inventory between pore water and marine sediments, the isotopic compositions of marine sediments are not affected by the interaction with pore water, such as alteration of volcanic material, ion exchange with NH_4^+ in pore water, and release of lithium under elevated temperatures.

Lithium isotopic compositions of sediments at ODP Sites 918 and 919 are well correlated with source material as defined by lithology and bulk geochemistry. Four major source materials of sediments are present at these sites: (1) volcaniclastic sediments which display MORB-like isotopic compositions (-3.2 and -4.9‰); (2) volcanic-rich IRD sediments containing basaltic dropstones and ash with relatively light isotopic values (~ -8‰); (3) chemically weathered plutonic, metamorphic and basaltic rocks on Greenland, which have isotopic values of about -8.5‰; and (4) fresh plutonic rocks with an isotopic composition (-10.5‰). The isotopic compositions of the marine sediments at Sites 918 and 919 are therefore mostly controlled by relative proportions of weathered or fresh plutonic/metamorphic component and volcanic component that were transported into the Irminger Basin. The

variation of lithology, chemical and isotopic compositions in the sediment sequence reflect the climatic and oceanographic history in the North Atlantic.

3.8 References

CHAN L. H. (1987) Lithium isotope analysis by thermal ionization mass spectrometry of lithium tetraborate. Anal. Chem., 59, 2662-2665.

CHAN L. H. AND EDMOND J. M. (1988) Variation of lithium isotope composition in the marine environment: A preliminary report. Geochim. Cosmochim. Acta 52, 1711-1717.

CHAN L. H., EDMOND J. M., THOMPSON G., AND GILLS K. (1992) Lithium isotopic composition of submarine basalts: Implications for the lithium cycle in the oceans. Earth Planet. Sci. Lett. 108, 151-160.

CHAN L. H., EDMOND J. M., AND THOMPSON G. (1993) A lithium isotope study of hot springs and metabasalts from mid-ocean ridge hydrothermal systems. J. Geophys. Res. 98, 9653-9659.

CHAN L. H., GIESKES J. M., YOU C. F., AND EDMOND J. M. (1994) Lithium isotope geochemistry of sediments and hydrothermal fluids of the Guaymas Basin, Gulf of California, Geochim. Cosmochim. Acta 58, No. 20, 4443-4454.

CHAN L. H. AND KASTNER M. (2000) Lithium isotope compositions of pore fluids and sediments in the Costa Rica subduction zone: implications for fluid processes and sediment contribution to the arc volcanoes. Earth Planet. Sci. Lett. 183, 275-290..

CROCK J. C. AND SEVERSON R. C. (1980) Four reference soil and rock samples for measuring lementent availability in western energy regions. USGS Circ. 841, 1-16.

FLESCH G. D., ANDERSON A. R. JR., AND SVEC H. J. (1973) A secondary isotopic standard for Li determinations. Intl. J. Mass Spectrom. Ion Phys. 12, 265-272.

GIESKES J. M., ELDERFIELD H. AND NEVSKY B. (1983) Interstitial water studies, Leg 65, DSDP. In ini. Reports of DSDP, 65 (eds. Lewis B. T. R., Robinson P. et al.), Washington, 441-449.

GIESKES J. M., SCHRAG D., CHAN L.-H., ZHANG L., AND MURRAY R. W. (1998) Geochemistry of interstitial waters. Proc. ODP. Sci. Results 152, 293 – 305.

HEIDEN K. A. AND HOLMES M. A. (1998) Grain-size distribution and significance of clay and clay-sized minerals in Eocene to Holocene sediments from Sites 918 and 919 in the Irminger Basin. Proc. ODP. Sci. Results 152, 39 –48.

JAMES H. J., RUDNICKI M. D., AND PALMER M. P. (1999) The alkali element and boron geochemistry of the Escanaba Trough sediment-hosted hydrothermal system. Earth Planet. Sci. Lett. 171, 157-169.

LARSEN H. C., SAUDERS A. D., CLIFT P. D., AND THE SHIPBOARD SCIENTIFIC PARTY (1994) Site 918, Proc. ODP. Ini. Report 152, 117-256, College Station, TX (Ocean Drilling Program).

LI Y. H. and GREGORY S. (1974) Diffusion of ions in seawater and in deep sea sediments. Geochim. Cosmochim. Acta 38, 703-714.

MANHEIM F. T. AND SYLES F. L. (1974) Composition and origin of interstitial waters of marine sediments based on deep sea drill cores. In Goldberg, E. D. (Ed.), The Sea (Vol. 5): New York (Wiley – Interscience), 527-568.

MURRAY R. W., GIESKES J. M., AND PHLAUMER. C. (1998) Data report: Major, trace, and rare earth element composition of interstitial water squeeze cakes. Proc. ODP. Sci. Results 152, 307-311.

SAITO S. (1998) Major and trace element geochemistry of sediments from East Greenland Continental Rise: an implication for sediment provenance and source area weathering. Proc. ODP. Sci. Results 152, 19 –28.

STOFFYN-EGLI P. AND MACKENZIE F. T. (1984) Mass balance of dissolved lithium in the oceans. Geochim. Cosmochim. Acta 48, 859-872.

VALLIER T., CALK L., STAX R. and DEMANT A. (1998) Metamorphosed sedimentary (volcaniclastic?) rocks beneath Paleocene basalt in Hole 917A, East Greenland margin. Proc. ODP. Sci. Results 152, 129-144.

YOU C. F. (1994) Lithium, beryllium, and boron isotope geochemistry: Implications for fluid processes in convergent margins. Dissertation, University of California, San Diego.

YOU C. F., CHAN L. H., SPIVACK A. J., AND GIESKES J. M. (1995) Lithium, boron, and their isotopes in sediments and pore waters of Ocean Drilling Program Site 808, Nankai Trough: Implications for fluid expulsion in accretionary prisms. Geology, 23, No. 1, 37 – 40.

YOU C. F. and CHAN L. H. (1996) Precise determination of lithium isotopic composition in low concentration natural samples. Geochim. Cosmochim. Acta 60, 909-915.

ZHANG L., CHAN L. H., AND GIESKES J. M. (1998) Lithium isotope geochemistry of pore waters from Ocean Drilling Program Sites 918 and 919, Irminger Basin, Geochim. Cosmochim. Acta 62, 2437–2450.

CHAPTER 4
LITHIUM AND ITS ISOTOPE DISTRIBUTION IN MARINE SEDIMENTS

4.1 Introduction

The lithium isotopic characteristics of the major reservoirs in the marine environment such as seawater, MORB (Mid-Ocean Ridge Basalt), and altered oceanic crust are relatively well defined due to recent studies of submarine hydrothermal activities and oceanic crust alteration (Chan et al., 1988, 1992, 1993, 1994a, 1996). However, the lithium isotopic compositions of different types of marine sediments are not well known. Chan et al (1994a) presented the lithium isotopic compositions of hemipelagic sediments and hydrothermally altered sediments of the Guaymas Basin, Gulf of California. Lithium isotopic data on the sediments of the Nankai Trough were reported (You et al., 1995) in a study of fluid expulsion in the décollement zone at ODP Site 808. Recently, lithium isotope composition of marine sediments from ODP Site 918, Irminger Basin, offshore of Greenland, has also been determined adding to the understanding of sediment water interactions (Zhang et al., 1998). Lithium isotope data were reported for the sediments from Escanaba Trough (ODP Site 1038) along with alkali elements, boron, and boron isotope data for these samples (James et al., 1999). Hoefs and Sywall (1997) observed large variations in lithium isotope compositions of biogenic carbonates with time. These studies represented limited attempts to characterize the distribution of lithium and its isotopes in marine sediments. Further characterization of the major constituents could shed light on the

controls of lithium isotope compositions in marine sediments. This chapter presents a reconnaissance study of sediments from the continental margin to the ocean-basin floor. Lithium concentrations and isotopic compositions are reported for river suspended materials, coastal sediments, hemipelagic sediments, pelagic clays, biogenic carbonates, biogenic silica, and metaliferous sediments. This work represents a first systematic study of lithium and its isotopic variation in the major sediment types.

Since marine sediments are relatively enriched in lithium compared to igneous rocks (Holland, 1984), they are considered to be an important sink for oceanic lithium. Holland (1984) argued that the lithium excess in sediments is due to uptake of oceanic lithium into igneous rocks during their sedimentary cycle. However, the uptake mechanism is unclear. Stoffyn-Egli and McKenzie (1984) proposed that lithium is incorporated into authigenic clay minerals. It has been demonstrated in Chapter 2 that lithium adsorption by marine sediments is a significant but not a major removal process in the oceans. To further test the hypothesis that marine sediment is an efficient sink, it is essential to define the lithium contents and isotopic compositions of different marine components such as marine carbonates and silica, and authigenic clay minerals. The magnitude of those sedimentary sinks can then be quantified based on their lithium content and their formation rate in the oceans. The lithium budget in the oceans will be examined in detail in Chapter 5 based on the magnitude of removal by various sediment components from this study.

Lithium is also enriched in marine sediments relative to the mantle and its mobility in fluids under elevated temperatures has been observed in laboratory experiments (Chan et al., 1994a and You, 1994). Available data show that the lithium isotope compositions of marine sediments are distinct from the mantle derived rocks. Because of these characteristics, lithium is a potentially important tracer for subduction processes and sediment recycling at convergent margins. Application of lithium and δ^6Li to understand the sediment recycling is largely dependent on the knowledge of lithium flux and isotopic signature of the sediments. This reconnaissance study provides a basis to define the end member compositions of subducted sediments. This permits us to evaluate the usefulness of lithium isotopes in the understanding of sediment contribution to arc magma. To summarize, the objectives of this work are (1) to characterize the isotopic composition of various types of marine sediments, (2) to gain a better understanding of the sedimentary cycle of lithium, and (3) to examine the implication for cycling of sediment-borne elements at convergent margins.

4.2 Sample description

Modern sediments were collected from the West Pacific Ocean, Gulf of Mexico, Antarctic Ocean, and Atlantic Ocean. Sample locations are shown in Figure 4.1 and are listed in Table 4.1. These samples with a widespread spatial distribution allow us to characterize the variation of lithium isotopic compositions of marine sediments worldwide.

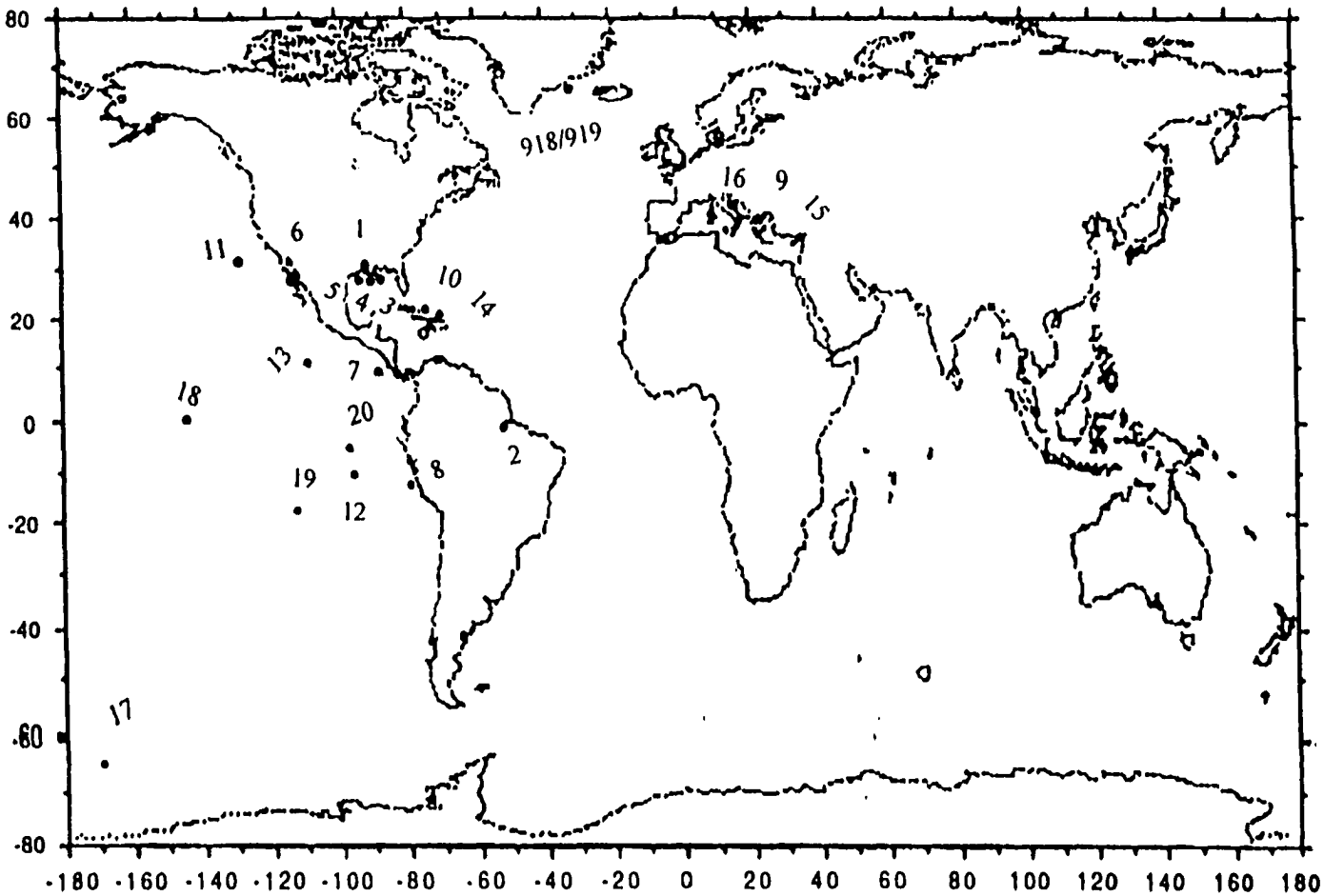

Figure 4.1 Sample location map (918/919 refers to ODP Sites 918 and 919. Marine sediments from those two sites are previously discussed in Chapter 3 and are included here for completeness. The other numbered samples are listed in Table 4.1)

Table 4.1 Lithium concentrations and isotope compositions of the analyzed sediment samples

Sample	Location	Latitude	Longitude	Depth (cm)	Li (ppm)	δ^6Li ± 2σ_m (‰)
River Suspended Sediments						
1. Amazon	confluence with Xingu				63.9	-1.1 ± 0.6
2. Mississippi	Baton Rouge, LA				49.3	-3.8 ± 0.8
Coastal Sediments						
3. B20	Gulf of Mexico			1-2	52.2	-9.3 ± 0.8
4. D65	Gulf of Mexico			1-2	56.5	-6.3 ± 0.6
5. G27	Gulf of Mexico			1-2	38.4	-4.3 ± 0.7
Hemipelagic and Continental Margin Sediments						
6. DSDP477-4-1	Guaymas Basin				37.5	-10.1 ± 0.7
7. VLCN 1-37 BC	MANOP H	6.57° N	-92.785° W	2-3	45.7	-14.6 ± 0.8
8. Y71-8-66	Peru Margin	-9.34° N	-80.678° W	2-3	52	-8.9 ± 0.7
9. SE-52-32	Aegean Sea				55.3	-12.2 ± 0.6
Pelagic Clay						
10. 543A-7-1	Caribbean Sea				66.2	-10.3 ± 0.7
11. Y74-3-58 MG3	MANOP R	33.17° N	-150.902° W	2-3	65.5	-10.9 ± 0.9
12. Y71-9-84	Nazca Plate				34.6	-11.5 ± 1.0

(table 4.1 continued)

(table 4.1 continued)

Sample	Location	Latitude	Longitude	Depth (cm)	Li (ppm)	δ^6Li ± 2σ_m (‰)
Marine Carbonates						
13. W8402-14GC	MANOP C	0.95° N	-138.955° W	2-3	0.4	-24.3 ± 1.3
14. Oolite	Bahama				1.0	-21.8 ± 0.7
15. SE-21-11.3	Aegean Sea				41.5	-18.2 ± 0.8
16. Senonian Chalk	Dead Sea				1.5	-12.1 ± 0.7
Siliceous Ooze						
17. KN7812-12BC	Antarctic Sea	-63.32 S	-169.73° W	0-2	1.2	-8.9 ± 1.0
Metaliferous Sediments						
18. PLUTO III-25BC	MANOP M	8.79° N	-103.988° W	2-3	36.2	-9.4 ± 0.7
19. OC73-3-27 MG	Southern EPR	-21.01° N	-114.732° W	2-3	0.45	-25.0 ± 1.0
Authigenic Fe-Montomorillonite						
20. LD3	Bauer Basin				18.2	-14± 0.7

Three pelagic clay samples 543A-7-1, Y74-3-58, and Y71-9-84 have been analyzed. Sample 543A-7-1 was retrieved from the margin of the Caribbean Accretionary Prism and consists of more than 95% pelagic clay and 4% silt (Biju-Duval et al, 1984). Sample Y74-3-58 is red clay from MANOP Site R in the eastern Pacific where the sediments are primarily made of oxidized eolian-rich clays (Huh and Ku, 1984). Y71-9-84 was collected as a part of the Nazca Plate Project (Dymond, 1981) and contains 50% biogenic materials and 50% eolian materials derived from South America.

Four hemipelagic and continental margin sediments are DSDP477-4-1, VLCN 1-37 BC, Y71-8-66, and SE-52-32. DSDP477-4-1 is collected from Guaymas Basin, California. This sample consists of approximately 40% diatomaceous ooze, 40% andesitic turbidite, 5-10% carbonate and 2-4% organic carbon (Kelts, 1982). Its lithium isotopic composition has been reported by Chan et al. (1994a) and is included here for comparison. VLCN 1-37 BC is from MANOP Site H. Due to its terrigenous-rich deposits with clayey-silt to silty clay, Site H is classified as "hemapelagic" (Lyle et al., 1984). The sample Y71-8-66 was acquired from the Peru margin, containing terrigenous-rich components (Dymond, 1981). SE-52-32 is a mudstone from Aegean Sea that consists of smectite (45%), kaolinite (13%), illite (9%), chlorite (5%), quartz (8%), plagioclase feldspar (5%), K-feldspar (4%), and calcite (2%) (Hsu et al., 1978).

Suspended sediments of two large rivers, the Mississippi and the Amazon were analyzed to characterize the lithium contents and δ^6Li in river

suspended material. Mississippi River suspended sediments were collected from the main channel at Baton Rouge during high flow in May 1983. The Amazon sample was collected at the mouth near the confluence with Xingu. In addition, three coastal sediments were collected from the Louisiana shelf, Gulf of Mexico.

Besides the siliciclastic sediments, marine carbonates and biogenic silica were also analyzed. Sample W8402-14GC is calcareous ooze collected from MANOP Site C in the eastern Pacific. This sample contains more than 95% carbonate. An oolite sample from Bahamas was also analyzed to determine the incorporation of lithium by inorganic carbonates. Sample SE-21-11.3 is lithified Marl ooze located in the Aegean Sea. It contains 40% nannofossils, 15% quartz, and 40% mica (Ryan et al., 1973). A Senonian chalk sample from the Dead Sea was also analyzed to have a better understanding of the lithium content and isotopic composition of ancient biogenic carbonates. Biogenic siliceous ooze KN7812-12BC was collected from the Antarctic Ocean (63.37° S).

Two metaliferous sediments analyzed are PLUTO III-25BC and OC73-3-27MG on the crest of EPR (East Pacific Rise). PLUTO III-25BC is from MANOP Site M which was chosen by the MANOP program to study hydrothermal deposits. However, it also has the highest flux of biogenic materials among the MANOP Sites. Since it is close to the Central American coast, it also receives a high flux of continentally derived materials (Lyle et al., 1984). OC73-3-27MG is on the south of crest of EPR with little biogenic and

detritus components (Dymond, 1981). LD3 is an authigenic clay mineral from Bauer Basin (Dymond, 1981) and consists of 90% Fe-montmorillonite and 4% carbonate.

4.3 Analytical methods

The carbonate samples were rinsed with distilled water before treatment with 0.1N HCl (prepared from double-distilled stock) at room temperature. When the carbonate fraction was dissolved, the slurry was immediately centrifuged. Then, the supernatant was filtered through 0.4μm filter paper. All aluminum silicate sediments were rinsed with distilled water to remove the interstitial salts and dried at 70°C. The dried samples were ground and homogenized in an agate mortar. The powders were then digested with ultrapure HF-$HClO_4$ following a procedure adapted from Crock and Severson (1980). All solids were dissolved completely. Since marl ooze contains carbonates and clays, it was prepared following the same procedure as for the aluminum silicate.

Lithium concentrations were determined by flame emission using the standard addition method. The precision was estimated as ±2%. Isotopic analyses were carried out on a Finnigan MAT 262 thermal ionization mass spectrometer. Lithium isotopic compositions were determined by thermal ionization mass spectrometry of lithium tetraborate. For detailed chemical separation and mass spectrometric procedures see Chan (1987). Isotopic compositions are expressed as δ^6Li relative to a NBS standard L-SVEC (Flesch et al., 1973):

$$\delta^6Li = [(^6Li/^7Li)_{sample} / (^6Li/^7Li)_{standard} - 1] \times 1000$$

where $(^6Li/^7Li)_{standard} = 0.083062 \pm 0.000054$.

4.4 Results

Lithium contents and isotopic compositions of different types of marine sediments are listed in Table 1 and illustrated in Figures 4.2 and 4.3. Marine biogenic and inorganic carbonates contain little lithium (0.4 – 1.5ppm) with δ^6Li values ranging from -12.1 to -24.3‰. The HCl soluble fraction of the calcareous ooze sample from MANOP Site C has extremely low lithium content (0.4ppm) and the heaviest isotopic composition (-24.3‰) among marine carbonates. The 0.5N acetic acid leach of the same sample yields a δ^6Li of -27‰ (Huh et al., 1998), confirming that the carbonate fraction of the ooze is relatively heavy in isotopic composition. The oolite sample from Bahamas suggests a similar apparent fractionation factor (1.010) in the Atlantic Ocean using -32.2‰ as the δ^6Li value for ocean water (Chan et al., 1988). The siliceous ooze sample KN7812-12BC from the Antarctic Ocean contains 1.2ppm of lithium with δ^6Li of -8.9‰. The apparent fractionation factor for biogenic silica in the Antarctic Ocean is approximately 1.023.

The three pelagic samples show a relatively narrow range of δ^6Li (-10.3 to -11.5‰). Red clays have the highest lithium concentrations (66ppm). Sample Y71-9-84 that contains 50% of biogenic and 50% eolian materials has a lithium concentration of 34.6ppm. The low lithium content is due to dilution by high percentage of biogenic component. Because the biogenic

component contains little lithium, δ^6Li value should largely reflect the signature of eolian material. Hemipelagic sediments have a relatively large range of δ^6Li from -8.9 to -18.2‰ with lithium content from 37.5 to 55.3ppm. The lowest concentrations are shown in the diatomaceous ooze from Guaymas Basin and the marl ooze from Aegean Sea. Like the pelagic samples, the range of lithium concentrations in hemipelagic sediments probably reflects the relative proportions of calcareous or siliceous components and siliciclastics.

Suspended sediments from the Mississippi River and the Amazon River have δ^6Li values of -1.1 and -3.8‰ respectively, which are isotopically lighter than pelagic clays and hemipelagic sediments. The sediments from the Louisiana Shelf have δ^6Li ranging from -4.3 to -9.3‰, falling between the Mississippi River suspended sediments and pelagic, hemipelagic clays. Lithium concentrations of the Louisiana Shelf sediments are also in the range for the river suspended sediments and hemipelagic sediments.

The Fe-rich montmorillonite Bauer Basin (LD-3) contains 18.2ppm with δ^6Li of -14‰. Two metaliferous sediments show extremely different lithium concentrations and isotopic compositions. PLUTO III-25BC contains 36.2ppm of lithium with isotopic composition of -9.4‰. In contrast, OC73-3-27MG has a concentration of 0.45ppm with the heavier isotopic composition (-25.0‰).

4.5 Discussion

4.5.1 Lithium isotopic compositions in various types of marine sediments

4.5.1.1 River Suspended Sediments and Coastal Sediments

The river suspended sediments from the Mississippi and the Amazon Rivers contain 49.3ppm and 63.9ppm lithium with isotopic composition of -1.1 and -3.8‰ respectively. Mississippi River water during high flow has a δ^6Li value of -17.7‰ (Chan et al., 1992) and Amazon River water above Xingu has -21.6‰ (Huh et al., 1998). The suspended sediments of the Orinoco River and tributaries also display lighter isotopic compositions (-6.4 to 0.9‰) relative to the dissolved load (Huh et al., 1999). The relatively light isotopic value in the suspended material is apparently due to the preferential retention of ^{6}Li in clays during the weathering process. The isotopic composition of weathering substrate also seems to depend on the intensity of weathering with the residue becoming increasingly enriched in ^{6}Li. The light isotopic composition of the Amazon River suspended sediment may be the result of extreme weathering on the tropical shields (Huh et al., 1998). In addition, the mineral and chemical composition of the suspended load can be modified by the transport process. Thus, the understanding of lithium partition, mobility and isotopic fractionation during the weathering process is more directly gained from soil profiles.

The coastal sediments in the Gulf of Mexico have heavier lithium isotopic composition (-4.3 to -9.3‰) compared to the Mississippi River suspended particulate. We note that sample (B20) directly outside the mouth

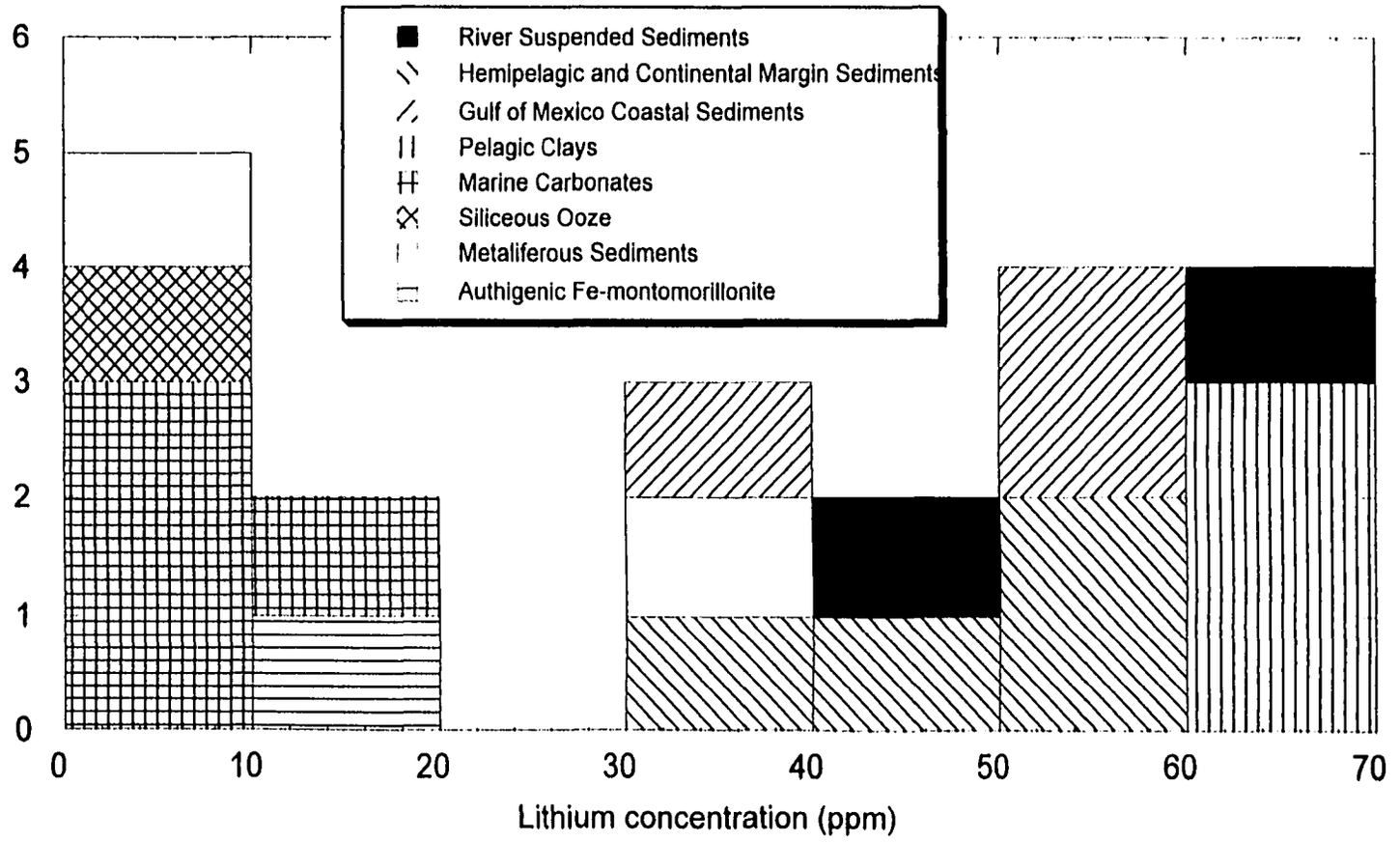

Figure 4.2 Stack histogram of lithium concentrations on different types of marine and river sediments.

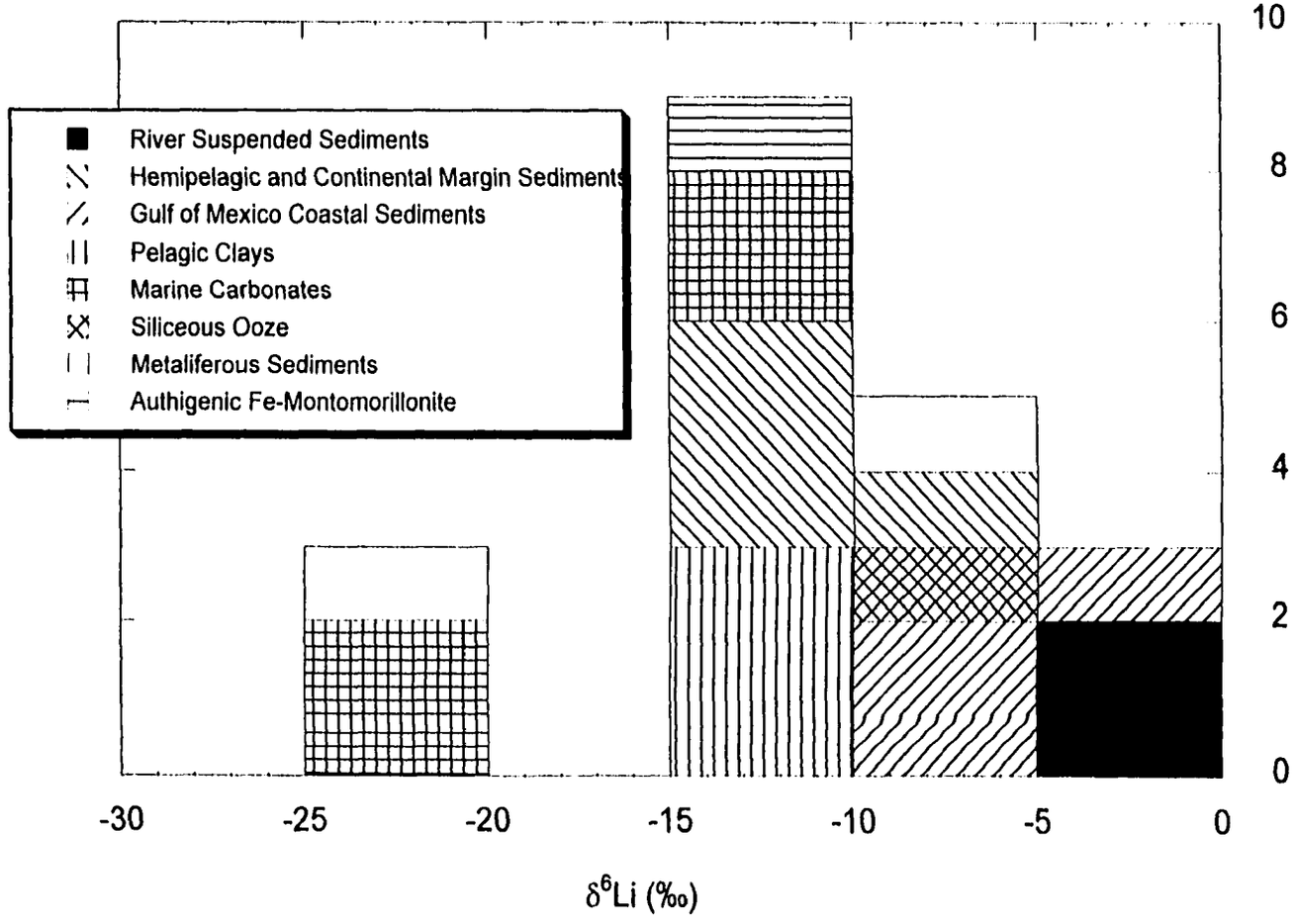

Figure 4.3 Stack histogram of lithium isotope compositions of different types of marine and river sediments

of the distributary has the lowest δ^6Li, demonstrating significant difference between river suspended material and deltaic deposits. The heavier isotopic compositions of deltaic and shelf sediments are probably due to higher concentration of coarse particles since they may contain bedload and sediments from longshore transport. They may therefore contain less clay mineral produced by chemical weathering but have a signature closer to that of the original continental rocks.

4.5.1.2 Hemipelagic Sediments

Most of the hemipelagic sediments are derived from terrigenous material transported by rivers. The shelf sediments contribute to the hemipelagic sediment formation at the continental margin through turbidity currents. Much of the sediment sections at Sites 918 and 919, Irminger Basin, offshore of Greenland are comprised of turbidites and glaciomarine sediments (Larsen et al., 1994). The lithium isotopic compositions of those sediments at Sites 918 and 919 vary between -7 to -12‰ and they largely reflect the signature of source materials with varying degree of weathering (Saito, 1998). The analyzed hemipelagic sediments have δ^6Li values ranging from -8.9 to -18.2‰, which are comparable to the values at ODP Sites 918 and 919. DSDP477-4-1 is collected from the Guaymas Basin, California and its isotopic composition (-10.1‰) represents that of andesitic turbidite (Chan et al., 1994a). VLCN 1-37 BC from MANOP Site H and Y71-8-66 from the Peru margin are located near active continental margins and probably derived from source materials from the volcanic arc.

4.5.1.3 Pelagic Clays

Compared with the Amazon and the Mississippi River suspended sediments (-1.1 to -3.8‰), pelagic clays in this study indicate relatively heavier lithium isotopic compositions (-10.3 to -11.5‰). From the adsorption experiments in Chapter 2, the partition of lithium onto clay mineral due to adsorption from seawater would be 2ppm at most, which has virtually no effect on the lithium isotopic composition of the pelagic clays. The heavier isotopic composition of pelagic clays cannot be derived from adsorption of oceanic lithium. The sample Y71-9-84, containing 50% biogenic carbonate and 50% eolian materials, has a δ^6Li value of -11.5‰. Because the lithium contribution from the carbonate fraction is minor, the value -11.5‰ reflects the isotopic composition of eolian materials. The sample Y74-3-58 is red clay from MANOP Site R that is primarily made of oxidized eolian-rich clays (Huh and Ku, 1984). The isotope composition of Y74-3-58 (-10.9‰) is very similar to the eolian signature of Y71-9-84. The sample 543A-7-1 is pelagic clay from the margin of the Caribbean Accretionary Prism. Its isotopic composition (-10.3‰) is probably also inherited from terrigenous component by river or eolian transport.

Aeolian deposits originate from wind erosion of the continental surface. The isotopic composition of the red clays can be compared to the available data of continental crustal rocks and loess. Available δ^6Li data of granitic and metamorphic rocks from N. America and S. Africa are mostly in the range of -8 to -17‰ (Chan, unpublished data). Shale from the Yellowstone area has -12

to -22‰. Loess provides a sampling of large regions of the continental surface (Taylor et al, 1983) but the lithium isotopic data of loess are as yet scanty. A Chinese loess sample contains 34.9ppm of lithium with isotopic composition of -6.5‰, and a Mississippi loess sample has 15ppm and a δ^6Li value of -15.2‰ (Chan, unpublished data). Based on these limited data, the isotopic compositions of deep-sea clays are bracketed by those of the continental crustal rocks and loess, and reflect the terrigenous origin of the sediments.

4.5.1.4 Marine Carbonates

The carbonate fraction of the calcareous ooze has a relatively heavy δ^6Li composition (-24.3‰). This yields an apparent isotopic fractionation from seawater (-32.3‰) of 1.008. The Bahamas oolite has a slightly lighter isotopic value (-21.8‰). The apparent fractionation factors for the oolite is 1.010. The isotopic compositions of these two samples suggest similar magnitudes of isotopic fractionation for lithium taken into carbonates by biological and inorganic processes. The isotopic fractionation of lithium in carbonates however is much smaller than the magnitude (1.019) for incorporation into clays as determined from seafloor weathered basalts (Chan et al. 1992).

While the two carbonate samples in this study yield similar results, there is a wide range of isotopic values reported for marine carbonates in literature. Huh et al. (1998) summarized the isotopic compositions of the carbonate sediments and limestones. Carbonates from ODP Site 851, which are known for extensive carbonate recrystallization, show δ^6Li of -6.2 and -

31.0‰ (You and Chan, 1996). Acetic acid leachates of nannofossil ooze at ODP Site 1039 have δ^6Li of -22.8 and -12.8‰ (Chan and Kastner, 2000). A wide range of values was also obtained for Quaternary and Tertiary foraminifera and carbonate ooze (Hoefs and Seawall, 1997). The authors attributed the large variations in part to diagenetic effects and admixture of lithium from the shale fraction during sample dissolution using 1N HNO_3. In this study, very dilute HCl solution (0.1N) was used and the calcareous ooze sample is from 2 – 3cm beneath the seafloor. It is therefore unlikely that diagenesis or impurities affected the sample. Ancient limestones also have variable isotopic values. A well-preserved marine chalk of Senonian age from the Judea Mountains has a lithium isotopic composition of -12.1‰. The acetic acid leachate of Jurassic and Mississippian limestone yield a value of -11 and -21.6‰ respectively (Chan, unpublished data). In summary, the lithium isotopic composition of marine carbonates and limestone vary widely, probably due to vital and diagenetic effects, admixed impurities, and analytical difficulty. Accurate determination of the carbonate-seawater fractionation factor requires further study of the fractionation behavior of calcareous organisms and inorganically precipitated carbonates.

4.5.1.5 Siliceous Ooze

The siliceous ooze sample contains 1.2ppm of lithium with a δ^6Li value of -8.9‰. The concentration and isotopic values resemble a siliceous nanofossil ooze sample from ODP Site 1040 which has a lithium content of 0.86ppm and δ^6Li of -9.4‰ (Chan and Kastner, 2000). The apparent

fractionation factor associated with lithium uptake into biogenic silica is therefore estimated at 1.024. These samples were totally digested in HF-$HClO_4$. Although the extremely low concentrations suggest high sample purity, some contamination by aluminum silicate cannot be excluded.

4.5.1.6 Marine authigenic clay minerals

Authigenic clays have been considered a possible sink of lithium in the ocean (Stoffyn-Egli and Mackenzie, 1984). The Bauer Basin sample was studied as an example of hydrothermal clay mineral formed authigenically in the ocean. Bauer Basin is located in the northwestern section of the Nazca Plate and its sediment composition is strongly influenced by the hydrothermal activity on the East Pacific Rise (Dymond, 1981). Sediments in this area have been modeled to contain 40% hydrothermal precipitates. LD3 used in this study is Fe-rich montmorillonite and is believed to be authigenically formed based on its isotopic and elemental composition. This Fe-montmorillonite sample contains 18.2ppm lithium with an isotope composition of -14‰. The apparent fractionation factor of lithium from seawater is 1.019, identical to the isotopic fractionation observed in seawater altered basalt on the seafloor (Chan et al., 1992). Unfortunately the formation rate of the authigenic minerals in the ocean is poorly known, and therefore the magnitude of this sink cannot be assessed. However, authigenic Fe-montmorillonite occurs in a restricted area that is influenced by hydrothermal process and therefore is probably not a quantitatively important sink of lithium.

4.5.1.7 Metaliferous Sediments

The metaliferous sediment sample (PLUTO III-25BC) near the East Pacific Rise has a δ^6Li of -9.4‰ with a lithium concentration of 36.2ppm. However, sample OC73-3-27MG from south of EPR contains much less lithium (0.45ppm) with δ^6Li value of -25.0‰. Both samples are close to the East Pacific Rise where the lithium isotopic compositions of hydrothermal solutions are from -6 to -11‰ (Chan et al., 1993). The Mn and other metal compositions of the surficial sediments are not purely hydrothermal in origin (Graybeal and Heath, 1984). A plausible explanation for the content and isotope composition of lithium in PLUTO III-25BC of Site M is that it was derived from the terrigenous component. Sediments at MANOP Site M receive a high flux of continentally derived materials (Lyle et al., 1984). The aluminum flux is 12μg/cm^2/year and Li/Al ratio of PLUTO III-25BC is 0.741mg/g, which is comparable to the detrital sediments (0.604 –0.665mg/g for Gulf of Mexico sediments). In addition, the isotope composition is also comparable to terrigenous detritus (-4.3 to -9.3‰ for Gulf of Mexico sediments, -8.9 to -14.6‰ for hemipelagic sediments). The sample OC73-3-27MG contains little lithium and its Li/Al ratio is 0.347mg/g that is significantly lower than detrital materials and probably reflects the presence of oxides. Hydrothermal Mn crusts from EPR have high lithium content (250 – 1000ppm) with an isotopic composition comparable to seawater value, indicating the scavenging from the Li-rich hydrothermal fluids, followed by isotope exchange with seawater lithium (Chan et al., 1994b). The isotopic signature (-25‰) of the sample OC73-3-

27MG may reflect hydrogenous lithium scavenged from seawater or hydrothermal lithium undergoing isotope exchange with seawater after precipitation.

4.5.2 Sedimentary cycle of lithium

The measured lithium concentrations and δ^6Li values of the modern marine sediments from this reconnaissance study and the downcore data from ODP Sites 918 and 919 are summarized in Figure 4.4. The published data from Guaymas Basin, Nankai Trough, Escanaba Trough, and Costa Rica Margin (James et al., 1999; You et al., 1995; Chan and Kastner, 2000) are also included to provide a view of global variation of lithium isotopic compositions in marine sediment. In addition, the sediment data are compared to the data of Jurassic and Cretaceous shales from Yellowstone area and the composition field of granitic and metamorphic rocks from South Africa and Canadian Shield (Chan et al., 1997; Huh et al., 1998; Chan et al., 1999; Chan, unpublished data). An overview of the sedimentary cycle of lithium isotopes based on these findings is presented below.

This data summarized in Figure 4.4 confirms previous findings that detrital sediments are enriched in lithium compared to igneous and metamorphic rocks (Holland 1984). During weathering, lithium is concentrated in clay minerals. The lithium content of the weathering product is dependent on the lithium content of the original rock and climate (Ronov et al., 1970). Studies of weathering profiles show that lithium is essentially constant in the parent rock and the weathering products (Horstman, 1957; Ronov et al.,

1970). However, mass balance indicates that 30 to 50% of the initial lithium may be lost from the weathering crust (Ronov et al., 1970). The isotopic composition of the clay is expected to vary with the degree of extraction. In a rock-dominated system, if the parent mineral has δ^6Li of -13.5‰, retention of 50% of lithium would result in a δ^6Li of -4‰ in the clay, assuming an isotopic fractionation factor of 1.019. On the other hand, if most of the lithium is retained in the weathered product, then the δ^6Li would resemble that of the parent material. Intense chemical weathering should leave the residue depleted in lithium and very light in isotopic composition, as discussed previously. The lithium contents and isotopic compositions of most sediment from ODP Sites 918/919 are similar to those of the continental rocks (Figure 4.4), indicating that physical weathering products dominate at the Greenland margin. Consequently the sediments inherit the isotopic signature of the source rocks. The coastal sediments of Gulf of Mexico, the hemipelagic sediments and pelagic sediments in the eastern Pacific, Caribbean sea, and Aegean sea are enriched in lithium and isotopically heavier than the river suspended particulate. Their isotopic values lie in the lighter region of the continental composition, suggesting the control by mixing of products of chemical weathering and physical weathering of source region. The unaltered sediments of Guaymas Basin have δ^6Li values similar to the pelagic sediments of the eastern Pacific (Chan et al., 1994a). Hydrothermally altered sediments at this site are depleted in lithium and have lighter lithium isotopic

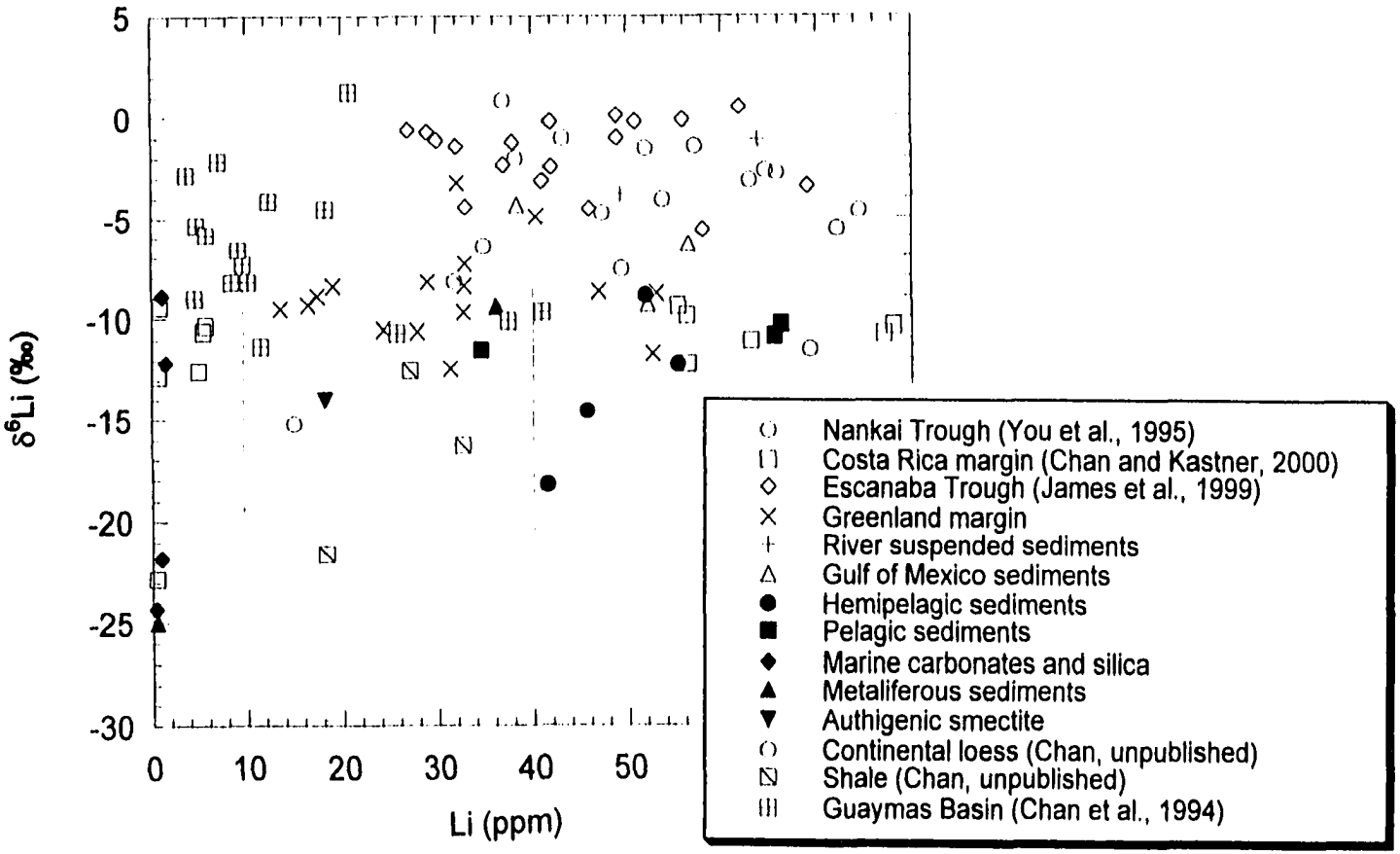

Figure 4.4 Lithium contents and isotopic compositions of river, coastal and marine sediments from this study. Also shown are available data from Guaymas Basin, Nankai Trough, Escanaba Trough, and Costa Rica subduction margin. The square field represents the compositional range of igneous and metamorphic rocks from South Africa and the Canadian Shield.

compositions. The Nankai Trough sediments display relatively light isotopic values (-8 to +1‰), which are due to its island arc origin (You et al., 1995). The concentration and isotopic data from Costa Rica margin (Chan and Kastner, 2000) are similar to those of the hemipelagic sediments at MANOP Site H which mainly reflects the terrigenous input from the Central American. The turbidite sediments from Escanaba Trough are derived from the Columbia River and Klamath Mountains of northern California and southern Oregon (James et al., 1999). Their relatively light lithium isotopic compositions (-5.6 to +0.5‰) must reflect the signature of the volcanic source in this region. The isotopic systematics is also consistent with Holland's conclusion that most of the sediments delivered to the ocean today are mixtures of old sedimentary rocks that have been eroded and the weathering products of igneous and metamorphic rocks (Holland, 1984). For sediments near continental margins, their isotopic compositions are strongly influenced by the regional source material.

The question remains whether the sediment composition is affected by reactions in seawater. Based on laboratory experiment, adsorption in seawater may contribute 2ppm of lithium. Low-temperature alteration of mafic minerals in the sediments will form smectite and result in a relatively heavy isotopic composition. The role of reverse weathering in the marine environment is poorly known and requires future study. The sediment data from the Greenland margin, Nankai Trough, Escanaba Trough, and the Costa Rica margin indicate the important role of the local source in controlling the

lithium isotopic composition of marine sediments. It appears that reactions in seawater have not significantly altered the signature of the terrigenous sediments.

4.5.3 Implication for sediment recycling and arc magma

Clays and hemipelagic sediment samples display isotopic compositions of -8.9 to –18.2‰. This isotopic range is similar to the values (-9 to -12‰) found for sediments in the Costa Rica subduction zone (Chan and Kastner, 2000). The lithium isotopic compositions of sediments are therefore heavier than that of the mantle as inferred from MORB (-3 to -5‰) (Chan et al., 1992). An exception is sediments from Nankai Trough and Escanaba Trough. The sediments in Nankai Trough display relatively light isotopic values (-8 to +1‰) due to its island arc origin (You et al., 1995). The turbidite sediments from Escanaba Trough also have light isotopic compositions that are derived from the Columbia River and Klamath Mountains of northern California and southern Oregon (James et al., 1999). Hydrothermal experiments have demonstrated that lithium is readily mobilized from sediments into fluids at elevated temperatures (You, 1994; Chan et al., 1994a). Mineral dehydration in the deep subduction zone causes release of fluids and mobilization of lithium from the descending sediments and altered ocean crust that is also isotopically heavier than MORB (Chan et al., 1992). The slab-derived fluid in turn metasomatizes the subarc mantle, transporting the subducted material to the arc magma source (Tatsumi, 1989; Morris et al., 1990). Addition of the

subducted sediments and oceanic crust would cause enrichment in ^{7}Li in the arc lavas.

Recently studies of the Central American Arc have indeed shown that the arc lavas are enriched in lithium and isotopically heavier than mantle-derived rocks (Chan et al., 1999). Although the sedimentary signature is indistinguishable from that of the altered ocean crust, lithium isotopic composition does provide a measure of the contribution of the subducted components. The arc volcanics from Izu Arc, Japan are also enriched in ^{7}Li relative to mantle wedge (Moriguti and Nakamura, 1998). Because the sediments in this region is isotopically light, the isotopic data suggests that altered ocean crust is the dominant subduction component. These studies underscore the importance of characterization of the subducted sediments for individual arcs in order to decipher the contribution of slab components to arc magma.

4.6 Summary and conclusion

Lithium isotopic compositions of the principal types of marine sediments have been characterized. The low lithium contents of marine carbonates and biogenic silica indicate that these components have little effect on the bulk isotopic compositions of marine sediments. The isotopic compositions of ooze carbonate and oolite suggest a smaller degree of lithium isotopic fractionation than clays. The suspended sediments of the Amazon and the Mississippi Rivers are isotopically light (-1 and -3.8‰), probably due to preferential uptake of the light isotope into fine-grained

materials, mainly clay minerals. Pelagic clays and hemipelagic sediments from many parts of the ocean display relatively heavy lithium isotopic compositions (-8.9 to –18.2‰), similar to the compositions of continental rocks and sediments. It is noted that sediments of Nankai Trough and Escanaba Trough display isotopic values that are lighter than those observed form this reconnaissance study. Lithium isotopic compositions of marine sediments are related to the characteristics of the source material. Thus the isotopic composition of marine sediments is dominated by terrigenous components that include both chemical and physical weathering products. This conclusion implies that the sediments delivered to the ocean today are mostly recycled sediments.

Clay-rich pelagic and hemipelagic sediments are enriched in lithium and isotopically distinct from mantle derived rocks. Lithium isotope systematics can be a powerful tracer for identifying the subducted component in island arc magmas.

4.7 References

BIJU-DUVAL B., MOORE J. C., et al. (1984) Initial Reports of the Deep Sea Drilling Project, Volume 78A, 227 – 300, Washington (U. S. Government Printing Office).

CHAN L. H. (1987) Lithium isotope analysis by thermal ionization mass spectrometry of lithium tetraborate. Anal. Chem. 59, 2662-2665.

CHAN L. H., ALT J. C., AND TEAGLE D. A. H. (1996) Alteration of the upper 1.8 kilometers of oceanic crust: A lithium isotope record at ODP Site 504B. Trans Am. Geophys. Union, 77, F805.

CHAN L. H. AND EDMOND J. M. (1988) Variation of lithium isotope composition in the marine environment: A preliminary report. Geochim. Cosmochim. Acta 52, 1711-1717.

CHAN L. H., EDMOND J. M., THOMPSON G., AND GILLS K. (1992) Lithium isotopic composition of submarine basalts: Implications for the lithium cycle in the oceans. Earth Planet. Sci. Lett. 108, 151-160.

CHAN L. H., EDMOND J. M., and THOMPSON G. (1993) A lithium isotope study of hot springs and metabasalts from mid-ocean ridge hydrothermal systems. J. Geophys. Res. 98, 9653-9659.

CHAN L. H., GIESKES J. M., YOU C. F., AND EDMOND J. M. (1994a) Lithium isotope geochemistry of sediments and hydrothermal fluids of the Guaymas Basin, Gulf of California, Geochim. Cosmochim. Acta 58, 4443-4454.

CHAN L. H., ZHANG L., AND HEIN J. R. (1994b) Lithium isotope characteristics of marine sediments. EOS, 75, No. 44, 314.

CHAN L. H., STURCHIO N. C. AND KATZ A. (1997) Lithium isotope study of the Yellowstone hydrothermal system. EOS, Trans. Amer. Geophys. Union 78, No. 46, F802.

CHAN L. H., LEEMAN W. P., AND YOU C. F. (1999) Lithium isotopic composition of Central American Volcanic Arc lavas: Implications for modification of subarc mantle by slab-derived fluids. Chem. Geol. 160, 255-280.

CHAN L. H. AND KASTNER M. (2000) Lithium isotope compostions of pore fluids and sediments in the Costa Rica subduction zone: Implications for fluid processes and sdiment contribution to the arc volcanoes. Earth Planet. Sci. Lett. 183, 275-290.

CROCK J. C. AND SEVERSON R. C. (1980) Four reference soil and rock samples for measuring lementent availability in western energy regions. USGS Circ. 841, 1-16.

DYMOND J. (1981) Geochemistry of Nazca plate surface sediments: An evaluation of hydrothermal, biogenic, detrital and hydrogenous sources. Geol. Soc. Amer. Memoir. 154, 133-173.

FLESCH G. D., ANDERSON A. R. JR., AND SVEC H. J. (1973) A secondary isotopic standard for Li determinations. Intl. J. Mass Spectrom. Ion Phys. 12, 265-272.

GRAYBEAL A. L. AND HEATH G. R. (1984) Remobilization of transition metals in surficial pelagic sediments from the eastern Pacific. Geochim. Cosmochim. Acta 48, 965-975.

HOEFS J. AND SYWALL M. (1997) Lithium isotope composition of Quaternary and Tertiary biogene carbonates and a global lithium isotope balance. Geochim. Cosmochim. Acta 61, 2679-2690.

HOLLAND H. D. (1984) The chemical evolution of the Atmosphere and the Oceans. Princeton Univ. Press.

HORSTMAN E. L. (1957) The distribution of lithium, rubidium, and caesium in igneous and caesium in igneous and sedimentary rocks. Geochim. Cosmochim. Acta 12, 1 – 28.

HSU K., MONTADERT L., et al. (1978) Initial Reports of the Deep Sea Drilling Project, Volume 42, Part 1, 305 – 320, Washington (U. S. Government Printing Office)

HUH C.-A. AND KU T.-L. (1984) Radiochemical observations on manganese nodules from three sedimentary environments in the north pacific. Geochim. Cosmochim. Acta 48, 951-963.

HUH Y., CHAN L. H., ZHANG L., AND EDMOND J. M. (1998) Lithium and its isotopes in major world rivers: implications for weathering and the oceanic budget. Geochim. Cosmochim. Acta 62, 2039-2051.

HUH Y., CHAN L. H., EDMOND J. (1999) Lithium and its isotopes in river water and suspended material. Annual V. M. Goldschmidt Conference, LDI Contribution No. 971, page 131, Lunar and Planetary Institute, Houston.

JAMES H. J., RUDNICKI M. D., AND PALMER M. P. (1999) The alkali element and boron geochemistry of the Escanaba Trough sediment-hosted hydrothermal system. Earth Planet. Sci. Lett. 171, 157-169.

KELTS K. R. (1982) Petrology of hydrothermally metamorphosed sediments at DSDP site 477, southern Guaymas Basin rift, Gulf of California. In Initial Reports of the Deep Sea Drilling Project, Volume 64, Pt. 2 (ed. J. R. Curray et al.), pp. 1123 – 1136. US Govt. Printing Office.

LARSEN H. C., SAUDERS A. D., CLIFT P. D., AND THE SHIPBOARD SCIENTIFIC PARTY (1994) Introduction: Breakup of the southeast Greenland margin and the formation of the Irminger Basin: Background and scientific objectives. Proc. ODP. Init. Reports 152.

LYLE M., HEATH R., AND ROBBINS J. M. (1984) Transport and release of transition elements during early diagenesis: Sequetial leaching of sediments from MANOP Site M and H. Geochim. Cosmochim. Acta 48, 1705-1722.

MORIGUTI T. AND NAKAMURA E. (1998) Across-arc variation of Li isotopes in lavas and implications for crust/mantle recycling at subduction zones. Earth Planet. Sci. Lett. 163, 140-167.

MORRIS J. D., LEEMAN W. P., TERA F. (1990) The subducted component in island arcs: Constraints from Be isotopes and B-Be systematics. Nature 344, 31-36.

RONOV A. B., MIGIDSOV A. A., VOSKERSENSKAYA N. T., AND KORZINA G. A. (1970) Geochemistry of lithium in the sedimentary cycle. Geochm. Int. 7, 75 –102.

RYAN W. B. F., HSU K. J., et al (1973) Initial Reports of the Deep Sea Drilling Project, Volume XIII, Part I. 243-322, Washington (U. S. Government Printing Office).

SAITO S. (1998) Major and trace element geochemistry of sediments from east Greenland continental rise: An implication for sediment provenance and source area weathering. Proc. ODP. Sci. Results 152, 19 – 28.

STOFFYN-EGLI P. AND MACKENZIE F. T. (1984) Mass balance of dissolved lithium in the oceans. Geochim. Cosmochim. Acta 48, 859 – 872.

TATSUMI Y. (1989) Migration of fluid phases and genesis of basalt magma in subduction zones, J. Geophys. Res. 94, 4697-4707.

TAYLOR S. R., MCLENNAN S. M., AND MCCULLOCH M. T. (1983) Geochemistry of loess, continental crustal composition and crustal model ages. Geochim. Cosmochim. Acta 47, 1897–1905.

YOU C. –F. (1994) Lithium, beryllium, and boron isotope geochemistry: Implications for fluid processes in convergent margins. Dissertation, University of California, San Diego.

YOU C. F., CHAN L. H., SPIVACK A. J., AND GIESKES J. M. (1995) Lithium, boron, and their isotopes in sediments and pore waters of Ocean Drilling Program Site 808, Namkai Trough: Implications for fluid expulsion in accretionary prisms. Geology 23, No. 1, 37 – 40.

You C. F. AND CHAN L. H. (1996) Precise determination of lithium isotopic composition in low concentration natural samples. Geochim. Cosmochim. Acta 60, 909 – 915.

ZHANG L., CHAN L. H., AND GIESKES J. M. (1998) Lithium isotope geochemistry of pore waters from Ocean Drilling Program Sites 918 and 919, Irminger Basin, Geochim. Cosmochim. Acta 62, 2437–2450.

CHAPTER 5
A RE-EVALUATION OF THE OCEANIC LITHIUM BUDGET

5.1 Introduction and background review

Lithium is generally considered to be a conservative element in the ocean with a residence time of 1 million years and does not show inter-ocean variation. There has been little variation in its concentration over past 40 million years as suggested by relatively constant Li/Ca ratio in planktonic foraminifera (Delaney and Boyle, 1986). The input of dissolved lithium to the oceans must, at steady state, be equal to the output in order to stabilize its relative composition in seawater. Elaboration of this steady-state model reveals some difficulties in explaining its budget in the oceans. Two major sources in the oceans are river input and hydrothermal input at ridge axes. The well-known major sink is low temperature basalt alteration, which cannot balance the combined input. The imbalance of the lithium budget is probably due to poorly constrained hydrothermal flux and unquantified sedimentary sinks. Clearly it is unsatisfactory to conclude due to the absence of a known sink of adequate magnitude, that lithium is accumulating in the oceans. Based on the findings from previous three chapters, in this chapter, we quantify the sinks such as adsorption by marine sediments, incorporation of biogenic carbonates and silica, and lithium diffusion into marine sediments on the sea floor to gain a better understanding of the oceanic budget.

Before evaluating these sedimentary sinks, it is essential to understand previous flux calculations. River input initially was estimated as

1.3 –1.6 x 10^{10}mole/yr based on the average concentration of 2.5 – 3.0μg/L of river waters (Stoffyn-Egli and Mackenzie, 1984). The average concentration is in agreement with the value of 3μg/L in the estimate of Edmond et al (1979) and Morozov (1969). Recently, Huh et al. (1998) has reevaluated the river-input flux using the flow-weighted mean of the lithium concentrations of thirteen major rivers of the world. The concentration means are reduced to 1.5μg/L (215nmol). Using a river flux of 37, 400km^3/yr, the river input is reduced from 1.3 – 1.6 to 0.8 x 10^{10}mole/yr. The seasonal and annual variability of rivers could give rise to significant uncertainty.

The global hydrothermal flux of lithium largely depends on the estimation of the hydrothermal water flux. To determine the hydrothermal water flux, we must first consider hydrothermal heat fluxes. The mass hydrothermal water flux (F) can then be calculated based on the following equation:

$$F = H/\Delta TC_p \qquad (1)$$

where H is hydrothermal heat flux, ΔT is the water temperature anomaly, and C_p is the specific heat capacity of seawater at seafloor pressure. There are three geophysical approaches to estimate submarine global heat fluxes: (a) estimation of the magmatic heat flux, (b) use of the global heat flow anomaly, (c) use of models of hydrothermal flow (Elderfield and Schultz, 1996). There is a reasonable agreement among those geophysical methods in the estimation of total and axial heat fluxes. The total hydrothermal heat flux falls in the range of 7 – 11 x 10^{12}W and the axial heat flux (on 0 – 1Ma crust) is

estimated from 2.1 to 3.1 x 10^{12}W (Elderfield and Schultz, 1996). The remainder of the hydrothermal heat flux occurs on older crust (1 – 65Ma) of the ridge flank. Thus the axial heat flow is approximately 20% of the total hydrothermal heat flow.

The axial heat flux can also be determined by the inventory of excess ^{3}He in the ocean and ^{3}He/heat ratios (Jenkins et al, 1978). There are no ^{3}He anomalies in low-temperature off-axis vents, and so the heat fluxes of 1 – 6 x 10^{12}W calculated for various vents must be ascribed wholly to axial hydrothermal heat flux. The higher limit exhibited by 21°N East Pacific Rise (Edmond et al., 1979) is almost as high as the total hydrothermal heat flux. The large variability is primarily a result of the different rates of extraction of heat and ^{3}He from basalt. Using a theoretical estimate based on the ^{4}He/heat production ratio by radioactive decay of U and Th and the ^{3}He/^{4}He in MORB, Lupton et al. (1989) arrived at a heat flux of 1 x 10^{12}W from the upper mantle. Even though the total hydrothermal heat flux is in reasonable agreement between geophysical and geochemical approaches, the problems arise in calculating the water fluxes.

One major problem is the partitioning of heat fluxes into axial and off-axis flow, as well as high-temperature and lower-temperature diffuse flow at the ridge axis. Assuming different partitions of heat to high-temperature and lower-temperature flow leads to totally different consequent water flux. If, at the ridge axis, 10% of the global hydrothermal budget results from high-temperature flow at 350°C and that 90% results from diffuse flow at 5°C,

Elderfield and Schultz (1996) estimate that the total water flux at high temperatures to be 0.3 – 0.6 x 10^{13}kg/year and the diffuse flow to be 280 – 560 x 10^{13}kg/year. On the other hand, if we assume all flows are at 350°C, the axial water flux would be 3 – 6 x 10^{13}kg/year. The water flux associated with off-axis flow is also highly uncertain. Elderfield and Schultz (1996) assumed the water flux at a temperature of 5 – 15°C and determined the water flux to be 370 – 1100 x 10^{13}kg/year. In conclusion, the high temperature and lower-temperature water fluxes using equation (1) are estimated with large uncertainty, which is mainly caused by the uncertainty in the heat partition at high-temperature and lower-temperature flows. This, in turn, strongly hampers the accurate estimation of lithium flux derived from circulation of seawater in the oceanic crust.

The hydrothermal water flux may be constrained by geochemical budgets. The high-temperature water flux is estimated at 8 – 9 x 10^{13}kg/year if we assume all the magnesium in the ocean is removed into the axial sink (Edmond et al., 1979). Based on the strontium isotope budget in the ocean, Palmer and Edmond (1989) obtain a high-temperature hydrothermal water flux of 9 – 15 x 10^{13}kg/year, which is compatible with the value based on the magnesium oceanic budget. However, they are larger than the geophysical estimation of 3 – 6 x 10^{13}kg/year assuming all axial flow at 350°C (Elderfield and Schultz, 1996). Palmer and Edmond (1989) argued that ridge flank flux has to be small relative to high-temperature ridge crest flux. Their most compelling argument is that if off-axis hydrothermal circulation were a major

component of the oceanic geochemical budget, it would have resulted in detectable physical and chemical plumes in the water column. At that time, no such plumes had been observed.

Recently, 62-64°C springs from Baby Bare, a 3.5 Ma-old basement outcrop on the flank of Juan de Fuca Ridge, were discovered (Wheat and Mottl, 2000). The chemical compositions of the springs indicate that the magnesium concentration decreases from the bottom seawater value of 52mmole/kg to 0.98mmole/kg and strontium increases from 86 μmole/kg to 110μmole/kg. Due to potentially large water flux from the ridge flank indicated by geophysical models, interaction of seawater with basement at moderate temperatures may result in a large input or removal flux. Without consideration of the reaction and isotopic exchange on ridge flanks, water flux calculation based on magnesium and strontium isotopes (Edmond et al., 1979; Palmer and Edmond 1989) may be in error.

5.2 The lithium balance in the ocean

The current estimates of the input and output fluxes are summarized in Table 5.1 with the highlighted values as the updated and prefered estimates. High-temperature hydrothermal flux of lithium has been computed to be 9.5 – 19 x 10^{10}mole/yr on the basis of the ^{3}He/heat ratio of ridge crest hot springs at Galapagos and the EPR (Edmond et al, 1979; Von Damm et al., 1985). However, the ^{3}He/heat ratios of hydrothermal vents vary by an order of magnitude, suggesting that the ratio observed at Galapagos and the EPR may not be representative of all hydrothermal systems (Lupton et al., 1989).

Stoffyn-Egli and Mackenzie (1984) argued that the lithium flux to the ocean couldn't exceed its inventory in the newly formed oceanic. New basaltic crust can only supply a maximum of 2.5 – 7.5 x 10^{10}mole/yr using 2.9g/cm^3 for the basalt density, 5 – 10ppm lithium in newly formed basalt, crust production rate of 2.94km^2/yr, and crust thickness of 4 – 6km (Stoffyn-Egli and Mackenzie, 1984). Since seawater may not reach the full depth of the new crust and therefore is not likely to remove 100% of the lithium contained in the basalt, the value of 2.5 – 7.5 x 10^{10}mole/yr has to be the upper limit of the hydrothermal flux. This flux is less than the 9.5 – 19 x 10^{10}mole/yr estimated by Edmond et al (1979). Based on the geophysical model (Mortan and Sleep, 1985), in which 1/6th of the convective heat loss occurs at the ridge axis, Stoffyn-Egli and Mackenzie (1984) estimated the lithium flux to be 1.6 – 2.7 x 10^{10}mole/yr, 1/6th of the ^{3}He-based flux of Edmond et al. (1979).

Chan et al. (1992) examined the oceanic lithium budget from the standpoint of isotope balance. The mean lithium isotopic composition of rivers was estimated to be -19 ± 6‰ and that of the hydrothermal input was taken to be -9 ± 2‰. The calculation shows that the hydrothermal flux must be comparable to the river flux in magnitude if preferential incorporation of light lithium in authigenic clays with an isotopic fractionation factor of 1.019 provides a mechanism for isotopic balance as required by a steady state ocean. Huh et al (1998) updated the calculation with a better-constrained riverine flux and mean isotopic composition based on measurement of the world's major rivers that account for one third of the global runoff. The mean

Table 5.1 Lithium fluxes in the oceans

Flux	Li (10^{10} mole/yr)	Reference
Sources		
(1) River input	1.3 – 1.6	Stoffyn-Egli and Mackenzie (1984)
	0.8	Huh et al., (1998)
(2) Hydrothermal input	1.6 – 2.7	Stoffyn-Egli and Mackenzie (1984)
	1.4	Huh et al., (1998)
(3) Diffusion from sediments	**0.06**	Stoffyn-Egli and Mackenzie (1984)
(4) Flux in continental margins	0.02 - 0.1	You et al, (1995)
	0.025 – 0.05	Chan and Kastner (2000)
Sinks		
(1) Low temperature ocean crust alteration	0.95	Thompson (1983)
	0.6 – 1.1	Seyfried et al., (1984)
	0.2 – 1.2	Stoffyn-Egli and Mackenzie (1984)
(2) Chlorite-rich greenschist metamorphism	**0.4 –0.6**	Stoffyn-Egli and Mackenzie (1984)
(3) Diffusion into sediments	**0.05**	This dissertation
(4) Adsorption on suspended matter	**0.41**	This dissertation
(5) Marine carbonates	**0.01 – 0.04**	This dissertation
(6) Biogenic silica	**0.01**	This dissertation
Total input	**2.28 – 2.31**	
Total output	**1.48 – 2.21**	

lithium concentration and δ^6Li are 215 nmol and -22.9‰. Using these values, the river flux was revised to 0.8 x 10^{10}mole/yr and the hydrothermal input is constrained to be 1.4 x 10^{10}mole/yr. Based on the lithium contents (411 – 1322μM) of high temperature vent fluids (Edmond et al., 1979. Von Damm et al., 1985), the calculated lithium flux yields a water flux of 1.1 to 3.4 x 10^{13}kg/yr. This is comparable to the geophysical estimate of 3 – 6 x 10^{13}kg/yr assuming all flow is at 350°C.

Fluids expelled from accretionary complexes at convergent margins may play an important role in the geochemical budgets of elements. Using the accepted water flux of 1 – 2 km^3/yr (Kastner et al., 1991), You et al (1995) estimated a lithium flux of 0.2 – 1 x 10^9mole/yr associated with the expelled fluid. Using a lithium content of 250μM at the décollement of ODP Site 1040 as the global mean, the lithium flux is 0.25 – 0.5 x 10^9mole/yr (Chan and Kastner, 2000).

The only major sink of lithium in the oceans is low temperature basalt alteration, which allows 0.95 x 10^{10}mole/yr to be removed from the oceans (Thompson, 1983). This estimate includes fluxes resulted from low and medium temperature reactions with the oceanic crust. This is comparable to the estimate of Seyfried et al. (1984) based on lithium data of ODP 418A rocks. Stoffyn-Egli and Mackenzie (1984) arrived at a range of 0.2 to 1.2 x 10^{10}mole/yr for the low temperature flux. The value is determined by assuming submarine basalts undergo alteration over a thickness of 200 – 600m during

their lifetime on the sea floor resulting an average lithium enrichment factor of 2.5.

The range proposed by Seyfried et al (1984), 0.6 – 1.1 x 10^{10}mole/yr, brackets the estimates above, except for the lower extreme of Stoffyn-Egli and Mackenzie (1984), and is therefore considered reasonable. Another possible removal mechanism is greenschist metamorphism of ocean crust at high water/rock ratios (Stoffyn and Egli and Mackenzie, 1984). However, the amount of basalt undergoing this reaction is poorly known and the calculated output flux (0.4 – 0.6 x 10^{10}mole/yr) is probably overestimated.

It is apparent that the mechanisms described above are not sufficient to balance the inputs from rivers and hydrothermal fluids. To better constrain the budget of lithium in the ocean, this dissertation examines the magnitudes of various sedimentary sinks. These include incorporation into marine carbonates and biogenic silica, diffusion into bottom sediments, and adsorption by detrital sediments.

5.3 Implication of the findings in this work

5.3.1 Role of marine carbonates and silica

Incorporation of lithium into non-detritus components is evaluated by estimating two different components: marine carbonate and silica. The data from the Chapter 4 indicates that biogenic and inorganic carbonates contain little lithium (0.4 – 1.5ppm). The accumulation rate of carbonates in the oceans is estimated as 18.9 x 10^{14}g/yr (Vengosh et al., 1991, and references therein) and 23.7 x 10^{14}g/yr (Wilkinson and Algeo, 1989) respectively. Using an

average value of 20 x 10^{14}g/yr for the marine carbonate accumulation rate and lithium content from 0.4 to 1.5ppm, total lithium removal by marine carbonates would be approximately 0.12 – 0.43 x 10^{9}mole/yr. The formation rate of biogenic silica is estimated as 3.2 – 4.4 x 10^{14}g/yr (Vengosh et al., 1991, and references therein), and lithium concentration of siliceous ooze is determined to be approximately 1.2ppm. Therefore, the removal flux by biogenic silica would be approximately 0.06 – 0.07 x 10^{9}mole/yr. These output fluxes combined cannot account for 2% of the total input.

5.3.2 Authigenic clay formation

The incorporation of lithium in Fe-montmorillonite from the Bauer Basin is an example of lithium removal by formation of hydrothermal clay minerals. However, it is difficult to quantify this sink because the global rate of authigenic clay formation is poorly known. Formation of authigenic clays is believed to be an insignificant process in areas remote from volcanic and hydrothermal sources (Kastner 1981).

5.3.3 Role of lithium diffusion into sediments

It has been speculated that diagenesis of volcanic material in sediments may be an important sink for lithium in the oceans (Stoffyn-Egli and Mackenzie, 1984) and diffusion may carry dissolved lithium into sediments due to the concentration gradient caused by the uptake of lithium into alteration clays. Lithium depletion in interstitial waters observed at many ODP sites has been linked to the presence of altered volcanic material in the sediment column (Stoffyn-Egli and Mackenzie, 1984 and references therein).

The lithium isotopic data at ODP Sites 918 and 919 support the suggestion that low lithium concentrations in the interstitial waters are due to alteration of volcanic material. Using the concentration gradient (10μM/10m) at Site 919 and a diffusion coefficient of 1.48 x $10^2 cm^2$/year for lithium (Li and Gregory, 1974) and a porosity of 50%, the diffusive flux of lithium into the sediments is estimated to be 3.7 x 10^{-4}μM/(cm^2 *year). The diffusive flux into the sediments in the entire ocean due to this diagenetic process is difficult to estimate because the content of volcanic matter and consequently the concentration gradient across the sediment-seawater interface would vary greatly geographically. At some locations the concentration gradient in the surface sediment is reversed, such as those observed in the Guaymas Basin (DSDP 477, Gieskes et al., 1982) and at the Peru margin (Martin et al., 1991). A review of pore fluid lithium data at the ODP sites indicates that 38% of the sites have pore water lithium concentrations lower than seawater in the uppermost sediments (James and Palmer, 2000). Assuming the diffusive flux estimated for Irminger Basin occurs over 38% of the entire ocean floor, the magnitude of dissolved lithium flux is approximately 0.5 x 10^9mole/yr. This value is very similar to that estimated for the removal during early diagenesis of marine sediments (James and Palmer, 2000). The amount of lithium removed by this process is about 2% of the combined hydrothermal and river inputs (Stoffyn-Egli and Mackenzie, 1984 and Huh et al., 1998). For this reason, post depositional alteration of volcanogenic components in the sediment cannot be a major sink of oceanic lithium.

5.3.4 Role of lithium adsorption by marine sediment

Since marine sediments are enriched in lithium in comparison to freshwater sediments (Holland, 1984), marine sediments are thought to be an important sink for oceanic lithium. Lithium adsorption onto marine sediment has been proposed as an important removal processes for lithium in the oceans (Seyfried et al., 1984). Using the partition coefficients determined in Chapter 2, it is possible to estimate the amount of lithium adsorbed by clay minerals in the oceans. Based on the adsorption experiments, partition coefficients for kaolinite and vermiculite in seawater are approximately 11.2 and 16.3 respectively. The Mississippi River suspended sediment contains mostly illite and the mixture of illite and smectite (Kennedy, 1965), and has a partition coefficient of 10.6. Based on this partition coefficient, 2ppm of lithium is expected to be adsorbed from seawater onto Mississippi River suspended sediment. Using the Mississippi River suspended sediment as representative of river sediments delivered to the ocean, and given a sediment load (suspended plus bed load) of 150 x 10^{14}g/yr for the world's rivers (Milliman and Meade, 1983), the total lithium removed from the oceans by the suspended sediments would be about 0.41 x 10^{10}mole/yr. This flux is approximately 20% of the sum of the latest estimated hydrothermal and river flux. Thus adsorption on suspended material appears to be a significant sink in the ocean.

Based on the updated estimates (Table 5.1), the total input flux of lithium to the ocean is 2.28 – 2.31 X 10^{10}mole/yr and the total output flux is

1.48 – 2.21 X 10^{10}mole/yr. Although uptake into marine carbonates and biogenic silica and lithium diffusion into marine sediments due to post depositional volcanic alteration contribute to the removal of lithium from the ocean, these mechanisms remain relatively minor. Adsorption by marine sediments appears to be a significant sink for lithium in the oceans. The upper limit of present estimation of sinks (Table 5.1) nearly balances total input estimated by Huh et al. (1998).

5.4 Future work

Two potential sinks are not well known and future work is required to achieve a better quantification. The first is the role of authigenic clay formation and the associated lithium isotope fractionation. This can further be used to constrain the hydrothermal flux. Michalopoulos and Aller (1995) have demonstrated that rapid authigenic clay formation can occur by reverse weathering reaction in Amazon delta sediments. It is estimated that authigenic clays can amount to 3 to 7% of the sediments deposited on the seafloor (Mackenzie and Garrels, 1966; Michalopoulos and Aller 1995). The iron rich clays potentially can incorporate lithium. If we conservatively take the lithium content of the Bauer Basin iron montmorillonite (18ppm) as typical, 0.12 – 0.27 x 10^{10}mole/yr additional lithium would be removed from the ocean. The second is the hydrothrmal flux associated with reaction at moderate temperatures on the ridge flank. This sink has been estimated by Thompson (1983) to be 0.5 x 10^{10}mole/yr based on altered basement rocks and included in the low-temperature alteration flux in Table 5.1. The discovery of warm

springs from the ridge flank provides insight from the viewpoint of fluid chemistry. The lithium content of the Baby Bare warm spring is 9.0μmole/kg, compared with 26μmole/kg in seawater (Wheat and Mottl, 2000). Considering that the large hydrothermal heat flux off axis, only a small change from seawater composition could produce globally significant fluxes. To illustrate, using the off-axis heat flux of 7 X 10^{12}W (Elderfield and Schultz 1996) and the temperature of 64°C for the hydrothermal springs at Baby Bare, the water flux would be 82 x 10^{13}kg/year. The flank hydrothermal flux could remove as much as 1.4 x 10^{10}mole lithium/yr. This value itself is almost equivalent to the hydrothermal input estimated by Huh et al. (1998). The fluxes resulted from low and medium temperature reactions with the oceanic crust may be underestimated. Because of the large temperature variation, however, the water flux is difficult to be determined with certainty. Further insight into the lithium balance in the ocean depends on the characterization of flank water flux in low and moderate temperature regimes and the chemistry of the waters.

5.5 References

CHAN L. H., EDMOND J. M., THOMPSON G., AND GILLS K. (1992) Lithium isotopic composition of submarine basalts: Implications for the lithium cycle in the oceans. Earth Planet. Sci. Lett. 108, 151-160.

CHAN L. H. AND KASTNER M. (2000) Lithium isotope compositions of pore fluids and sediments in the Costa Rica subduction zone: Implications for fluid processes and sediment contribution to the arc volcanoes. Earth Planet. Sci. Lett. 183, 275-290.

DELANEY M. L. AND BOYLE E. A. (1986) Lithium in foraminiferal shells: Implications for high-temperature hydrothermal circulation fluxes and oceanic crustal generation rates. Earth Planet. Sci. Lett. 8, 91-105.

EDMOND J. M., MEASURES C., MCDUFF E., CHAN L. H., COLLIER R., GRANT B., GORDON L. I., AND CORLISS J. B. (1979) Ridge crest hydrothermal activity and the balances of the major and minor elements in the ocean: the Galapagos data. Earth Planet. Sci. Lett. 46, 1-18.

ELDERFIELD H. AND SCHULTZ A (1996) Mid-ocean ridge hydrothermal fluxes and the chemical composition of the ocean. Annu. Rev. Earth Planet. Sci. 24, 191-224.

JENKINS W. J., EDMOND J. M., AND CORLISS J. B. (1978) Excess ^{3}He and ^{4}He in Galapagos submarine hydrothermal waters. Nature 272, 156-158.

GIESKES J. M., ELDERFIELD H., LAWRENCE J. R., JOHNSON J., MEYERS B. AND CAMPBELL A. (1982) Geochemistry of interstitial waters and sediments, Leg 64, Gulf of California. In Initial Reports of the DSDP, 64, Pt. 2 (eds. Curray J. R., Moore D. G. et al.), Washington, 675-694.

HOLLAND H. D. (1984) The Chemical Evolution of the Atmosphere and the Oceans. Princeton Univ. Press.

HUH Y., CHAN L. H., ZHANG L., AND EDMOND J. M. (1998) Lithium and its isotopes in major world rivers: implications for weathering and the oceanic budget. Geochim. Cosmochim Acta 62, 2039-2051.

JAMES R. H. AND PALMER M. R. (2000) Marine geochemical cycles of the alkali elements and boron: The role of sediments. Geochim. Cosmochim. Acta 64, 3111-3122.

KASTNER M. (1981) Authigenic silicates in deep sea sediments: formation and diagenesis. In The Sea, Vol. 7 (ed. Emiliani C.) pp. 915 – 980, J. Wiley.

KASTNER M., ELDERFIELD H. AND MARTIN J. B. (1991) Fluids in convergent margins: What do we know about their composition, origin, role in diagenesis and importance for oceanic chemical fluxes? Phil. Trans. Roy. Soc. London Sr. A 335, 243-259.

KENNEDY U. C. (1965) Mineralogy and cation-exchange capacity of sediments from selected streams, U. S. Geol. Surv. Prof. Paper 433-D, pp 28.

LI Y. H. AND GREGORY S. (1974) Diffusion of ions in seawater and in deep sea sediments. Geochim. Cosmochim. Acta 38, 703-704.

LUPTON J. E., BAKER E. T., AND MASSOTH G. J. (1989) Variable ^{3}He/heat ratios in submarine hydrothermal systems: evidence from two plumes over the Juan de Fuca ridge. Nature 337. 161-164.

MACKENZIE F. T. AND GARRELS R. M. (1966) Chemical mass balance between rivers and oceans. Amer. J. Sci. 264, 507-525.

MARTIN J. B., KASTNER M. AND ELDERFIELD H. (1991) Lithium: Sources in pore fluids of Peru slope sediments and implications for oceanic fluxes. Marine Geology, 102, 281 – 292.

MICHALOPOULOS AND ALLER R. C. (1995) Rapid clay mineral formation in Amazon delta sediments: Reverse weathering on dooceanic elemental cycles. Science 270, 614-617.

MILLIMAN J. D. AND MEADE R. H. (1983) World-side delivery of river sediments to the oceans. J. of Geol. 91, 1-21.

MOROZOV N. P. (1969) Geochemistry of the alkali metals in rivers. Geochem. Int. 6, 585-594.

MORTON J. L. AND SLEEP N. H. (1985) A mid-ocean ridge thermal model: constraints on the volume of axial hydrothermal heat flux. J. Geophys. Res. 90, 11345 – 11353.

PALMER M. R. AND EDMOND J. M. (1989) The strontium isotope budget of the modern ocean. Earth Planet. Sci. Lett. 92, 11-26.

SEYFRIED W. E. JR., JANECKY D. R., AND MOTTL M. J. (1984) Alteration of the oceanic crust: Implications for geochemical cycles of lithium and boron. Geochim. Cosmochim. Acta 48, 557 – 569.

STOFFYN-EGLI P. AND MACKENZIE F. T. (1984) Mass balance of dissolved lithium in the oceans. Geochim. Cosmochim. Acta 48, 859 – 872.

THOMPSON G. (1983) Hydrothermal fluxes in the ocean. In Chemical Oceanography (ed. J. P. Riley and R. Chester) Vol. 8, pp. 272 – 337. Academic Press.

VENGOSH A., KOLODNY., STARINGSKY A., CHIVAS A. R., AND MCCULLOCH M. T. (1991) Coprecipitation and isotopic fractionation of boron in modern biogenic carbonates. Geochim. Cosmochim. Acta 55, 2901 – 2910.

VON DAMM K. L., EDMOND J. M., GRANT B., MEASURES C. I., WALDEN B., AND WEISS R. F. (1985) Chemistry of submarine hydrothermal solutions at 21°N, East Pacific Rise. Geochim. Cosmochim. Acta 49, 2179–2220.

WHEAT G. C. AND MOTTL M. J. (2000) Composition of pore and spring waters from Baby Bare: Global implications of geochemical fluxes from a ridge flank hydrothermal system. Geochim. Cosmochim. Acta 64, 629–642.

WILKINSON B. H. AND ALGEO T. J. (1989) Sedimentary carbonate record of calcium-magnesium cycling. Amer. J. Sci. 289, 1158 - 1194.

YOU C. F., CHAN L. H., SPIVACK A. J., AND GIESKES J. M. (1995) Lithium, boron, and their isotopes in sediments and pore waters of Ocean Drilling Program Site 808, Nankai Trough: Implications for fluid expulsion in accretionary prisms. Geology 23, 37 – 40.

CHAPTER 6
SUMMARY AND CONCLUSION

Several aspects of the lithium isotope geochemistry of marine sediments are addressed in this dissertation. By conducting the laboratory experiments in which clay minerals and river suspended sediment were allowed to interact with river water and seawater, the extent of lithium adsorption on marine sediments and the magnitude of isotopic fractionation associated with the adsorption process were determined. A comprehensive study of the sediments from the Greenland margin was included to accompany a previous study of the pore fluids in the same sediments to gain further understanding of the diagenetic reactions in the sediments. By characterizing the isotopic compositions of various types of marine sediments including hemipelagic and pelagic clays, and biogenic carbonates and siliceous ooze, the sedimentary cycle of lithium isotopes and the control of the lithium isotopic compositions of marine sediments are discussed. With the enhanced isotope database, the oceanic lithium budget is re-evaluated.

The partition of lithium between clay minerals and water, and the isotopic fractionation factor associated with adsorption were determined from the adsorption experiments. Lithium is taken up by kaolinite and vermiculite but not Na-montmorillonite in seawater and river media. Greater magnitude of adsorption was observed from river water than seawater demonstrating the effect of competition of major ions for sorption sites. The lighter isotope, ^{6}Li, is favored in the adsorption process. The isotopic fractionation factors for adsorption on kaolinite, vermiculite and Mississippi River suspended

sediment are similar within analytical uncertainty, and the mean value have been determined to be 1.024 ± 0.003.

Complementary to the pore water lithium study, the detailed lithium concentration and isotopic profiles of marine sediments are reported. The concentration profile of the marine sediments displays a shape similar to the dissolved lithium profile. The similarity between solid and pore water profiles suggests that the sediments largely control the distribution of lithium in pore water. The pore water lithium isotope profiles are controlled by a variety of exchange reactions with the solid phases such as volcanic alteration, cation exchange with NH_4^+, and lithium release from marine sediments under elevated temperatures. However, due to at least two orders of magnitude difference in lithium inventory between pore water and marine sediments, the isotopic compositions of marine sediments are not affected by the interaction with pore water. The isotopic compositions (δ^6Li = -11 to –11.7‰) are well correlated with source material as defined by lithology and bulk geochemistry and are mostly controlled by relative proportions of weathered or fresh plutonic/metamorphic component and volcanic component.

A reconnaissance study of the lithium isotopic compositions of river sediments and the major types of marine sediments, including pelagic clay, hemipelagic sediments, biogenic carbonates, biogenic silica, coastal sediments, and metaliferous sediments was conducted to understand the sedimentary cycle of lithium isotopes. The low lithium contents of marine carbonates and biogenic silica indicate that these components have little

effect on the bulk isotopic compositions of marine sediments. The isotopic compositions of ooze carbonate and oolite suggest a smaller degree of lithium isotopic fractionation than clays. The suspended sediments of the Amazon and the Mississippi Rivers are isotopically light (-1 and –3.8‰), probably due to preferential uptake of the light isotope into fine-grained materials, mainly clay minerals. Pelagic clay and hemipelagic sediments from various locations of the ocean display relatively heavy lithium isotopic compositions (-8.9 to –18.2‰), similar to the compositions of continental rocks and sediments. Thus the isotopic composition of marine sediments is dominated by terrigenous components that include both chemical and physical weathering products. This conclusion implies that the sediments delivered to the ocean today are mostly recycled sediments. Clay-rich pelagic and hemipelagic sediments are enriched in lithium and isotopically distinct from mantle-derived rocks. Lithium isotope systematics can be a powerful tracer for identifying the subducted component in arc magmas.

The results of this work permit estimation of the magnitudes of various sedimentary sinks, including incorporation into marine carbonates and biogenic silica, diffusion into bottom sediments, and adsorption by marine sediments. The total amount of lithium removed by marine carbonates and biogenic silica cannot account for 1% of the total input. Assuming the diffusive flux estimated at ODP Site 919 occurs over 38% of the entire ocean floor, the magnitude of dissolved lithium flux is approximately 0.5×10^9mole/yr. Therefore, post depositional alteration of volcanogenic components in the

sediment cannot be a major sink of oceanic lithium. Using the partition coefficient determined for Mississippi River suspended sediment in the adsorption experiment, the total lithium removed from the oceans by the suspended sediments would be about 0.41 x 10^{10}mole/yr, which is approximately 20% of the combined of the latest estimated hydrothermal and river flux. Thus adsorption on suspended material appears to be a significant sink in the oceans.

With the enhanced knowledge of the sedimentary sinks, the lithium budget in the ocean is re-examined. Based on the latest estimates, the total input flux of lithium to the ocean is 2.28 – 2.31 x 10^{10}mole/yr and the total output flux is 1.48 – 2.21 x 10^{10}mole/yr. The present estimation of sinks is close to the total input given the uncertainty in the estimation of each flux. However, it is unsatisfactory to suggest that oceanic lithium budget is balanced since two potential sinks are not well known. The first is the role of authigenic clay formation and the associated lithium isotope fractionation. It is difficult to quantify this sink because the global rate of authigenic clay formation is poorly known. Formation of hydrothermal clays is believed to be an insignificant process in areas remote from volcanic and hydrothermal sources. The extent of reverse weathering is poorly known. The second is the hydrothrmal flux associated with reaction at moderate temperatures on the ridge flank. The discovery of warm springs from the ridge flank provides new insight on the oceanic lithium budget from the viewpoint of fluid chemistry. Using the geophysically estimated off-axis heat flux, only a small change from

seawater composition could produce globally significant fluxes. It is possible that the role of oceanic crust alteration is underestimated. Further insight into the lithium balance in the ocean depends on the characterization of flank water flux in low and moderate temperature regimes and the chemistry of the waters.

VITA

Libo Zhang was born August 3, 1965, in Linjiang City, Jilin Province, People's Republic of China. From 1982 to 1986, he attended Beijing University and majored in geology. In 1986, he graduated with distinction and then joined the master's program in the Department of Geology, Beijing University. In 1989, He graduated with master's degree in geology. In August 1992, he attended Louisiana State University and graduated with master's degrees in computer science, and geology and geophysics in 1997. At present, he is working on his doctoral degree in the Department of Geology and Geophysics. He will receive the degree of Doctor of Philosophy in May, 2001.

DOCTORAL EXAMINATION AND DISSERTATION REPORT

Candidate: Libo Zhang

Major Field: Geology

Title of Dissertation: Lithium Isotope Geochemistry of Marine Sediments

Approved:

Dwi-Hsung Chan
Major Professor and Chairman

Dean of the Graduate School

EXAMINING COMMITTEE:

Gavin M. Lin

Lorenzo

C D White

Gary Byerly

Ajoy Bakshi

Date of Examination:

November 29, 2000